

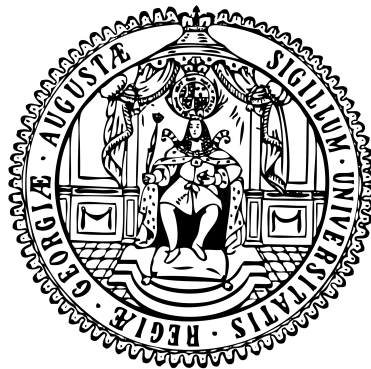
*Clostridioides difficile*:  
Analysis on Single Cell Motility  
and on Antibiotic Resistance

DISSERTATION

for the award of the degree

“Doctor rerum naturalium”

of the Georg–August–Universität Göttingen



within the doctoral program

Microbiology & Biochemistry

at the Göttingen Graduate Center

for Neurosciences, Biophysics,

and Molecular Biosciences

submitted by

Julian Schwanbeck

from Henstedt–Ulzburg, Germany

Göttingen MMXX





### **Thesis committee**

Prof. Dr. med. Uwe Groß                      Supervisor & First Reviewer  
Institut für Medizinische Mikrobiologie, Universitätsmedizin Göttingen

Prof. Dr. Jörg Stülke                      Second Reviewer  
Institut für Mikrobiologie und Genetik, Georg-August-Universität Göttingen

Prof. Dr. Fabian Commichau  
Institut für Biotechnologie,  
Brandenburgische Technische Universität Cottbus – Senftenberg

### **Further members of the examination board**

Prof. Dr. Rolf Daniel  
Institut für Mikrobiologie und Genetik, Georg-August-Universität Göttingen

Prof. Dr. Burkhard Morgenstern  
Institut für Mikrobiologie und Genetik, Georg-August-Universität Göttingen

PD Dr. Michael Hoppert  
Institut für Mikrobiologie und Genetik, Georg-August-Universität Göttingen

Date of Submission:                      31. 08. 2020



# Danksagung

An erster Stelle möchte ich meinem Doktorvater Uwe danken – dafür, dass er mich als Doktorand für dieses spannende Thema angenommen hat, sowie für die interessanten Herausforderungen, die sich im Laufe der Zeit ergeben haben. Es hat mir sehr viel Spaß gemacht, in deinem Institut zu arbeiten und weit über den ursprünglich geplanten Rahmen meiner Arbeit Erfahrungen zu sammeln. Vielen Dank, dass du es mir ermöglichst hast.

Ebenso möchte ich mich bei Prof. Jörg Stülke und Prof. Fabian Commichau, nicht nur für eure Rolle im Thesis Committee, sondern auch für die Zeit davor bedanken. Die Arbeit mit euch hat mir immer viel Spaß gemacht und hatte einen großen Einfluss darauf, dass ich in dem Feld weiter arbeiten wollte.

Ebenfalls Dankeschön an Prof. Rolf Daniel, Prof. Burkhard Morgenstern und PD Dr. Michael Hoppert, sowohl für die Teilnahme in der Prüfungskommission, als auch für eure generelle Hilfsbereitschaft, und dafür, dass ihr immer eine offene Tür habt.

Besonders lieben extra großen super Dank mit Sahne an Rosi, für die vielen Stunden auf dem Balkon, die langen Abende, die diversen gebrauten Weine und schönen Erinnerungen.

For my fellow comrade-in-arms Sabrina, who worked for the same boss, my sincerest gratitude for various bruises, both on my arm and my diaphragm due to laughter, fun conferences, and for sharing interesting in-jokes<sup>1</sup> as well as bets<sup>2</sup>. It wouldn't have been half as fun without you.

¡Muchas gracias Emi! Not just for my now vastly expanded spanish vocabulary (¡Ocho!), but also for the many fun hours. I have come to miss not having the amazing Emis “encouragements” thrown, deservedly, at my head.

Vielen lieben Dank an Pia – für die langen Abende, den Beistand in schweren Zeiten, die Späße in guten, die fachlichen Diskussionen, die unfachlichen Diskussionen, die überraschend seltenen Unterhaltungen auf dem Arbeitsweg, und den ein oder anderen Wein.

Ebenfalls ein Dankeschön an Rike und Noémie für die Bürostimmung, Frisbee-Aktionen, netten Witze, schlechten Witze, Mediziner-Witze, Biologen-Witze, impromptu-parties und generelle Bereitschaft für Blödsinn bzw. Einschreitung gegen selbigen.

Auch an Ruth, Maik, Frau Althaus und Herrn Zickenrott vielen lieben Dank für die unzählige Unterstützung.

---

<sup>1</sup>You need sugar!

<sup>2</sup>I owe you five bottles, in the name of dark DNA.

Lieben Dank an meine Mitstreiterin Avi, für die fachlichen Diskussionen, das ein oder andere Bierchen, die diversen Korrekturen, die sehr therapeutischen Abende und die große Hilfe bei der gemeinsamen Prokrastination. Möge die dunkle DNA mit dir sein.

Many thanks to Cera, for broadening my horizon regarding movies, the discussions both during RNA purification and outside of it, the various nice evenings, as well as for calling my bullshit.

Einen Großen dank an Katrina, Kelly, Carina, Anna und Igor. Es hat mir viel Spaß gemacht, mit euch zu Arbeiten. Vieles ist mit euch erst möglich geworden.

Lieben Dank auch an Vincent, Ruben und Tenzin, für die gute Stimmung im Büro und die ein oder andere blödsinnige Aktion.

Vielen Dank ebenfalls an Raimond, Carsten und Oli, für diverse Tips und Tricks, allgemeine Hilfestellung und aufbauende Sprüche.

Lieben Dank an Markus, der mit mir angefangen hat. Nicht nur für die massige IT-Hilfe, sondern auch die netten Gespräche zwischendrin.

Ebenfalls möchte ich meiner Familie, Andrea, Rebecca, Luise, Astrid und Joachim, für die große und diverse direkte sowie indirekte Hilfe danken. Ihr steht mir immer mit Rat und Tat zur Seite.

Einen lieben Dank an Andreas, für die aufbauenden Kommentare, interessanten neuen Forschungsthemen, und die gute Zusammenarbeit.

Mein ganz besonderer Dank gilt Ines. Du hast mir nicht nur am Anfang die ganzen interessanten praktischen Tricks und Kniffe beigebracht, sondern mir durchgehend auf unzählige Art und Weise geholfen. Ohne dich wäre das nicht möglich gewesen.

Mein größter Dank an dieser Stelle gilt Wolfgang, der mich in den letzten drei Jahren und drei Monaten ertragen musste. Als direkter Betreuer fungierte er als Ratgeber in allen Lebenslagen, Fontäne praktischer Ratschläge, Stimmungsaufheller, und lebender Blitzableiter<sup>3</sup>. Es freut mich sehr, dass er meine Begeisterung an der Thematik teilt<sup>4</sup>. Auch wenn ich sie häufig auf die Probe stellte, bewies er durchgehend sagenhafte Reserven an Geduld<sup>5</sup>

Spaß beiseite, danke Wolfgang: für deine offene Tür, deine Bereitschaft mich Dinge ausprobieren zu lassen, dein Verständnis für Fehler, deine editorischen Fähigkeiten und deine Beratung. Es hat mir sehr viel Spaß gemacht, mit dir zu Arbeiten.

---

<sup>3</sup>Wagemutig schützte er mich vor dem, dank ungezogener Stromversorgung, unter Spannung stehendem Erdungskabel des anaeroben Zeltens.

<sup>4</sup>Zitat Wolfgang: Ich hab mich nie als Mikrobiologe gesehen, das kam jetzt erst mit dieser Geschichte hier. Aber ist ja auch ganz nett.

<sup>5</sup>Einzige Ausnahme: Papierkrieg jeglicher Art.

*Triploblasts played a crucial role in evolution, precisely because they did have internal organs, and in particular they could ingest food and excrete it. Their excreta became a major resource for other creatures; to get an interestingly complicated world, it is vitally important that shit happens.*

(Terry Pratchett, Ian Stewart, Jack Cohen; *The Science of Discworld*, 1999)



# Publications

1. Schwanbeck, J., Riedel, T., Laukien, F., Schober, I., Oehmig, I., Zimmermann, O., Overmann, J., Groß, U., Zautner, A. E., and Bohne, W. 2019. Characterization of a clinical *Clostridioides difficile* isolate with markedly reduced fidaxomicin susceptibility and a V1143D mutation in *rpoB*. *J. Antimicrob. Chemother.*, **74**(1):6–10.
2. Schwanbeck, J., Oehmig, I., Dretzke, J., Zautner, A. E., Groß, U., and Bohne, W. 2020. YSMR: a video tracking and analysis program for bacterial motility. *BMC Bioinformatics*, **21**(1):166.
3. Tilkorn, F. K. M. T., Frickmann, H., Simon, I. S., Schwanbeck, J., Horn, S., Zimmermann, O., Groß, U., Bohne, W., and Zautner, A. E. 2020. Antimicrobial Resistance Patterns in *Clostridioides difficile* Strains Isolated from Neonates in Germany. *Antibiotics*, **9**(8):481.





# Contents

<b>Acknowledgements</b>	<b>I</b>
<b>Publications</b>	<b>V</b>
<b>Contents</b>	<b>VII</b>
<b>Summary</b>	<b>XI</b>
<b>1 Introduction</b>	<b>1</b>
1.1 <i>C. difficile</i> prevalence, infection & treatment . . . . .	2
1.2 Motility . . . . .	9
<b>I Antibiotic Resistance in <i>Clostridioides difficile</i></b>	<b>15</b>
<b>2 Characterization of a clinical <i>Clostridioides difficile</i> isolate with markedly reduced fidaxomicin susceptibility and a V1143D mutation in <i>rpoB</i></b>	<b>17</b>
2.1 Abstract . . . . .	17
2.2 Introduction . . . . .	18
2.3 Methods . . . . .	19
2.3.1 <i>C. difficile</i> strains . . . . .	19
2.3.2 Media and strain cultivation . . . . .	19
2.3.3 Susceptibility testing . . . . .	19
2.3.4 Amplification and sequencing of <i>rpoB</i> and <i>rpoC</i> . . . . .	20
2.3.5 SMRT sequencing of strain Goe-91 (DSM 105001) . . . . .	20
2.3.6 MLST . . . . .	20
2.3.7 Measurement of toxin A/B production . . . . .	20
2.3.8 Sporulation assay . . . . .	20
2.3.9 Growth curves . . . . .	21
2.4 Results and discussion . . . . .	21
2.5 Appendix . . . . .	25
2.5.1 Acknowledgements . . . . .	25
2.5.2 Funding . . . . .	25
2.5.3 Transparency declarations . . . . .	25
2.5.4 Supplementary data . . . . .	25

<b>3 Rifaximin resistance of <i>C. difficile</i> is associated with <i>rpoB</i> alleles and MLST clades</b>	<b>27</b>
3.1 Abstract . . . . .	27
3.2 Introduction . . . . .	28
3.3 Results . . . . .	29
3.3.1 Phenotypic rifaximin resistance testing of <i>C. difficile</i> isolates . . .	29
3.3.2 <i>rpoB</i> sequence polymorphisms in RFX resistant <i>C. difficile</i> isolates	30
3.3.3 Epidemiological parameters associated with RFX resistance . . .	30
3.4 Discussion . . . . .	32
3.5 Materials and Methods . . . . .	34
3.5.1 Patient samples and Isolate collection . . . . .	34
3.5.2 Bacterial culture of <i>C. difficile</i> . . . . .	34
3.5.3 Antimicrobial resistance testing of <i>C. difficile</i> . . . . .	35
3.5.4 DNA isolation, PCR and <i>rpoB</i> sequencing . . . . .	35
3.5.5 Whole genome sequencing and bioinformatics . . . . .	35
3.6 Conclusions . . . . .	36
3.7 Appendix . . . . .	36
3.7.1 Author Contributions . . . . .	36
3.7.2 Funding . . . . .	37
3.7.3 Acknowledgments . . . . .	37
3.7.4 Conflicts of Interest . . . . .	37
<b>4 Evolving higher replication rates while maintaining a Fidaxomicin resistance in <i>C. difficile</i></b>	<b>39</b>
4.1 Abstract . . . . .	39
4.2 Introduction . . . . .	40
4.3 Materials and Methods . . . . .	41
4.3.1 Media and strain cultivation . . . . .	41
4.3.2 Used strains . . . . .	41
4.3.3 Strain evolution . . . . .	41
4.3.4 Growth curves . . . . .	42
4.3.5 Sequencing . . . . .	42
4.3.6 Mutation site analysis . . . . .	42
4.4 Results and Discussion . . . . .	42
4.4.1 Mutations in <i>rpoB</i> and <i>rpoC</i> . . . . .	42
4.4.2 Other Mutations . . . . .	46

<i>CONTENTS</i>	IX
4.5 Conclusion . . . . .	46
4.6 Appendix . . . . .	47
4.6.1 Acknowledgements . . . . .	47
4.6.2 Funding . . . . .	47
4.6.3 Declarations . . . . .	47
4.6.4 Author contributions . . . . .	47
<b>II <i>Clostridioides difficile</i> Single Cell Motility</b>	<b>49</b>
<b>5 YSMR: a video tracking and analysis program for bacterial motility</b>	<b>51</b>
5.1 Abstract . . . . .	51
5.1.1 Background . . . . .	51
5.1.2 Results . . . . .	51
5.1.3 Conclusion . . . . .	52
5.2 Background . . . . .	52
5.3 Software . . . . .	53
5.3.1 File requirements . . . . .	53
5.3.2 Bacteria detection by grey value . . . . .	53
5.3.3 The tracking process . . . . .	55
5.3.4 Track selection . . . . .	55
5.4 Data processing, analysis and illustration . . . . .	57
5.5 Comparison to TrackMate . . . . .	57
5.6 Discussion and Conclusion . . . . .	58
5.7 Availability and requirements . . . . .	59
5.8 Declarations . . . . .	59
5.8.1 Authors' contributions . . . . .	59
5.8.2 Acknowledgements . . . . .	59
<b>6 <i>C. difficile</i> single cell swimming strategy</b>	<b>61</b>
6.1 Abstract . . . . .	61
6.2 Importance . . . . .	62
6.3 Introduction . . . . .	62
6.4 Materials & Methods . . . . .	63
6.4.1 Used <i>C. difficile</i> strains . . . . .	63
6.4.2 Media and strain cultivation . . . . .	63
6.4.3 Video Microscopy . . . . .	63

6.4.4	Video Microscopy with polyvinylpyrrolidone (PVP) or Mucin . . .	64
6.4.5	YSMR settings . . . . .	64
6.4.6	Insertion of <i>erm</i> into <i>cheY</i> . . . . .	65
6.5	Results . . . . .	65
6.5.1	Quantification of <i>C. difficile</i> motility parameters . . . . .	65
6.5.2	<i>C. difficile</i> swimming motility in BHIS medium . . . . .	65
6.5.3	The motility phenotype changes in the presence of the high molecular weight polymer PVP . . . . .	67
6.5.4	<i>C. difficile</i> displays a distinct motility phenotype . . . . .	69
6.5.5	Dependency of <i>C. difficile</i> motility on the availability of various metabolites . . . . .	71
6.6	Discussion . . . . .	74
6.7	Appendix . . . . .	77
6.7.1	Acknowledgements . . . . .	77
6.7.2	Funding . . . . .	77
6.7.3	Transparency declaration . . . . .	77
6.7.4	Author contributions . . . . .	77
6.7.5	Supplementary data . . . . .	78
<b>7</b>	<b>Discussion</b>	<b>79</b>
7.1	Antibiotic Resistance in <i>Clostridioides difficile</i> . . . . .	79
7.1.1	Outlook . . . . .	83
7.2	Motility of single cell <i>Clostridioides difficile</i> . . . . .	85
7.2.1	Outlook . . . . .	90
	<b>List of Figures</b>	<b>93</b>
	<b>References</b>	<b>95</b>
	<b>Curriculum vitae</b>	<b>117</b>

## Summary

*Clostridioides difficile*, formerly in the genus *Clostridium*, is a Gram positive obligatory anaerobic spore forming bacterium. *C. difficile* is the leading nosocomial gastrointestinal pathogen in the western world. In symptomatic patients it causes diarrhoea and in some cases pseudo-membranous colitis. It can cause toxic megacolon, a potentially lethal complication. After treatment, a large percentage of patients suffer a recurrence. A healthy gastrointestinal microbiome offers some protection against *C. difficile* infection.

Fidaxomicin is an antibiotic effective against *C. difficile* which has a lesser negative effect on the microbiome compared to other antibiotic regimen. Fidaxomicin resistant *C. difficile* strains have previously only been created under laboratory conditions. Most mutations conferring decreased susceptibility to Fidaxomicin occur in the RNA polymerase, with the strongest resistance effect caused by mutations in the  $\beta$ -subunit at amino acid 1143, valine to aspartate (*rpoB*<sub>V1143D</sub>). The change in charge of the side chain likely interferes with the binding of Fidaxomicin to the RNA polymerase. Mutations at position 1143 in *rpoB* come with strong negative side effects, namely reductions in growth rate, sporulation, and toxin formation. We have verified the resistance and side effects of the *rpoB*<sub>V1143D</sub> in our lab strain *C. difficile* 630 $\Delta$ *erm*.

In a strain screening we identified a Fidaxomicin resistant *C. difficile* strain, Goe-91, isolated from a symptomatic patient who was treated with Fidaxomicin. The strain carried a *rpoB*<sub>V1143D</sub> mutation, but had no discernible growth rate reduction when compared to our lab strain *C. difficile* 630 $\Delta$ *erm*. This indicates that Goe-91 has a compensatory mechanism for the negative side effects of the *rpoB*<sub>V1143D</sub> mutation, which allow it to remain viable and infectious. Using the *C. difficile* 630 $\Delta$ *erm* *rpoB*<sub>V1143D</sub> strain, we performed an evolutionary experiment selecting for increases in growth rate under Fidaxomicin as selective agent. After a growth period of 16 to 20 days, the resulting three isolates which had a significant increase in growth rate were genome sequenced. Two strains had mutations in the RNA polymerase, proline 244 to threonine in *rpoB* and glutamate 768 to valine in *rpoC*. Both mutations likely change how the DNA is guided through the RNA polymerase holoenzyme, which could alleviate the negative effects caused by the *rpoB*<sub>V1143D</sub> mutation. As the original Goe-91 strain, as well as one of the three strains from the evolutionary experiment, had no additional mutations in the RNA polymerase, further compensatory mechanisms may exist. The time scale of the evolutionary experiment further fits into an extended pulsed Fida-

xomicin regimen, increasing the chance that Fidaxomicin resistant strains will become more common in the future.

Most *C. difficile* strains have an intact motility and chemotaxis operon, but the role of motility and chemotaxis of *C. difficile* was up to now not fully clear. In order to assess the motility of single cell bacteria on a statistically significant level without human intervention, *YSMR*, an open-source python program, was created in this work. It allows for the detection and tracking of several thousand objects on simple desktop PCs and the analysis of speed, percentage of motile cells, stop events, average direction of travel, displacement and run phase length on a population level.

Motile *C. difficile* cells in liquid media display a futile motility phenotype, rapidly moving back and forth in place without achieving displacement. When long chained molecules are added, such as polyvinylpyrrolidone or mucin, it instead performs long run phases, achieving displacement exceeding five cell lengths. When stopping, it inverts its direction of travel and proceeds in a reverse direction. *C. difficile* has no discernible difference in curvature during run phases regardless of heading, nor a preferred direction of travel. Its motility phenotype therefore does not fit any previously described, and we propose it forms a new phenotype which we termed run and turnaround. The adaptation of the motility system of *C. difficile* to a medium containing long chained or net like molecules is logical, as *C. difficile* must swim through the mucin layer which protects the epithelial cells.

When cysteine is added to the medium at a concentration of 5 mM, *C. difficile* strains with an intact chemotaxis system react with a slow-down during run phases resulting in a net decrease in displacement. A *C. difficile*  $\Delta cheY$  strain in contrast had no change in behaviour. The chemotaxis system in *C. difficile* therefore works different to that of other described bacteria. Instead of leading to a reorientation of the cell or change in mode of travel, it reduces the rate of rotation of the flagella without affecting the turnaround phases. Cysteine is exported at the membrane of the epithelial cells as part of the gastrointestinal redox system.

We propose a motility model for *C. difficile* in which cysteine serves as a positional indicator which leads to motility reduction and, as a consequence, to an accumulation of cells at their preferred ecological niche.

# Chapter 1

## Introduction

*C. difficile* was first described as a bacterium isolated from newborn infants in 1935. Ivan C. Hall and Elizabeth O'Toole analysed faecal matter of ten newborn infants from meconium, the earliest passed stool after birth, through to milk stool, during the first ten days after birth (Hall and O'Toole, 1935). With the aid of selective cultivation methods, strain selection, as well as various staining methods they tried to identify when bacteria start to colonise the intestine of the infants, as well as which bacteria can be isolated. Except for the first stool, which was at times perceived to be sterile, they cultivated strains from each specimen and obtained 18 different species in total. One of the species had not previously been described in literature: initially named *Bacillus difficilis*, it was cultivated from the stool of four infants as early as the second day after birth. It was classified as *Bacillus*, Latin for “little staff”, and named *difficilis*, Latin for “difficult, troublesome”, due to the difficulty the authors had in both its study and isolation. Hall and O'Toole described it as a Gram-positive rod-shaped anaerobe, with a visible ability to form spores (fig. 1.1). They could observe motility and were able to show flagella through staining (fig. 1.1). When tested on rabbits and guinea pigs through subcutaneous injection, each strain of *Bacillus difficilis* was highly pathogenic, usually leading to the death of the animal. Guinea pigs exhibited a wide array of symptoms, several of them neurological. Hall and O'Toole could not cultivate *Bacillus difficilis* from heart blood, lesions, or subcutaneous oedema of either rabbits or guinea pigs during autopsy. Due to their inability to recultivate *Bacillus difficilis*, the symptoms which affected several areas of the animals, as well as various clues in the autopsies of the animals, they predicted *Bacillus difficilis* would produce exotoxins.

*Bacillus difficilis* was later renamed to *Clostridium difficile* due to metabolic and phenotypical similarities to the *Clostridium* genus in the Clostridiaceae family. Genetic relationships based on 16s RNA sequencing necessitated another reclassification to the *Clostridioides* genus in the Peptostreptococcaceae family (Lawson *et al.*, 2016). The name *Clostridioides* is composed of *Clostridium* from Latin “a small spindle”, -oides from the Latin suffix “resembling, similar”. It is the type strain of the genus, which has one other member, *Clostridioides manganotii*, which has been isolated from the faecal matter of a timber rattlesnake (McLaughlin *et al.*, 2014).

*Clostridioides difficile* is the causative agent of *Clostridioides difficile* infection (CDI),

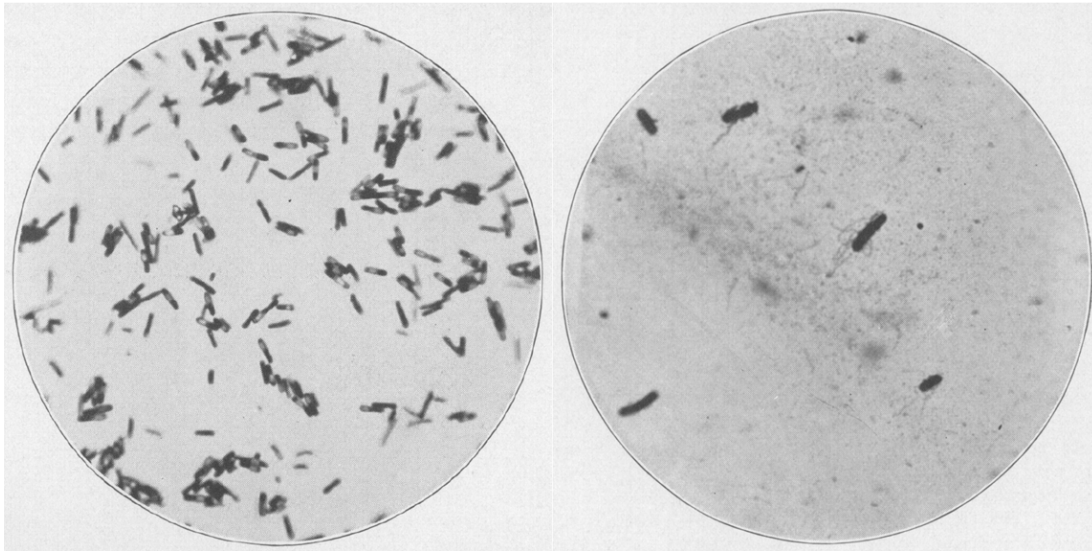


Figure 1.1: **Original microscopy pictures from Hall and O'Toole.** Left: Gram stained *C. difficile* smear from a 48 hour blood agar slant with visible endospores; 500 $\times$  magnification. Right: *C. difficile* from a 24 hour blood agar slant with Bailey's method stained flagella; 1000 $\times$  magnification (Hall and O'Toole, 1935).

a gastrointestinal infection. CDI is transmitted via the faecal-oral route through spores, as the obligate anaerobic *C. difficile* cannot survive in an oxygen rich environment. Spores of *C. difficile* from the infection herd in the gastrointestinal tract are continually shed with the stool of the host. From there they can be transmitted more directly, helped by insufficient hygiene measures, or indirectly, through environmental spreading, to other hosts. Due to their natural resilience, spores can persist in most environments.

## 1.1 *C. difficile* prevalence, infection & treatment

*C. difficile*, or rather its spores, could be found in various different environments. It has been detected in soil samples, manure, private residences, and it was isolated from wildlife animals, urban pests, livestock, as well as household pets (Al Saif and Brazier, 1996, Bandelj *et al.*, 2018, Dharmasena and Jiang, 2018, Himsforth *et al.*, 2014, Krijger *et al.*, 2019, Rothenburger *et al.*, 2018, Wei *et al.*, 2019). Worryingly, the prevalence in food is at around 4.1 % globally and 1.9 % in Europe (Rodriguez-Palacios *et al.*, 2020, Songer *et al.*, 2009). It is prevalent in waters, where it was found in sea water, swimming pools, and in 40-80 % of river samples. The isolated strains from rivers were mostly detected as transient; most likely rivers are contaminated with wastewater from colonised humans or animals (Al Saif and Brazier, 1996, Zidaric *et al.*, 2010).

The persistence of *C. difficile* spores is due to their resilience. Spores of *C. difficile*



are highly resistant towards various adverse environmental conditions and can remain viable through many usually employed hygiene measures. *C. difficile* spores have high resistance towards ethanol, ethanol-water mixtures in all ranges, as well as other solvents such as butanol and chloroform (Edwards *et al.*, 2016). Ethanol-water mixtures are common base ingredients of disinfectants and work by dehydration and denaturation of proteins. Heat stress at 85 °C for 20 min, even with wet spores, does not completely eradicate spores (Edwards *et al.*, 2016). Regular washing decreases spore loads on contaminated bed sheets by 40 % and can cross-contaminate other washed items (Tarrant *et al.*, 2018). A wide selection of sporicidal wipes designed for surface cleaning has been found to not work as required and some broke up spore aggregates, potentially spreading spores further (Siani *et al.*, 2011).

*C. difficile* spores can be made unviable by UV-C light, which has been used as a decontamination procedure for hospital rooms and medical devices (Wallace *et al.*, 2019). Hydrogen peroxide solutions are likewise sporicidal at concentrations > 0.003 %. (Edwards *et al.*, 2016). Aerosolic hydrogen peroxide treatment of hospital rooms has been tested, but is fraught with health and safety hazards (Steindl *et al.*, 2015).

A *C. difficile* biofilm is resistant against most hospital disinfectants, which are commonly based on chlorine, hydrogen peroxide, formaldehyde, ortho-phthalaldehyde, or quaternary ammonium compounds (Rashid *et al.*, 2020). Neither hydrogen peroxide nor UV-C is completely sporicidal against larger aggregates of organic matter and spores. A preceding mechanical cleaning therefore enhances effectiveness of any decontamination procedure. Regarding hand hygiene, rigorous hand washing using coarse soap offered the best reduction of cells and spores when compared to routine hand disinfection using alcohol rub (Oughton *et al.*, 2009).

A healthy gut microbiome offers protection towards colonisation by *C. difficile*. Metabolites commonly produced by commensalist bacteria have been correlated with a negative impact on *C. difficile* (Weingarden *et al.*, 2016). The strongest inhibitory compounds produced by commensalist bacteria are the secondary bile acids deoxycholate and lithocholate. Presence of bacteria carrying genes for the production of these secondary bile acids correlates with resistance towards *C. difficile* colonisation (Buffie *et al.*, 2015, Theriot *et al.*, 2016). *C. difficile* reacts to non-lethal bile acid shock stress with an increase in expression of chaperones and cell wall binding proteins as well as proteins involved in cell division, whereas long term bile acid stress induces a more varied response depending on the bile acid. *C. difficile* grown in long term bile acid stress with lithocholate, and to some extent with deoxycholate, have a dramatic

decrease in FliC expression. FliC is the main building block of the flagellum. Transmission electron micrographs of cells show a decrease in flagella under deoxycholate and next to no flagella under lithocholate (Sievers *et al.*, 2019). The microbiome further protects from *C. difficile* infection by out-competing *C. difficile* for nutrient resources, effectively starving the pathogen (Sorg *et al.*, 2018).

A strong risk factor for infection with *C. difficile* is a preceding course of antibiotics (Drózdź *et al.*, 2018, Lee *et al.*, 2019, Teng *et al.*, 2019). Antibiotics reaching the gastrointestinal tract change the gut microbiome and metabolome. Depending on the antibiotic, different bacterial groups can be impacted (Antunes *et al.*, 2011, De Gunzburg *et al.*, 2018, Palleja *et al.*, 2018, Theriot *et al.*, 2016, Young and Schmidt, 2004). The effect of antibiotics on the microbiome cumulates over various stages: the initial affected organisms decrease during the course of treatment with antibiotics. The total amount of bacteria decreases, which can be measured as a loss in total amount of detectable bacterial DNA. Organisms resistant to the antibiotic increase in relative abundance. After the course of antibiotics, organisms with higher growth rates can re-colonise faster. Likewise, sporulating organisms re-emerge from their hibernating status and can directly recolonise. Lost organisms have to re-enter the gut. The impact on the microbiome is therefore complex and long lasting (Burdet *et al.*, 2019, Palleja *et al.*, 2018, Xu *et al.*, 2020).

Antibiotics associated diarrhoea (AAD) can further decrease the total amount of bacteria in the gut (Young and Schmidt, 2004). Antibiotics-associated diarrhoea is a possible side effect during a course of antibiotics which occurs in total in around 4.9 % of antibiotic courses. The frequency is dependent on length of treatment and choice of antibiotic, with courses of three or fewer days at a significantly lower risk for AAD (Wiström *et al.*, 2001). In at least 20 % of cases, Antibiotic associated diarrhoea in a hospital setting are caused by *C. difficile* (Nasiri *et al.*, 2018).

Recommended treatment for a first occurrence of non-severe CDI is currently an antibiotics course of either Vancomycin, Metronidazole, or Fidaxomicin. In addition, the Rifampicin derivative Rifaximin was also previously suggested as a treatment option (Johnson *et al.*, 2007). Resistances against Rifampicin also confer resistance to Rifaximin (O'Connor *et al.*, 2008). Resistance rates against Rifampicin for *C. difficile* are at 11.8 % in Europe (Freeman *et al.*, 2020). In mild cases stopping an on-going antibiotic treatment and observation is an option if possible. In severe cases of CDI, Vancomycin or Fidaxomicin is recommended. First recurrence of CDI is treated primarily with Vancomycin, or optionally with Fidaxomicin. In cases of multiple recurrent CDI Fi-

daxomicin is recommended or optionally vancomycin followed by tapered or pulsed vancomycin. For recurrent CDI, Faecal Microbiota Transplant (FMT) is recommended in addition to antibiotic courses (Ooijevaar *et al.*, 2018). FMT is aimed at restoring a protective gut microbiome and offers good prospects but faces regulatory issues (Keller *et al.*, 2019, Rohlke and Stollman, 2012).

Antibiotics must act as either strong growth inhibitor (bacteriostatic agent) or have a lethal effect on to the targeted organism (germicide), but have negligible or ideally no negative effects on the host (McDonnell and Russell, 1999). Targets for antibiotics are therefore usually distinct features of the organism which are not present or sufficiently different in the host. Commonly affected areas of antibiotics against bacteria can be subdivided into targets in areas of cell wall synthesis, protein synthesis, and nucleic acid synthesis. Within the nucleic acid synthesis pathway, common targets include the folate synthesis pathway, the DNA gyrase, and the RNA polymerase (Kapoor *et al.*, 2017).

The antibiotic Fidaxomicin targets the RNA polymerase. It ultimately stops the RNA polymerase from transcribing from a DNA template to the messenger RNA (mRNA). Without mRNA, cells are unable to form new proteins, which is lethal. In order to transcribe mRNA from a template, bacterial RNA polymerases recognise and bind to a promoter region in DNA which signifies the start of a transcribed RNA sequence. For this interaction, two regions in front of the code sequence are important; one is roughly ten base pairs before the start codon (the -10 promoter region), the other 35 (the -35 promoter region). When these regions are bound, the polymerase converts to the closed complex. In the closed complex the double stranded DNA is melted into two single strands, and transcription from the template strand begins. Fidaxomicin binds to the  $\beta$ - and  $\beta'$ -subunit of the RNA polymerase (Lin *et al.*, 2018). RNA polymerases which have bound Fidaxomicin can no longer switch from the open complex to the closed complex. The polymerase can therefore no longer interact with the -35 and -10 region simultaneously, which prohibits transcription initiation. The area in which Fidaxomicin binds is a proposed site with which specific RNA loops interact. These loops act as pause-inducing or transcription terminating signals. Fidaxomicin has a less pronounced effect on the microbiome than other antibiotics (Ajami *et al.*, 2018, Theriot *et al.*, 2014). Its, in comparison to other antibiotics, narrower effect on the microbiome is a primary feature which is thought to help prevent recurrent CDI. Recurrent infection after treatment with Fidaxomicin has been linked to new strain colonisation rather than a recurrence with the same strain (Eyre *et al.*, 2014).

Antibiotics act as natural selection pressures for increased tolerance against themselves. Any bacterium with tolerance or resistance can out-compete strains affected by the antibiotic. In the comparatively nutrient rich environment of the human gut, resistant strains have therefore an immediate growth advantage (Palleja *et al.*, 2018, Xu *et al.*, 2020). Therefore, the selective pressure on bacteria for evolved resistance is great. During a course of antibiotics, the relative abundance of resistant bacteria increases, which could be an arising issue as the likelihood of horizontal transfer of resistance genes between different species increases (Xu *et al.*, 2020).

Resistance against antibiotics can be mediated by stopping the antibiotic reaching its target, for example through exporter systems which transport the antibiotic out of the cell faster than it can be imported. Resistance can also be mediated by changing the target region of the antibiotic, preventing interaction. Differences in target sites which negatively impact interaction can be achieved via single mutations. Another resistance mechanism is the inactivation of the antibiotic by producing, and in some cases exporting, degrading enzymes. Both degradation and exporter systems can sometimes be overcome by increasing the antibiotic dosage (Munita and Arias, 2016). Smaller resistance effects achieved during low-level antibiotic exposure can cumulatively confer a strong resistance towards an antibiotic (Wistrand-Yuen *et al.*, 2018). Some resistance effects prohibit the simultaneous resistance towards other antibiotics, as the resistance mediators are mutually exclusive or lethal in combination. Finding such combinatory antibiotic treatments is an important research question (Suzuki *et al.*, 2017).

Evolved resistance towards Fidaxomicin in *C. difficile* under laboratory conditions as well as from patient isolates was often mediated through a single mutation of the valine at position 1143 in the  $\beta$ -subunit of the RNA polymerase (Goldstein *et al.*, 2011, Kuehne *et al.*, 2017). The highest resistance (MIC > 64 mg/L) is achieved via a mutation from the 1143 valine to aspartate (Kuehne *et al.*, 2017, Schwanbeck *et al.*, 2019). The hydrophobic, nonpolar side chain of valine is exchanged for the hydrophilic, negatively charged side chain of aspartate. The change in side chain most likely interferes with the binding of fidaxomicin to its target location. Other mutations conferring higher tolerance at the 1143 position are Glycine (MIC 8-16 mg/L), and phenylalanine (MIC 2 mg/L), which differ from valine in their steric properties. Further mutations conferring low tolerances towards Fidaxomicin have been found in either the  $\beta$ - or  $\beta'$ -subunits of the RNA polymerase (Babakhani *et al.*, 2014, Leeds *et al.*, 2014, Seddon *et al.*, 2011). One strain with a tolerance of 1 mg/L had no mutations within the RNA polymerase but a frame shift within the gene CD22120, a MarR homologue

(Leeds *et al.*, 2014). MarR is a repressor to the multiple antibiotic resistance locus found in enteric bacteria, which acts by modulating efflux pump and porin expression in *E. coli* (Seoane and Levy, 1995, Sharma *et al.*, 2017).

Even though tolerances have been generated under laboratory conditions, actual concentration of Fidaxomicin employed during treatment can be far higher. One study showed Fidaxomicin concentrations of  $> 1$  mg/g in stool (Sears *et al.*, 2012). Additionally, Fidaxomicin has been shown to attach to spores, which would expose newly germinating *C. difficile* cells to high local concentrations of Fidaxomicin (Chilton *et al.*, 2016).

*C. difficile* infection (CDI) is subdivided into community-onset CDI and hospital-associated CDI. Community-onset CDI is acquired outside a healthcare-facility in which the patient presents with CDI symptoms during admission. Hospital-associated CDI develops during hospitalisation and is often associated with a preceding course of broad-spectrum antibiotics. Colonisation and subsequent infection with *C. difficile* begin with the spores entering the gastro-intestinal tract. Dormant spores traverse the stomach and, upon interaction with germinants, start to degrade their cortex layer. The cortex layer consists of a thick layer of modified peptidoglycan protecting the spores against environmental stresses. The main germinants are the primary bile acids taurocholic acid and cholate, produced by the gall bladder, which are recognised by the spore through the CspC receptor. Various amino acids and calcium ions act as co-germinants, which further increase the germination rate (Howerton *et al.*, 2011, Rohlfing *et al.*, 2019, Shrestha and Sorg, 2017, Sorg and Sonenshein, 2008). The pH value is also involved in controlling germination rates (Wetzel and McBride, 2019). Due to the concentrations of germinants and pH, spores likely start to reactivate between the duodenum and jejunum (Buffie *et al.*, 2015, Sorg and Sonenshein, 2008). *C. difficile* cells become vegetative in a nearly anaerobic environment, at luminal partial O<sub>2</sub> pressure of  $< 0.13 - 1.5$  kPa ( $< 1 - 11$  mmHg), which is less than 10 % the concentration of O<sub>2</sub> in air at sea level (Albenberg *et al.*, 2014, Zheng *et al.*, 2015). *C. difficile* would therefore become viable shortly before the areas most affected by histological changes, the caecum and colon (Koenigsnecht *et al.*, 2015).

An infection with *C. difficile*, when symptomatic, can present as diarrhoea in the form of watery, loose stool, fever, nausea, and abdominal pain. *C. difficile* colonises the colon and releases exotoxins, as predicted by Hall and O'Toole, which damage the enterocytes, the upper cell layer lining the small and large intestine (Debast *et al.*, 2014, Hall and O'Toole, 1935, Ng *et al.*, 2010). This damage can lead to diarrhoea and

inflammation, accompanied by nausea and abdominal pain. Possible complications include pseudomembranous colitis, in which necrotic enterocytes, fibrin, mucous and leukocytes form a membrane-like layer on the inflamed colon. Damage to the epithelial cells can cause a perforation of the colon, which in turn can lead to sepsis. A further possible complication is toxic mega-colon, in which loss of the mucosal barrier leads to damage and paralysis of the smooth muscles in the colon. This in turn prevents the function of the colon which can result in faecal stasis, a life threatening condition (Debast *et al.*, 2014, Ooijselaar *et al.*, 2018).

*C. difficile* strains can express up to three different toxins, Toxin A (TcdA), Toxin B (TcdB), and the binary *C. difficile* transferase toxin (CDT). All three ultimately cause cells to lose their cytoskeletal integrity, which can lead to apoptosis or cell lysis. CDT enters the cell via lipolysis-stimulated lipoprotein receptor (Hemmasi *et al.*, 2015). It ribosylates actin, which stops actin from polymerisation (Aktories *et al.*, 2018, Schwan *et al.*, 2014). The Microtubules of eukaryotic cells use the actin filament as boundaries: without an actin filament, microtubules do not stop growing and can rupture the cell membrane, causing cell lysis. For cell invasion, Toxin A uses sucrose-isomaltase and the glycoprotein 96 as receptor, Toxin B uses chondroitin sulphate proteoglycan 4 and the poliovirus receptor-like 3. Toxins A and B, after import through cell receptors and escape of the N-terminal glucosyltransferase from endosomes, inactivate GTP-binding proteins of the Rho family. Rho-GTPases are regulatory proteins of the actin cytoskeleton and of tight and adherent junctions. Inactivation of Rho-GTPases through glucosylation by the toxins leads to the cytoskeletal disorganisation, cell rounding, increased epithelial permeability, and cell death. The cytotoxic effect of toxin A and B is associated with the activation of the inflammasome (Di Bella *et al.*, 2016, Ng *et al.*, 2010). *C. difficile* strains carrying either toxin A, toxin B, or both can be pathogenic whereas strains lacking all toxins appear to be apathogenic (Kuehne *et al.*, 2010). The virulence of *C. difficile* is further facilitated by lytic enzymes, such as collagenase, hyaluronidase, and chondroitin-sulfatase (Seddon *et al.*, 1990).

Other factors facilitating increased pathogenicity include adherence and motility. Within the gut, adherence is a critical step in colonisation and allows pathogens to overcome the natural displacement due to peristaltic movement. Non-adherent bacteria are continually displaced, which hinders their collective growth rate (McGuckin *et al.*, 2011). Adherence in *C. difficile* is in part mediated through the surface layer (S-layer). The S-layer consists in *C. difficile* of heterodimeric proteins, both of which are derived from the gene *slpA*, but may contain up to further 30 different proteins (Bradshaw *et al.*,

2018). The S-layer plays a role in attachment: the high molecular weight variation of SlpA can adhere to the epithelium lining (Calabi *et al.*, 2002, Merrigan *et al.*, 2013). Adherence can likely be further enhanced by the type IV pili, as cells lacking them are cleared from the intestine more quickly. Type IV pili knock-out mutants associated less with cecal mucosa than their parent strains (McKee *et al.*, 2018a).

## 1.2 Motility

As explained by Edward Mills Purcell in his 1976 lecture, the Reynolds number shows which effects are important for movement in any medium (Purcell, 1977). The Reynolds number, a dimensionless value, expresses whether the viscosity or the density play a larger role for movement through the medium. For smaller numbers viscosity takes precedent, for larger numbers density. The Reynolds number changes depending on the size of the object, as well as on the viscosity of the medium. At miniscule Reynolds numbers, viscosity becomes dominant and inertia irrelevant. For a perceivable change in Reynolds number, the difference between viscosity and density must be large. Simply doubling the viscosity of water, for example, is not sufficient for a change in human swimming behaviour (Gottfing and Cussler, 2004). In part due to viscosity, a human can swim through water but would suffocate when attempting to swim in molasses (Jabr, 2013). Besides viscosity, the Reynolds number depends on the size of the object. To take Purcell's example, the Reynolds number is  $10^4$  for a human in water. For a guppy, however, it would be closer to  $10^2$ . For bacteria in water, the Reynolds number is around  $10^{-4}$  to  $10^{-5}$ . At such low Reynolds numbers, inertia is next to irrelevant and only currently active forces determine a change in position. This in turn determines the usable propulsion mechanisms. Bacteria need to exert a constant force to stay in motion, yet this force cannot be time-reversible, such as the slow opening and rapid closure of a clam. Thus, bacterial flagella follow a screw like rotary motion which fulfils these requirements.

Motility in bacteria allows the exploration of a habitat, forming a trade-off with the ability to grow faster in-place. Faster migration allows a species to reach and occupy a habitat before another slower moving species can move in. Focusing on growth rate, on the other hand, allows a species to dominate its immediate surroundings. The outperformance and extinction of a less optimised organism is not the only possible outcome in such a scenario. Depending on the growth rate and migration speed, several species can inhabit the same niche within a system and coexist due to their different migration and growth properties. Taxa better at dispersing are locally outcompeted

for nutrients by faster growing ones, however, can reach and occupy other areas faster (Gude *et al.*, 2020). In an evolution experiment, starting from a single progenitor strain, a stable community of three descendant strains with differing growth rate and motility properties could be established. Each of the strains dominated a specific area on a plate but was outcompeted in others, even though initially, all cells started from the same space (Liu *et al.*, 2019). Motility therefore is an influential factor for the choice of bacterial habitat and niche, as well as for community establishment.

The mucin layer in the intestine forms a challenging medium for motility of bacteria. It consists of both attached and free, long chained, and reversibly linked mucins. The inner mucus layer in the colon is in the range 50-100  $\mu\text{m}$  for mice and rats and likely longer for humans. The unbound mucins can reach several micrometres (Johansson *et al.*, 2011, Lai *et al.*, 2009). As both a barrier to pathogens and gate for nutrients, it must be able to selectively pass particles. At sizes below 55 nm the diffusion rate is close to that of water, which allows free passage of most nutrients. Between 55 and 500 nm the viscosity shifts mainly due to the inter-fibre spacing, which causes steric hindrances (Lai *et al.*, 2007, Olmsted *et al.*, 2001). Interestingly, surface modification in particles plays a large role, as polyethylene glycol-coated particles of up to 500 nm can diffuse relatively fast. Presumably the charge of the coating and its interaction with the charged mucin strands is responsible for this effect. For both polyethylene glycol as well as viruses shown to quickly diffuse, the surface charge is net neutral and hydrophilic (Lai *et al.*, 2007, Olmsted *et al.*, 2001). Pathogenic bacteria which need to attach to the epithelial layer, such as *C. difficile*, must traverse the mucin layer despite these hindrances.

Bacterial cell shape is determined by a trade-off between three aspects: cell elongation, swimming efficiency, and construction cost (Schuech *et al.*, 2019). Longer cells have an advantage in chemotactile behaviour, as Brownian rotation has a lesser impact on cell orientation during straight runs. This in turn increases the signal to noise ratio for the cell. Spherical cells are the most cost efficient cell shape to build. *In silico* models show curvature increases swimming efficiency, though likely not enough to explain the building costs. Curvature may therefore offer habitat specific advantages. It has been implicated in preventing slippage in viscous media, higher minimal immobilising viscosity limits, better persistence under flow, and resistance to expulsion by peristalsis in the gastrointestinal tract (Taylor *et al.*, 2019). Both cell curvature and elongation increase construction costs, meaning that bacteria must optimise between the three properties. Given the three aspects, most bacteria are pareto-optimal.



Besides for attachment, bacteria can use pili for movement. Pili can facilitate motility by attaching to an object and pulling the bacterium and the anchor point together by retraction of the pilus in an ATP dependent manner. In the case of *Neisseria gonorrhoeae*, this happens at a speed of  $\sim 1 \mu\text{m/s}$ , whereas *Clostridium perfringens* has a median speed of 23.6 nm/s. The term for pili facilitated movement depends on the form of movement. When bacteria proceed in short bursts it is called “twitching motility”, whereas a surface mediated, jerk-free variety is sometimes incorrectly termed “gliding motility” (Chlebek *et al.*, 2019, Merz *et al.*, 2000, Varga *et al.*, 2006). In general, gliding motility is understood as a form of surface mediated motility which does not involve either pili or flagella (Kearns, 2010). Gliding motility is facilitated in *Myxococcus xanthus* through externally rotating proteins anchoring the cell to a surface. Mediated by the Glt complex, this is used for an intricate and social form of movement which enables the colony to move in ripples. In *M. xanthus* it is further involved in the formation of complex fruiting bodies (Luciano *et al.*, 2011).

In *C. difficile*, Type IV pili have been shown to increase attachment to cells, as well as playing a role in persistence and virulence in an animal model (McKee *et al.*, 2018a). The PilJ of *C. difficile*, the protein which constitutes the stem of a pilus, appears to have a unique structure compared to other Type IV pilins. Its exact function during infection and whether it can facilitate motility in *C. difficile* is currently unknown (Piepenbrink *et al.*, 2014).

A general form of social movement is categorised as swarming motility. This cooperative movement is necessitated when the surrounding medium does not contain enough water or surface friction is too high. To enable movement along terrain impassable for single cells, some bacterial strains can form rafts. The connection within the raft is supported by flagellar bundles between different bacteria. Some species can additionally form surfactants, which aid movement over the surface by forming a thin layer over which the rafts can glide (Kearns, 2010, Partridge and Harshey, 2013). A conserved feature in strains which perform swarming motility is the suppression of tumbling events. Increasing the length of run phases leads to longer association times between different cells which aids in maintaining the rafts (Partridge *et al.*, 2020).

The flagellum is a complex supramolecular structure which, in Gram-negative bacteria, generally consists of 36 different proteins, 28 of which have been identified or characterised in *C. difficile* (Kanehisa, Morimoto and Minamino, 2014, Stevenson *et al.*, 2015). The flagellum can broadly be divided into a rotary motor assembly, a type III secretion system, a hook acting as joint, and a helical filament. The rotary motor

assembly is anchored to the peptidoglycan layer via a stator. With an electrochemical potential across the membrane it uses the flow of the gradient to generate torque which can turn the flagellum in either direction (Morimoto and Minamino, 2014). The hook connects the basal body with the filament and acts as universal joint. The curvature during unidirectional rotation is maintained by shortening the distance between subunits along the inner curvature (Mukherjee and Kearns, 2014, Samatey *et al.*, 2004).

Each filament consists of FliC, the flagellin protein. The flagellum, in *E. coli*, is elongated through a proton-motif force (PMF) driven ejection-diffusion mechanism through the type III secretion system (Renault *et al.*, 2017). The PMF is used to transport flagellin proteins through the hook assembly, whereupon they self-assemble at the end of the flagellum. The rate of growth of the filament is inversely correlated with the length of the flagellum, with faster growth rates for shorter flagella. The filament is connected to the hook assembly through a single layer of FlgK on the hook side and FlgL on the filament side, which act as a binding intermediary (Stevenson *et al.*, 2015). The cap of the filament is formed by a pentamer of FliD, which acts as a plug stopping further FliC export through the filament.

The cap structure of *C. difficile* has been shown do bind to the mouse caecum (Tasteyre *et al.*, 2001). When assessing the role of flagellar importance for inflammation, *C. difficile* strains with functional flagella had a stronger response than those without. Interestingly, mutant strains with present but non-functional flagella elicited the same inflammatory response as their wild type counterparts (Batah *et al.*, 2017).

Directed motility in bacteria was first described in 1882 by Theodor Wilhelm Engelmann who studied the influence of different light wavelengths on plants (Engelmann, 1882). He noted that bacteria would accumulate in areas illuminated by red light, which he took to be a good indicator for the oxygen production by chlorophyll. In 1884, Wilhelm Pfeffer studied how bacteria react to the presence of meat extract and dismembered fly legs. The bacteria appeared to move towards and accumulate on the meat and open wounds on the fly legs. He coined the term chemotaxis for this apparently gradient directed motility behaviour (Pfeffer, 1884). For bacteria to react to a sensation they need to be able to directly or indirectly perceive it. For detection of molecules in solution a signal needs to be detected and passed through at least one membrane and the cell wall. Depending on the starting concentration and rate of change, the signal must be amplified. The predicted receptor in *C. difficile* stems from a transmembrane signal transducer family termed the methyl-accepting chemotaxis protein (MCP). Homologues of MCP in other organisms act as trans-membrane

signal transducers spanning both the cell wall and cell membrane. They connect to trimers of dimers to form a sensory cluster region via a HAMP domain (Hall *et al.*, 2012). In most bacteria the receptors form sensory clusters at specific positions on the cell surface. Such clusters allow for a fast reaction to a signal from a known direction. The sensory patches are often located at a cell pole, likely due to easier formation, better chemotaxis performance, or better stability in curved membranes (Hall *et al.*, 2012, Sourjik and Armitage, 2010, Thiem *et al.*, 2007). As a protein class, MCPs can recognise a wide array of molecules. Interaction partners of the MCP are determined by the structure of its binding domain, though the range of interaction partners of a MCP can be extended by adding further adaptor proteins. According to homology, the interaction of the MCP with its target in *C. difficile* likely takes place in a four alpha helix domain (Matilla and Krell, 2017). Upon interaction, the last helix physically shifts. This shift is translated along the MCP into the cell, which further transduces the chemotaxis signalling pathway (Ottemann, 1999). The signal is then transferred to CheA, which needs the activator protein CheD for its kinase activity. The activated CheA phosphorylates CheY, which can diffuse freely through the cell and acts as secondary messenger. It is recognised by the flagellum, which in turn can initiate motility (Sarkar *et al.*, 2010).

The signal cascade needs to be regulatable. If cells would act upon each activation of the receptor equally, they would be unable to detect changes in a gradient and not be able to target the desired source. As soon as the activation threshold would be reached, movement would be initiated without regard for the direction. Chemotaxis therefore requires a form of short term memory. Bacteria achieve this through several regulatory mechanisms which increase or decrease the net sensitivity to the signal. The MCP itself is methylated, which changes its ability to transmit the signal. The methylation is carried out by CheR and CheB, two methyltransferases. The position of the methyl groups in relation to each other are responsible for signal adaptation (Zimmer *et al.*, 2000). Differences in methylation status changes the necessary signal strength for activation of CheA. The concentration of phosphorylated CheY (CheY-p), further downstream, is self-regulatory and is bound by the phosphatase CheC. The CheC-CheY-p complex is then able to compete with the kinase CheA for its activator CheD in a negative feedback-loop. CheC's phosphatase activity increases when bound by CheD. CheY-p is finally dephosphorylated by FliY, a phosphatase located at the flagellar C-ring. Interaction of CheY-p with the flagellum influences turning direction of the filament. In both *Escherichia coli* and *Bacillus subtilis* counterclockwise rotation

of the flagellum leads to a run and clockwise rotation leads to reorienting tumbling behaviour (Cluzel *et al.*, 2000, Parkinson *et al.*, 1983). The interaction between CheY-p and the flagellum does not have a uniform effect across different bacteria. In *B. subtilis*, interaction causes the flagellum to rotate clockwise, leading to a reorientation. In *E. coli*, CheY-p interaction causes a run phase (Sarkar *et al.*, 2010).

For chemotaxis bacteria need to be able to perform a swimming pattern that allows them to search for the attractant. Various modes are known for this, though they generally can be divided into two phases, run and reorientation phase. In the run phase the bacterium swims along a path with little curvature. This allows it to follow along a gradient or reach a new area. Run phases are either signal dependent or intermittently interrupted by reorientation phases. If no or an undesired change in gradient is detected, the cell reorients itself and starts a new run phase. The two phases in consort allow for a stochastic search pattern which favours runs in the right direction. *E. coli* forms the model scenario as it switches between a “run” and “tumble” mode. During the run phase the flagella turn counter-clockwise and form a bundle which pushes the cell forward. The tumble phase is achieved by a short clockwise rotation of the flagella, which breaks the flagellar bundle and gives the cell a pulse in a new direction (Sarkar *et al.*, 2010). In *Vibrio alginolyticus*, which has a single flagellum, the forward motion of the run phase is followed by a shorter reverse swimming phase and a “flick”, which reorients the cell (Stocker, 2011, Xie *et al.*, 2011). The *Rhodobacter sphaeroides* flagellum is fixed in its rotational direction. Its run phase is interrupted by a “stop and coil” pattern, during which it is immobile and reoriented by Brownian motion (Armitage and Macnab, 1987). *Pseudomonas putida* has three distinct running modes mediated by a tuft of flagella on one cell pole. The flagellar tuft can push, pull, or wrap around the cell. Reorientation of the cell occurs during mode switches (Hintsche *et al.*, 2017).

## Part I

# Antibiotic Resistance in *Clostridioides difficile*

*But I would like to sound one note of warning. Penicillin is to all intents and purposes non-poisonous so there is no need to worry about giving an overdose and poisoning the patient. There may be a danger, though, in underdosage. It is not difficult to make microbes resistant to penicillin in the laboratory by exposing them to concentrations not sufficient to kill them, and the same thing has occasionally happened in the body. The time may come when penicillin can be bought by anyone in the shops. Then there is the danger that the ignorant man may easily underdose himself and by exposing his microbes to non-lethal quantities of the drug make them resistant.*

(Sir Alexander Fleming, 1945)



## Chapter 2

# Characterization of a clinical *Clostridioides difficile* isolate with markedly reduced fidaxomicin susceptibility and a V1143D mutation in *rpoB*

Authors: Julian Schwanbeck<sup>1</sup>, Thomas Riedel<sup>2,3</sup>, Friederike Laukien<sup>1</sup>, Isabel Schober<sup>2</sup>, Ines Oehmig<sup>1</sup>, Ortrud Zimmermann<sup>1</sup>, Jörg Overmann<sup>2,3</sup>, Uwe Groß<sup>1</sup>, Andreas E. Zautner<sup>1,4</sup>, Wolfgang Bohne<sup>1,4,5</sup>.

Author contributions: Conceptualization, Ortrud Zimmermann (OZ), Uwe Groß (UG), Andreas E. Zautner (AEZ), Wolfgang Bohne (WB); methodology, Thomas Riedel (TR), OZ, WB; software, TR; validation, Julian Schwanbeck (JS), Friederike Laukien (FL), Ines Oehmig (IO); formal analysis, JS, TR, FL; investigation, JS, TR, FL, IO; resources, Jörg Overmann (JO), UG, AEZ, WB, ; data curation, JS, TR, FL, OZ; writing-original draft preparation, JS, TR, AEZ, WB; writing-review and editing, JS, TR, JO, UG, AEZ, WB; visualization, JS; supervision, OZ, JO, UG, AEZ, WB; project administration, JO, UG, AEZ, WB; funding acquisition, JO, UG.

First sent to the Journal of Antimicrobial Chemotherapy on the 9th May 2018; returned on the 11th July 2018; revised on the 14th August 2018; accepted on the 23rd August 2018. DOI: 10.1093/jac/dky375 (Schwanbeck *et al.*, 2019).

## 2.1 Abstract

**Objectives:** The identification and characterization of clinical *Clostridioides difficile* isolates with a reduced fidaxomicin susceptibility.

**Methods:** Agar dilution assays were used to determine fidaxomicin minimum inhibitory concentrations (MICs). Genome sequence data were obtained by single-molecule real-time (SMRT) sequencing in addition to amplicon sequencing of *rpoB* and *rpoC*

---

<sup>1</sup>Institute for Medical Microbiology, University Medical Center, Göttingen, Germany

<sup>2</sup>Leibniz Institute DSMZ-German Collection of Microorganisms and Cell Cultures, Braunschweig, Germany

<sup>3</sup>German Center for Infection Research (DZIF), Partner Site Hannover–Braunschweig, Braunschweig, Germany

<sup>4</sup>Authors share senior authorship

<sup>5</sup>Corresponding Author. Tel.: 0049-551-395869, E-Mail: wbohne@gwdg.de

alleles. Allelic exchange was used to introduce the identified mutation into *C. difficile* 630 $\Delta$ *erm*. Replication rates, toxin A/B production and spore formation were determined from the strain with reduced fidaxomicin susceptibility.

Results: Out of 50 clinical *C. difficile* isolates, isolate Goe-91 revealed a markedly reduced fidaxomicin susceptibility (MIC >64 mg/L). A V1143D mutation was identified in *rpoB* of Goe-91. When introduced into *C. difficile* 630 $\Delta$ *erm*, this mutation decreased fidaxomicin susceptibility (MIC >64 mg/L), but was also associated with a reduced replication rate, low toxin A/B production and markedly reduced spore formation. In contrast, Goe-91, although also reduced in toxin production, showed normal growth rates and only moderately reduced spore formation capacities. This indicates, that the *rpoB*<sub>V1143D</sub> allele associated fitness defect is less pronounced in the clinical isolate.

Conclusions: This is the first description of a pathogenic clinical *C. difficile* isolate with markedly reduced fidaxomicin susceptibility. The lower than expected fitness burden of the resistance mediating *rpoB*<sub>V1143D</sub> allele might be an indication for compensatory mechanisms that take place during *in vivo* selection of mutants.

## 2.2 Introduction

Infections with *Clostridioides* (*Clostridium*) *difficile* are currently a leading cause for hospital-associated diarrhoea and membranous colitis worldwide (Leffler and Lamont, 2015, Lessa *et al.*, 2015). For severe or recurrent infections, treatment with fidaxomicin is advised, since it has a smaller impact on the microbiome than metronidazole and vancomycin, and recurrence is less likely (McDonald *et al.*, 2018). An additional advantage of fidaxomicin treatment is the low level of resistance observed for clinical *C. difficile* isolates up to now. Interestingly, lower fidaxomicin susceptibility develops easily *in vitro* after culturing laboratory strains with increasing fidaxomicin concentrations (Leeds, 2016). Fidaxomicin targets the RNA polymerase (Artsimovitch *et al.*, 2012, Lin *et al.*, 2018) and all artificially created strains with lower fidaxomicin susceptibilities had mutations either in the  $\beta$  or  $\beta'$  subunit of the RNA polymerase (*rpoB* and *rpoC*, respectively) (Goldstein *et al.*, 2011, Kuehne *et al.*, 2017). Most mutations occurred in the valine at position 1143 of *rpoB*: V1143D (>32 mg/L), V1143G (8 - 16 mg/L) and V1143F (2 mg/L) (Goldstein *et al.*, 2011, Kuehne *et al.*, 2017). However, these *rpoB* mutants were also shown to have severe fitness defects and this reduced fitness is believed to account for the low frequency with which these strains were isolated from clinical specimens (Kuehne *et al.*, 2017). In this study, to the best of our knowledge, we report the identification of the first clinical *C. difficile* isolate that possesses markedly



reduced fidaxomicin susceptibility with an MIC 64 mg/L and a V1143D mutation in *rpoB*. This isolate has lower-than-expected fitness costs.

## 2.3 Methods

### 2.3.1 *C. difficile* strains

We used the following *C. difficile* strains: *C. difficile* 630 $\Delta$ *erm* (DSM 28645, RT012, CP016318.1) (Dannheim *et al.*, 2017), Goe-91 (DSM 105001), *C. difficile* 630 $\Delta$ *erm* *rpoB*<sub>V1143D</sub> (this study), *C. difficile* DSM 29678 (RT014/020), *C. difficile* DSM 29744 (RT001/072), *C. difficile* R20291 (DSM 27147, RT027) and *C. difficile* 630 $\Delta$ *erm*  $\Delta$ *spo0A*.

### 2.3.2 Media and strain cultivation

*C. difficile* strains were grown at 37 °C in BHIS (37 g/L brain heart infusion broth with 5 g/L yeast extract and 0.3 g/L cysteine), with 15 g/L agar for plates or on Columbia agar with 5% sheep blood (COS, bioMérieux, Germany). For sporulation, chromID™ *C. difficile* agar plates (CDIF, bioMérieux) were used. Growth was always performed under anaerobic conditions using a COY anaerobic gas chamber (COY Laboratory Products, USA). The atmosphere used consisted of 85% N<sub>2</sub>, 10% H<sub>2</sub> and 5% CO<sub>2</sub>. For antibiotic susceptibility testing, 28 g/L Brucella broth supplemented with 5% defibrinated sheep blood, 5 mg/L haemin, 1 mg/L vitamin K1 and 15 g/L agar was used. For single-molecule real-time (SMRT) genome sequencing, strain Goe-91 was cultivated anaerobically in Wilkins-Chalgren Anaerobe Broth (Thermo Scientific, UK), followed by DNA extraction as described previously (Riedel *et al.*, 2015a,b).

### 2.3.3 Susceptibility testing

Susceptibility testing was performed as described by Schwalbe *et al.* (2007) by agar dilution methods, with slight modifications. Cultures were grown overnight in 4 mL of BHIS and diluted to an OD<sub>600</sub> of 0.1 in BHIS, from which 2  $\mu$ L was spotted on Brucella plates with log<sub>2</sub> fidaxomicin concentrations between 0.008 and 64 mg/L. A control without fidaxomicin was always performed. *Bacteroides fragilis* ATCC 25285 was used as the positive growth control. Plates were incubated overnight.

### 2.3.4 Amplification and sequencing of *rpoB* and *rpoC*

The *rpoB* and *rpoC* loci of Goe-91 were initially sequenced by amplification with primers JS001–JS010 (Table S1, available as Supplementary data at JAC Online<sup>6</sup>). The same primers were used for sequencing (Microsynth Seqlab, Germany).

### 2.3.5 SMRT sequencing of strain Goe-91 (DSM 105001)

The genome was sequenced on the PacBio RSII (Pacific Biosciences, Menlo Park, CA, USA) using P6 chemistry and one SMRT cell. Genome assembly was performed with the ‘RS\_HGAP\_Assembly.3’ protocol included in the SMRT Portal version 2.3.0, utilizing 75264 post-filtered reads with an average read length of 7578bp. The obtained chromosomal contig was trimmed, circularized and adjusted to *dnaA* as the first gene. Long-read genome quality was enhanced by using the ‘RS\_BridgeMapper.1’ protocol in SMRT Portal version 2.3.0. Further, a final genome sequence quality of QV60 was attained after mapping Nextseq Illumina reads with the Burrows–Wheeler Aligner (Li and Durbin, 2009, 2010) onto the genome sequence obtained by PacBio sequencing. The chromosomal sequence has been deposited at GenBank under accession number CP028361.

### 2.3.6 MLST

MLST was performed with WGS data from Goe-91 using [pubmlst.org/cdifficile/](http://pubmlst.org/cdifficile/) (Griffiths *et al.*, 2010) and revealed that strain Goe-91 belongs to MLST type 49 (ribotypes 007, 014, 025), which is grouped in clade 1 (Table S2<sup>6</sup>).

### 2.3.7 Measurement of toxin A/B production

Toxin production was assessed via Serazym ‘*Clostridioides difficile* Toxin A + B ELISA’ (Seramun, Germany). Bacteria grown on COS plates were resuspended in the supplied reagent buffer to an OD<sub>600</sub> of 0.05, 0.1 and 0.15; 100 µL of the suspension was processed as described by the manufacturer.

### 2.3.8 Sporulation assay

Sporulation assays were performed as described by Sachsenheimer *et al.* (2018), with slight modifications. Strains were inoculated into BHIS and incubated overnight; 4 mL

---

<sup>6</sup><https://academic.oup.com/jac/article-lookup/doi/10.1093/jac/dky375#supplementary-data>

of BHIS was inoculated with 40  $\mu$ L from this overnight culture and grown to an OD<sub>600</sub> of 0.2 - 0.4. A new 4 mL BHIS tube was inoculated with 40  $\mu$ L of this culture and incubated for: (i) 1 min; or (ii) 120 h. Cultures were split and one sample was incubated at 60 °C for 25 min to kill vegetative cells. The other sample was left untreated. Both samples were spotted on CDIF plates in 10<sup>0</sup> to 10<sup>6</sup> dilution steps.

### 2.3.9 Growth curves

From a BHIS overnight culture, 4 mL of BHIS was inoculated to an OD<sub>600</sub> of 0.05 in Hungate tubes (Macy *et al.*, 1972). OD<sub>600</sub> was measured in a NanoColor<sup>R</sup> VisII spectrophotometer (Macherey–Nagel, Düren, Germany).

## 2.4 Results and discussion

We determined the susceptibility to fidaxomicin for 50 *C. difficile* isolates that were obtained from patients with severe CDI by agar dilution assay. One isolate, named as Goe–91, showed markedly reduced susceptibility (MIC 64 mg/L). This MIC is considerably higher than the MIC of 16 mg/L determined for previously isolated clinical isolates with reduced fidaxomicin susceptibility (Eyre *et al.*, 2014, Goldstein *et al.*, 2011).

The *rpoB* and *rpoC* loci of Goe–91 were amplified by PCR and sequenced. A single T to A nucleotide polymorphism at base 3428 in *rpoB*, resulting in a V1143D mutation, was identified and later confirmed by SMRT sequencing data (accession number CP028361). In vitro studies identified the V1143D exchange as the mutation with the highest impact on fidaxomicin susceptibility (Kuehne *et al.*, 2017, Seddon *et al.*, 2011). The MICs of 32 - 64 mg/L reported for laboratory strains harbouring the *rpoB*<sub>V1143D</sub> allele correspond well to the MIC determined for Goe–91 (Kuehne *et al.*, 2017, Seddon *et al.*, 2011).

Since the *rpoB*<sub>V1143D</sub> allele was shown to be associated with a reduced replication rate in strain R20291 (Kuehne *et al.*, 2017), we analysed growth kinetics of Goe–91 in comparison with *C. difficile* R20291 and *C. difficile* DSM 29678. Both reference strains, like Goe–91, belong to phylogenomic clade 1. Surprisingly, Goe–91 displayed very similar growth characteristics to the reference strains with no indication of a reduced replication rate (fig. 2.1 A).

To analyse whether the previously observed fitness cost of the *rpoB*<sub>V1143D</sub> allele for the clade 2 strain R20291 might be restricted to this particular strain, we introduced

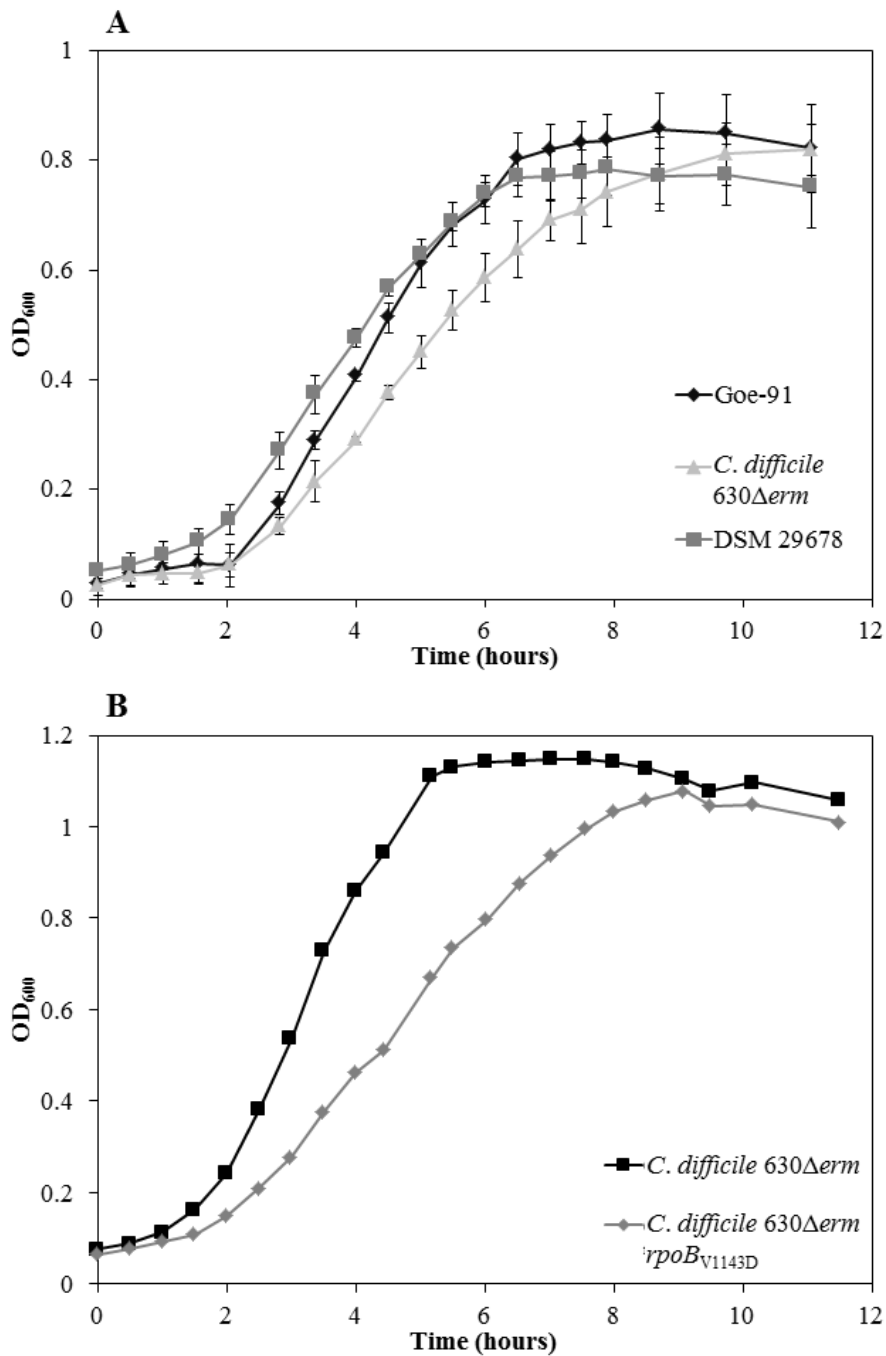


Figure 2.1: (a) Growth curve of strain Goe-91. For comparison, the clade 1 strains *C. difficile* 630Δerm and *C. difficile* DSM 29678 are included. Strains were inoculated to a starting OD<sub>600</sub> of 0.05. Error bars show the standard deviations (n = 3). (b) Growth curve of *C. difficile* 630Δerm *rpoB*<sub>V1143D</sub> in comparison with *C. difficile* 630Δerm. Strains were inoculated to a starting OD<sub>600</sub> of 0.05. The time to peak OD<sub>600</sub> value and the minimal generation time were substantially increased in the *rpoB*<sub>V1143D</sub> mutant.

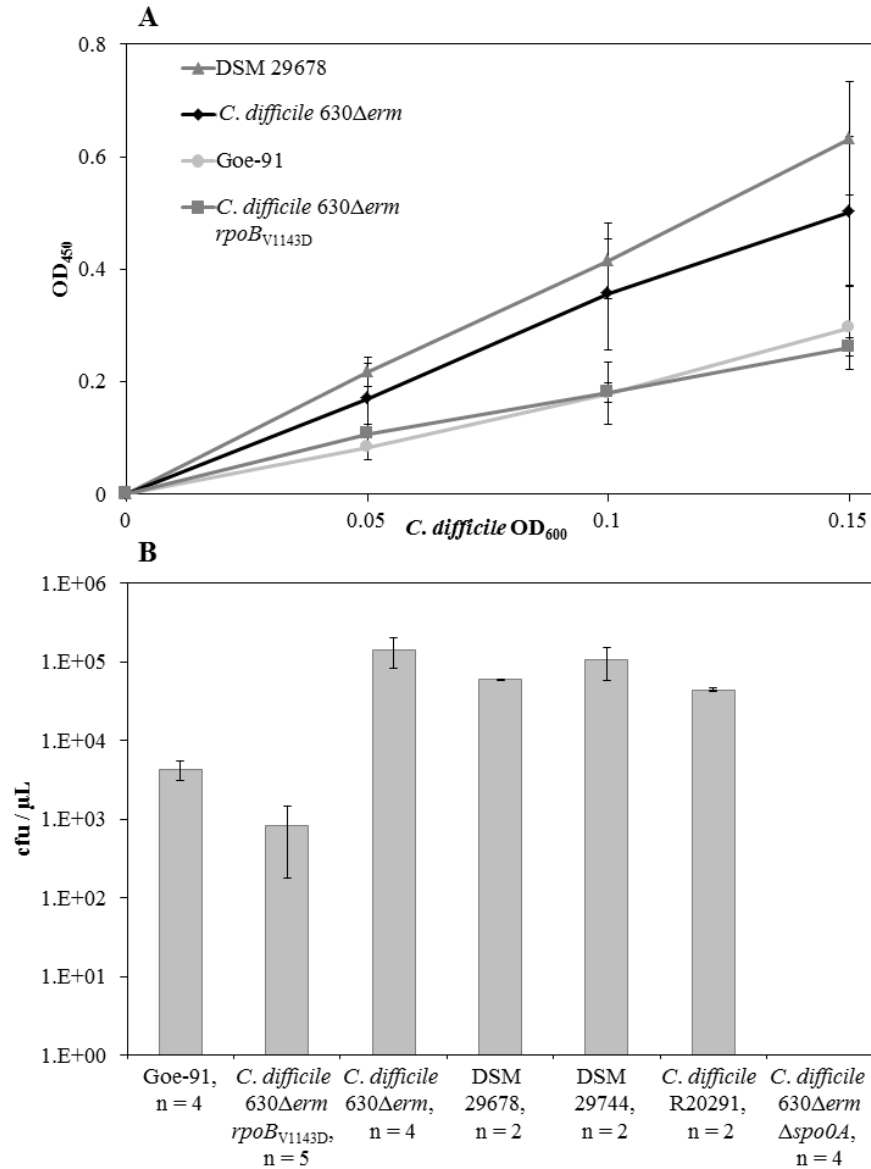


Figure 2.2: (a) Toxin A/B production. The toxin A/B ELISA was performed with three bacterial dilutions for each strain ( $OD_{600}$  of 0.05, 0.1 and 0.15) to demonstrate the linearity of the assay. Toxin A/B-producing strains *C. difficile* DSM 29678 and *C. difficile* 630Δ*erm* were used as positive controls. Error bars show the standard deviations from three biological replicates. (b) Sporulation assay. Spore formation was quantified after 1 min and after 120 h of incubation in BHIS. An aliquot was heat-shocked to kill off viable cells. Heat-shocked and untreated samples were plated in serial dilutions. Displayed are cfu/μL of the heat-shocked fraction after 120 h. The 1 min control sample contained <2 spores/μL. *C. difficile* 630Δ*erm* with a mutation in *spo0A* was used as a negative control. The clade 1 isolates *C. difficile* DSM 29678 and *C. difficile* DSM 29744 were used as positive controls.

this mutation into *C. difficile* R20291 by allelic exchange (see the Supplementary data available at JAC Online<sup>6</sup>). The obtained clones displayed reduced fidaxomicin susceptibilities with MICs 64 mg/L and showed a reduced replication rate (fig. 2.1 B), indicating that the *rpoB*<sub>V1143D</sub> allele associated fitness defect is a more general effect that can be observed for members of at least two different clades. The exact mechanism of how the V1143D mutation leads to the reduced fitness is unknown. However, Goe-91 appears to possess a genetic background that can compensate for the otherwise growth-reducing effect of the *rpoB*<sub>V1143D</sub> allele. At the present stage it is unclear whether this suitable genetic background was present before or after the V1143D mutation in *rpoB* occurred in Goe-91. A hypothetical scenario is that the *rpoB*<sub>V1143D</sub> allele first resulted in a reduced growth rate, but that compensatory mutations in unknown genomic loci occurred afterwards, which led to a partial restoration of the fitness defect.

The *rpoB*<sub>V1143D</sub> mutant in strain R20291 was also shown to have lessened toxin production and reduced sporulation (Kuehne *et al.*, 2017). This phenotype was confirmed for 630 $\Delta$ *erm* *rpoB*<sub>V1143D</sub>, which displayed reduced toxin A/B production and a 100-fold lower spore-formation capacity (fig. 2.2). Analysis of the Goe-91 genome sequence revealed a complete pathogenicity locus (PaLoc) containing *tcdR*, *tcdB*, *tcdE*, *tcdA* and *tcdC*, whereas *cdtA* and *cdtB* of the binary toxin are present as pseudogenes and are not functional. Goe-91 produced comparable toxin A/B levels to *C. difficile* R20291 *rpoB*<sub>V1143D</sub>, suggesting that toxin production might be impaired (fig. 2.2 A). The spore-forming capacity of Goe-91 was reduced by at least an order of magnitude when compared with the positive controls; however, to a lower extent than in *C. difficile* R20291 *rpoB*<sub>V1143D</sub> (fig. 2.2 B).

Taken together, our results reveal that the *rpoB*<sub>V1143D</sub> allele, which was formerly only generated under *in vitro* conditions, and which was believed to be associated with such a high fitness burden that it was expected to be unlikely to be competitive, is indeed occurring in a clinical isolate. At the present stage, we cannot make any judgement about the clinical relevance of the *rpoB*<sub>V1143D</sub> allele. EUCAST resistance breakpoints for fidaxomicin have not been established so far. It is known that faecal concentrations of fidaxomicin can reach high levels of >1 mg/g during *C. difficile* infection treatment (Sears *et al.*, 2012). Whether that is sufficient to efficiently suppress the replication of *C. difficile* harbouring the *rpoB*<sub>V1143D</sub> allele is unknown. The prevalence of clinical isolates with decreased fidaxomicin susceptibility is fortunately still low. However, the detection of an isolate with highly decreased fidaxomicin susceptibility that has lower-than-expected fitness defects is a finding that requires future monitoring.

## **2.5 Appendix**

### **2.5.1 Acknowledgements**

We thank Cathrin Spröer, Simone Severitt, Carola Berg and Carolin Pilke at the Leibniz Institute DSMZ for helpful advice and technical assistance.

### **2.5.2 Funding**

This work was funded by the Federal State of Lower Saxony, Niedersächsisches Vorab (VWZN2889/3215/3266).

### **2.5.3 Transparency declarations**

None to declare.

### **2.5.4 Supplementary data**

Supplementary data, including Tables S1 and S2, are available at JAC Online: <https://academic.oup.com/jac/article-lookup/doi/10.1093/jac/dky375#supplementary-data>.





## Chapter 3

# Rifaximin resistance of *Clostridioides difficile* is associated with *rpoB* alleles and MLST clades

Authors: Julian Schwanbeck<sup>1,7</sup>, Friederike Laukien<sup>1,7</sup>, Thomas Riedel<sup>2,3</sup>, Jörg Overmann<sup>2,3</sup>, Paul Cooper<sup>4</sup>, R. Lia Kusumawati<sup>5</sup>, Uwe Groß<sup>1</sup>, Wolfgang Bohne<sup>1</sup>, and Andreas E. Zautner<sup>1,6</sup>

In preparation for submission. Contributions: see subsection 3.7.1 on page 36.

### 3.1 Abstract

**Background:** Rifaximin (RFX) was recently proposed as an alternative therapy option for *Clostridioides difficile* infection. The aim of the study was to perform a survey regarding RFX-susceptibility in a *C. difficile* test cohort that was representative for five clinically relevant clades. At a MIC[RFX]  $\geq 32$   $\mu\text{g}/\text{mL}$  the *rpoB* gene was sequenced to determine the underlying resistance alleles.

**Methods:** Agar dilution assays were used to determine RFX MICs of 129 clinical *C. difficile* isolates from Germany (86), Indonesia (29) and Ghana (14). Genome sequence data were obtained in addition to amplicon sequencing of *rpoB* genes in order to deduce ribotypes and multi locus sequencing typing sequence types (MLST-ST).

**Results:** 10.1% of the isolates were found to be resistant against RFX. The resistance rate is distributed among the individual regions as follows: 4.7% for Germany, 27.6% for Indonesia, and 7.1% for Ghana. Three different *rpoB* alleles could be associated with RFX-resistance. One of them had not been described before. The presence of a specific *rpoB* allele correlates with the MLST clade of the isolate, i.e. the RFX-resistant isolates belonged to the MLST STs 1,2, and 4.

---

<sup>1</sup>Institute for Medical Microbiology, University Medical Center Göttingen, Göttingen, Germany

<sup>2</sup>Leibniz Institute DSMZ-German Collection of Microorganisms and Cell Cultures, Braunschweig, Germany

<sup>3</sup>German Center for Infection Research (DZIF), Partner Site Hannover–Braunschweig, Braunschweig, Germany

<sup>4</sup>St. Martin de Porres Hospital, Eikwe, W/R, Ghana

<sup>5</sup>Department of Microbiology, Faculty of Medicine, Universitas Sumatera Utara, Medan, Indonesia

<sup>6</sup>Correspondence: azautne@gwdg.de; Tel.: +49-(0)551-395927

<sup>7</sup>These authors contributed equally to this work.

**Conclusion:** A significant increased RFX-resistance rate, especially in Indonesian isolates, may be due to the use of rifampicin e.g. in the treatment of tuberculosis.

## 3.2 Introduction

*Clostridioides difficile*, a Gram-positive spore-forming bacterium, is the leading cause of nosocomial diarrhea worldwide and therefore a substantial burden to the healthcare systems (Abt *et al.*, 2016). The incidence of infections with *C. difficile* (CDI) has increased within the last years in Germany and other mainly western countries (Cassini *et al.*, 2016). Most of the CDI occur after antibiotic exposure and are the foremost cause of hospital-acquired diarrhea. Typical antibiotics that reduce the microbiome to such an extent that a CDI occurs are clindamycin, ampicillin, amoxicillin, cephalosporins, and fluoroquinolones (Brown *et al.*, 2013). After antibiotic exposure and in combination with risk factors CDI can lead to severe complications, like pseudomembrane colitis or toxic megacolon. Standard therapy includes the oral administration of vancomycin and metronidazole (Debast *et al.*, 2014). However, the relapse rate after these primary therapy schemes is up to 20%. Additionally vancomycin treatment, but also metronidazole treatment, has been demonstrated to select vancomycin resistant enterococci (VRE) and thus leads to a growing hygiene problem (Al-Nassir *et al.*, 2008).

Rifaximin (RFX), a derivate of rifampicin, was recently proposed as a possible alternative therapy option for *C. difficile* infection (CDI), especially in recurrent cases. In several studies RFX was described as a follow-up therapy after an unsuccessful vancomycin therapy (Johnson *et al.*, 2009, Major *et al.*, 2019). It is poorly absorbed in the gastrointestinal tract, making it suitable for non-systemic intra-intestinal use comparable to vancomycin (Huhulescu *et al.*, 2011). Like rifampicin, RFX acts as an inhibitor of the bacterial RNA polymerase and thus inhibits bacterial transcription (Campbell *et al.*, 2001, O'Connor *et al.*, 2008). RFX is licensed for the treatment of traveller's diarrhoea and hepatic encephalopathy in patients with liver cirrhosis in Germany, the UK and other European countries (Shayto *et al.*, 2016). In these countries the treatment of the CDI with RFX is therefore still an off-label use. Whereas in other countries, such as the USA, RFX is also used for the treatment of pseudomembrane colitis due to *C. difficile*, small bowel bacterial overgrowth, irritable bowel syndrome and diverticulitis (Shayto *et al.*, 2016). Promising treatment successes have already been observed in the treatment of recurrent CDI with RFX, but the use of RFX is not recommended in patients with previous exposure to any rifamycin due to the rapid development of resistance (Babakhani *et al.*, 2014, Curry *et al.*, 2009, Johnson *et al.*,

2007, 2009).

The aim of the study was to perform a survey regarding RFX susceptibility in a *C. difficile* test cohort that was representative for five clinically relevant clades out of eight established clades of this microbial species. For this purpose, 129 clinical *C. difficile* isolates from Germany, Indonesia and Ghana have been assessed using agar dilution susceptibility testing. At a MIC [RFX]  $\geq 32$   $\mu\text{g}/\text{mL}$  resistance of the isolate to RFX was assumed and the *rpoB* gene was sequenced to determine the underlying resistance alleles. All RFX-resistant isolates were whole genome sequenced to determine their phylogenetic relatedness.

### 3.3 Results

#### 3.3.1 Phenotypic rifaximin resistance testing of *C. difficile* isolates

Testing of the 129 *C. difficile* isolates determined an epidemiological cut-off of RFX at a maximum MIC of 0.5 mg/L. As a result, 116 isolates demonstrated an MIC[RFX]  $\leq 0.5$  mg/L. The group of RFX resistant isolates clearly separates with a MIC  $\geq 32$  mg/L. The number of isolates at each MIC was 3 at 0.5 mg/L, 16 at 0.25 mg/L; 15 at 0.125 mg/L, 4 at 0.064 mg/L, 17 at 0.032 mg/L, 42 at 0.016 mg/L, 19 at 0.008 mg/L; and finally, 13 isolates at an MIC[RFX]  $\geq 32$  mg/L (see fig. 3.1).

Accordingly, 89.92% (116/129) of the tested isolates are to be considered RFX susceptible and 10.08% (13/129) as RFX resistant. Looking at the RFX resistance rate separately for the three countries included in the study, 4.65% (4/86) of the isolates from Germany, 27.59% (8/29) of the isolates from Indonesia and 7.14% (1/14) of the isolates from Ghana were tested resistant to RFX (see table 3.1).

Table 3.1: **Total and RFX resistant number of strains per country.** 129 Strains were collected from screenings in Germany, Indonesia and Ghana.

Origin	No. of strains	RFX resistant (No.)	RFX resistant (%)
Germany	86	4	4.65
Indonesia	29	8	27.59
Ghana	14	1	7.14
Sum	129	13	10.08

Thus, a significantly ( $p < 0.05$ ) increased RFX resistance rate was observed for the Indonesian *C. difficile* isolates compared to the German isolates. There is also a clear difference in the RFX resistance rate between the Indonesian isolates and the Ghanaian isolates (27.59% vs. 7.14%), but not at a significant level ( $p = 0.07$ ) due to

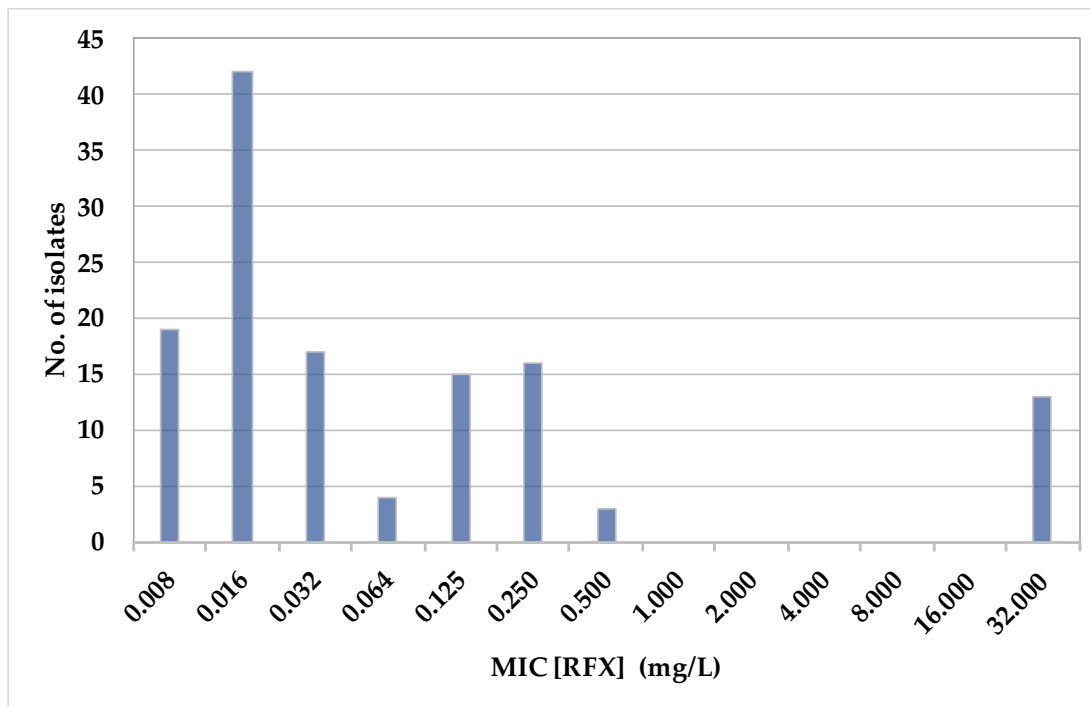


Figure 3.1: **Frequency distribution of MIC [RFX]**. The epidemiological cut off was determined at 0.5 mg/L, while RFX resistance was determined at an MIC  $\geq$  32 mg/L.

the relatively low number of *C. difficile* isolates from Ghana available to us.

### 3.3.2 *rpoB* sequence polymorphisms in RFX resistant *C. difficile* isolates

By sequencing the *rpoB* gene, three different *rpoB* alleles could be identified within the 13 RFX resistant strains (table 3.2). In the four isolates from Germany, only one *rpoB* allele was found, which, compared to the reference strain *C. difficile* 630 $\Delta$ *erm* (DSM 28645, CP016318.1), was characterized by the amino acid substitutions R505K, I548M, E1037Q, A1205V, N1207A, A1208T, and D1232E. The one RFX resistant isolate from Ghana, DSM 100002, is characterized by the amino acid substitutions H502N and R505K. Within the Indonesian RFX resistant strains, two isolates were also found that exhibited the amino acid substitution H502N and R505K. In six, and thus the majority of the Indonesian strains, a further additional amino acid substitution, I750M, was detected, which was not found in the German isolates and the Ghanaian isolate.

### 3.3.3 Epidemiological parameters associated with RFX resistance

Of the 13 *C. difficile* strains tested RFX resistant in this study, the complete genome was sequenced and from the resulting genome sequences MLST sequence type, clade

Table 3.2: Amino acid substitutions in the RpoB subunit of the RFX resistant tested *C. difficile* isolates compared to reference strain *C. difficile* 630 $\Delta$ *erm* (DSM 28645, CP016318.1).

Strain	MIC[RFX]	AA substitutions in RpoB
DSM 29628	$\geq 32.0$ $\mu\text{g}/\text{mL}$	H502N, R505K, I750M1
DSM 29630	$\geq 32.0$ $\mu\text{g}/\text{mL}$	H502N, R505K
DSM 29640	$\geq 32.0$ $\mu\text{g}/\text{mL}$	H502N, R505K
DSM 29646	$\geq 32.0$ $\mu\text{g}/\text{mL}$	H502N, R505K, I750M1
DSM 29648	$\geq 32.0$ $\mu\text{g}/\text{mL}$	H502N, R505K, I750M1
DSM 29695	$\geq 32.0$ $\mu\text{g}/\text{mL}$	H502N, R505K, I750M1
DSM 29696	$\geq 32.0$ $\mu\text{g}/\text{mL}$	H502N, R505K, I750M1
DSM 29697	$\geq 32.0$ $\mu\text{g}/\text{mL}$	H502N, R505K, I750M1
DSM 100002	$\geq 32.0$ $\mu\text{g}/\text{mL}$	H502N, R505K
DSM 28196	$\geq 32.0$ $\mu\text{g}/\text{mL}$	R505K, I548M, E1037Q, A1205V, N1207A, A1208T, D1232E
DSM 105800	$\geq 32.0$ $\mu\text{g}/\text{mL}$	R505K, I548M, E1037Q, A1205V, N1207A, A1208T, D1232E
DSM 105801	$\geq 32.0$ $\mu\text{g}/\text{mL}$	R505K, I548M, E1037Q, A1205V, N1207A, A1208T, D1232E
DSM 105802	$\geq 32.0$ $\mu\text{g}/\text{mL}$	R505K, I548M, E1037Q, A1205V, N1207A, A1208T, D1232E

and ribotype were derived. Additionally, the toxin gene presence was investigated (table 3.3). The RFX resistant *C. difficile* isolates collected in Germany belonged exclusively to MLST-ST 1 and thus to clade 2. Ribotyping of the 4 German isolates yielded the highly virulent ribotype 027, and as it is characteristic for this ribotype, both toxins A and B and the gene for the *C. difficile* binary toxin CDT were present. The only RFX resistant *C. difficile* isolate from Ghana is of MLST-ST 48 and therefore belongs in clade 1, has ribotype 084, but is atoxigenic. The highest biodiversity among the RFX resistant isolates is found among the Indonesian isolates. This subgroup includes 5 isolates that have MLST-ST 37 and thus belong to clade 4 and ribotype 017. These 5 isolates had only the Toxin B gene but were negative for Toxin A and CDT. Another clade 4 isolate shows ST 39 and ribotype 131 and was atoxigenic. In addition, two of the Indonesian isolates were clade 1 isolates. However, these belonged to different sequence types and ribotypes. One isolate belonged to ST 35 and ribotype 046 and was positive for the toxin genes A and B, whereas the second Indonesian clade 1 isolate that belonged to ST 15 and ribotype 010 was atoxigenic.

Looking at the RpoB alleles in relation to the clade grouping, a clear association between clade and RpoB allele is evident in our test cohort. All clade 1 isolates carry the amino acid substitutions H502N and R505K, all clade 2 isolates the amino acid

Table 3.3: Epidemiological parameters derived from the genome sequences of the RFX resistant *C. difficile* isolates

Strain	Origin	MLST-ST	RT	Clade	Toxins
DSM 29628	Indonesia	39	131	4	–
DSM 29630	Indonesia	35	046	1	AB
DSM 29640	Indonesia	15	010	1	–
DSM 29646	Indonesia	37	017	4	B
DSM 29648	Indonesia	37	017	4	B
DSM 29695	Indonesia	37	017	4	B
DSM 29696	Indonesia	37	017	4	B
DSM 29697	Indonesia	37	017	4	B
DSM 100002	Ghana	48	084	1	–
DSM 28196	Germany	1	027	2	AB CDT
DSM 105800	Germany	1	027	2	AB CDT
DSM 105801	Germany	1	027	2	AB CDT
DSM 105802	Germany	1	027	2	AB CDT

substitutions R505K, I548M, E1037Q, A1205V, N1207A, A1208T, and D1232E, and all clade 4 isolates the amino acid substitutions H502N, R505K, and I750M.

### 3.4 Discussion

One of the main findings from our study was the large difference in the RFX resistance rate between the Indonesian isolates of 27.59% compared to the German (4.65%) and Ghanaian (7.14%) *C. difficile* isolates. This increased RFX resistance rate among Indonesian isolates is mainly due to the high prevalence of RFX resistant isolates of ribotype 017. Of the 8 RFX resistant isolates from Indonesia, 5 were assigned to ribotype 017 (these 5 isolates were not copy strains). In a very recent East Asia-wide study by Lew and coworkers, it was shown that 67.7% of the ribotype 017 isolates were resistant for RFX (Lew *et al.*, 2020). Ribotype 017 is the most common *C. difficile* ribotype in Asia (Collins *et al.*, 2013), and according to Lew and colleagues, RFX resistance is very widespread in East Asia, including Indonesian *C. difficile* isolates of ribotype 017. The exception here were ribotype 017 isolates from Australia, Japan and Singapore in which RFX resistance is rather rare (Lew *et al.*, 2020). While we were able to detect RFX resistance in the ribotypes 010, 046, and 131 in Indonesia, Lew and colleagues occasionally detected RFX resistance in the ribotypes 002 and 018 (Lew *et al.*, 2020).

Pecava and colleagues have conducted a study with 348 *C. difficile* isolates from Austria, Slovenia and England in which Rifaximin resistance was also investigated (Pecavar *et al.*, 2012). In this study, 20.11% (70/348) of the examined *C. difficile*

isolates proved to be RFX resistant. However, this was not a representative resistance study, as it investigated a pre-selected isolate collection, using strains from a previous study by Huhulescu and coworkers. In this study on 898 Austrian patient isolates only 7.46% (67/898) were tested as RFX resistant (Huhulescu *et al.*, 2011). In our study, which is more representative of the clinical average in the sub-cohort of German *C. difficile* isolates and which to our knowledge is the first of this kind in Germany, we found a comparatively low RFX resistance rate of 4.65%. On the other hand, Reigadas and colleagues have conducted a study on phenotypic RFX resistance in Spain that examined 276 *C. difficile* isolates. There, 32.2% (89/276) of all isolates were tested RFX resistant, which is also significantly higher than we determined (Reigadas *et al.*, 2017). A similar study from the USA, conducted by Curry and colleagues, identified RFX resistance in 36.8% (173/470) of *C. difficile* isolates in a large American teaching hospital (Curry *et al.*, 2009).

Typically for central European and US-American *C. difficile* isolate collections, here, as well as in the studies of Pacavar *et al.*, O'Connor *et al.*, and Curry *et al.*, the majority of the RFX resistant isolates are classified as ribotype 027 (North American pulsed-field type 1 = NAP1) (Curry *et al.*, 2009, O'Connor *et al.*, 2008, Pecavar *et al.*, 2012). In contrast, the majority of RFX resistant isolates in Spain were classified as ribotype 001 (Reigadas *et al.*, 2017).

In the study of Pecava *et al.* 13, and in the study of Curry *et al.* 5 different *rpoB* alleles were associated with RFX resistance. R505K was the most frequent amino acid substitution in RpoB associated with RFX resistance (Curry *et al.*, 2009, Pecavar *et al.*, 2012). Also, in our study all RFX unsusceptible isolates showed the R505K amino acid substitution. In addition, some further amino acid substitutions were found in comparison to the reference strain allele. One of them, the amino acid substitution I750M in the Indonesian isolates of ribotype 017, was described here for the first time. It should be noted that these *rpoB* alleles are only associated with phenotypic RFX resistance while the exact mechanism of RFX resistance in *C. difficile* has not been fully elucidated, though antibiotic interaction with the  $\beta$ -subunit and the  $\gamma$ -subunit of bacterial RNA polymerase has been implicated (Campbell *et al.*, 2001).

In Ghana, we were able to find only a single RFX resistant isolate, which can be assigned to ribotype 084. Like the other clade 1 isolates of ribotype 010 and 046 cultivated in Indonesia, it carries the RpoB amino acid substitutions H502N and R505K. These amino acid substitutions have already been described earlier (Curry *et al.*, 2009), but the assignment to these somewhat rarer ribotypes has not yet been made before.

As Curry and colleagues have already shown on a small series of 8 patients, therapy with a rifamycin antibiotic, typically rifampicin, leads to a selection of RFX and rifampicin-resistant *C. difficile* strains (Curry *et al.*, 2009). This is very plausible since the underlying resistance mechanisms are identical (Campbell *et al.*, 2001). This was further confirmed by the fact that rifampicin and RFX MICs correspond to each other and thus RFX susceptibility can be derived from rifampicin susceptibility (O'Connor *et al.*, 2008, Reigadas *et al.*, 2017). Since Indonesia is one of the top three tuberculosis burden countries together with India and China (Kim *et al.*, 2020) and rifampicin remains a standard therapy for tuberculosis (Faust *et al.*, 2020), it seems only plausible that in East Asia and especially in Indonesia there are very high rates of RFX resistance in *C. difficile* isolates.

## 3.5 Materials and Methods

### 3.5.1 Patient samples and Isolate collection

A total of 129 clinical *C. difficile* isolates from Germany (86), Indonesia (29) and Ghana (14) have been selected in such a way that the test cohort represents the high genetic diversity, but also the clinically most relevant and prevalent five of the eight established clades of this microbial species. The isolates originate from two previously conducted studies at St. Martin de Porres Hospital in Eikwe, Ghana (Janssen *et al.*, 2016), at the Adam Malik Hospital and Pematang Siantar Hospital in Medan, Indonesia, the University Medical Center Göttingen, Germany, and the Asklepios Hospital Schildautal in Seesen, Germany (Seugendo *et al.*, 2018). Initial species re-confirmation was performed using the MALDI Biotyper system (Bruker Daltonics, Bremen, Germany). Results with MALDI Biotyper identification score values  $\geq 2.000$  were assessed as correct.

### 3.5.2 Bacterial culture of *C. difficile*

*C. difficile* strains were maintained in store as cryobank stocks (Mast Diagnostica, Reinfeld, Germany) at  $-80$  °C. For investigation they were thawed and grown at  $37$  °C on Columbia agar with 5% sheep blood (COS, bioMérieux, Germany). Growth was performed either under anaerobic conditions using a COY anaerobic gas chamber (COY Laboratory Products, USA), with an atmosphere consisting of 85% N<sub>2</sub>, 10% H<sub>2</sub>, and 5% CO<sub>2</sub>, or alternatively in an Anaerocult®chamber (Merck, Darmstadt, Germany) using a GENbox anaer atmosphere generator (bioMérieux, Nürtingen, Germany).



### 3.5.3 Antimicrobial resistance testing of *C. difficile*

Agar dilution susceptibility testing of the *C. difficile* isolates was performed with slight modifications as described by Schwalbe and coworkers (Schwalbe *et al.*, 2007). Every strain to be tested was grown over night in 4 mL BHIS (37 g/L Brain Heart Infusion broth with 5 g/L yeast extract and 0.3 g/L cysteine). Bacterial suspension of each strain was suspended in BHIS to obtain a McFarland of 0.5 (corresponds to an OD<sub>600</sub> of 0.1). The adjusted suspensions were diluted 1:10 in sterile saline and 2 µL were spotted on Brucella plates with log<sub>2</sub> RFX concentrations between 0.008 µg/mL and 32 µg/mL (RFX was solved in Methanol). Additionally, an antibiotic-free control plate was carried along to ascertain overall strain growth, and on each plate a culture of *Bacteroides fragilis* ATCC 25285 was plated as positive growth control. Inoculated plates were incubated for 48 h under anaerobic conditions at 37 °C and subsequently checked for bacterial growth (fig. 3.2).

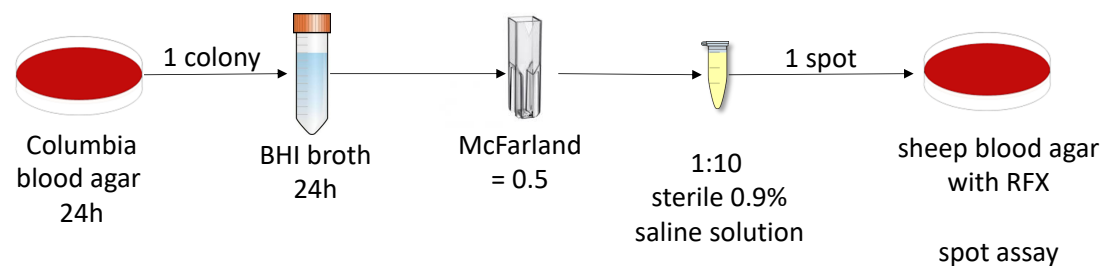


Figure 3.2: Scheme of the Antimicrobial Susceptibility Testing workflow.

### 3.5.4 DNA isolation, PCR and *rpoB* sequencing

DNA extractions from culture materials were performed using a Magna Pure LC 2.0 (Roche Diagnostics, Mannheim, Germany) automated system. For sequencing of *rpoB* the primer pairs JS001 & JS002, JS003 & JS004, and JS005 & JS006 were used as described before (Schwanbeck *et al.*, 2019). The primers have an overlapping region with the next pair of at least 150 bp. The first 379 bp of *rpoB* were not covered as it was deemed unlikely to find mutations in this part.

### 3.5.5 Whole genome sequencing and bioinformatics

Whole genome sequencing was performed as described before (Schwanbeck *et al.*, 2019). In short, the genomes of the 13 RFX resistant *C. difficile* strains were sequenced on the PacBio RSII system (Pacific Biosciences, Menlo Park, CA, USA) using P6 chemistry and one SMRT cell per isolate. Genome assembly was accomplished applying

the “RS\_HGAP\_Assembly.3” protocol included in the SMRT Portal version 2.3.0. The obtained chromosomal contig of each strain was trimmed, circularized and adjusted to *dnaA* as the first gene. Long-read genome quality was enhanced by using the “RS\_BridgeMapper.1” protocol also included in the in SMRT Portal version 2.3.0. Further, a final genome sequence quality of QV60 was attained after mapping Nextseq Illumina reads with the Burrows–Wheeler Aligner (Li and Durbin, 2009, 2010) onto the genome sequence obtained by PacBio sequencing. MLST Sequence Type, clade, ribotype and toxin gene configuration were derived from the genome sequence. Multi-locus sequence typing (MLST) was carried out making use of the *Clostridioides difficile* MLST Database <https://pubmlst.org/cdifficile/> (Griffiths *et al.*, 2010).

## 3.6 Conclusions

The overall RFX resistance rate in our test cohort was 10.08%, largely due to the significant increased RFX resistant rate of Indonesian *C. difficile* isolates of 27.59%. This may be a consequence of the use of rifampicin, e.g. in the treatment of tuberculosis in Indonesia. We were able to identify three different *rpoB* alleles in the tested strains associated with phenotypic RFX resistance. One of these alleles characterized by the three amino acid substitutions H502N, R505K, and I750M compared to the *rpoB* sequence of the reference strain *C. difficile* 630 $\Delta$ *erm* was previously unpublished. RFX resistant isolates belong to the three different clades 1, 2, and 4 and to the six different ribotypes 010, 017, 027, 046, 084, and 131. RFX is therefore only an alternative CDI therapy option in regions with low rifamycin application rate or after proof of susceptibility.

## 3.7 Appendix

### 3.7.1 Author Contributions

Conceptualization, Jörg Overmann (JO), Paul Cooper (PC), R. Lia Kusumawati (RLA), Uwe Groß (UG), Wolfgang Bohne (WB), Andreas E. Zautner (AEZ); methodology, Julian Schwanbeck (JS), WB; software, Thomas Riedel (TR); validation, JS; formal analysis, JS, AEZ; investigation, JS, Friederike Laukien (FL), PC, RLA; resources, JO, UG; data curation, JS, FL, TR; writing-original draft preparation, JS, AEZ; writing-review and editing, JS, TR, UG, WB, AEZ; visualization, AEZ; supervision, JO, UG, WB, AEZ; project administration, JO, UG, WB, AEZ; funding acquisition, JO, UG.

### **3.7.2 Funding**

This research was funded by the Federal State of Lower Saxony, Niedersächsisches Vorab (VWZN2889/3215/3266), Germany and by the Deutsche Forschungsgemeinschaft (DFG ZA 697/6-1), Germany.

### **3.7.3 Acknowledgments**

We thank Ines Oehmig for excellent technical assistance.

### **3.7.4 Conflicts of Interest**

The authors declare no conflict of interest.



## Chapter 4

# Evolving higher replication rates while maintaining a Fidaxomicin resistance in *Clostridioides difficile*

Authors: Julian Schwanbeck<sup>1</sup>, Thomas Riedel<sup>2,3</sup>, Katrina Funkner<sup>1</sup>, Ines Oehmig<sup>1</sup>, Jörg Overmann<sup>2,3</sup>, Uwe Groß<sup>1</sup>, Andreas E. Zautner<sup>1,4</sup>, Wolfgang Bohne<sup>1,4,5</sup>.

In preparation for submission. Contributions: see subsection 4.6.4 on page 47.

### 4.1 Abstract

Fidaxomicin is an antibiotic currently employed in cases of recurrent *C. difficile* 630 $\Delta$ *erm* infection (CDI). Resistance mutations against Fidaxomicin most often occur in the  $\beta$ -subunit of the RNA polymerase (*rpoB*) at position 1143 in *Clostridioides difficile*. The *rpoB*<sub>V1143D</sub> mutation is the cause for the strongest known tolerance towards Fidaxomicin in *C. difficile* with a MIC of > 64  $\mu$ g/ml. However, this mutation is also associated with fitness defects as decreased sporulation, low or no toxin expression, and most notably a decrease in growth rate. In this study, we performed an in vitro evolution experiment in order to test the hypothesis that compensatory mutations might lead to increased fitness in a *rpoB*<sub>V1143D</sub> mutant over time. We passaged *C. difficile* *rpoB*<sub>V1143D</sub> daily in the presence of sublethal Fidaxomicin concentrations. After 20 days, we could observe a marked increase in growth rate of the population in comparison to the progenitor strain. Individual clones obtained from this population also showed the increased growth rate. We performed whole genome sequencing on three of these clones, of which two carried mutations in the RNA polymerase within the  $\beta$  and  $\beta'$  units. Both mutations likely change the interaction of the holoenzyme with the non-coding strand of the DNA. We conclude that the growth defect incurred by a Fidaxomicin resistance muta-

---

<sup>1</sup>Institute for Medical Microbiology, University Medical Center, Göttingen, Germany

<sup>2</sup>Leibniz Institute DSMZ-German Collection of Microorganisms and Cell Cultures, Braunschweig, Germany

<sup>3</sup>German Center for Infection Research (DZIF), Partner Site Hannover–Braunschweig, Braunschweig, Germany

<sup>4</sup>Authors share senior authorship

<sup>5</sup>Corresponding Author. Tel.: 0049-551-395869, E-Mail: wbohne@gwdg.de

tion can be restored by further mutations and that restorative mutations can occur on multiple different sites. Sustained resistance against Fidaxomicin in viable strains will therefore likely become a larger issue in the future.

## 4.2 Introduction

*Clostridioides difficile*, formerly in the genus *Clostridium*, is a human pathogen which can infect the upper colon (Lawson *et al.*, 2016, Ooijselaar *et al.*, 2018). It is an obligate anaerobe which spreads as spores via the fecal-oral route (Crobach *et al.*, 2018). *C. difficile* 630 $\Delta$ *erm* is a major problem in modern health care settings and most often causes diarrhoea, though in extreme cases it can lead to toxic megacolon (Smits *et al.*, 2016). Usually, a healthy microbiome offers protection against *C. difficile* 630 $\Delta$ *erm* infection (CDI) (Buffie *et al.*, 2015, Theriot *et al.*, 2016). Dysbiosis is a risk factor for CDI. The loss of diversity of the microbiome associated with various antibiotics is thought to be a major contributing factor in developing CDI (Buffie *et al.*, 2015, Gómez *et al.*, 2017, Theriot and Young, 2015). The recommended initial antibiotic treatment of CDI consists of vancomycin or metronidazole (Ooijselaar *et al.*, 2018). These in turn can have a negative impact on the microbiome (Ajami *et al.*, 2018, Igarashi *et al.*, 2014). A continually disturbed microbiome facilitates a heightened risk for CDI, which can lead to recurrent CDI. Recurrent CDI can, in severe cases, lead to death (Ooijselaar *et al.*, 2018).

Fidaxomicin is currently recommended for use in patients with recurrent CDI (Ooijselaar *et al.*, 2018). Fidaxomicin, a macrocyclic antibiotic, targets the RNA polymerase. It stops the formation of the closed complex of the holoenzyme by interfering with the simultaneous binding of the -10 and -35 elements of the promoter region (Lin *et al.*, 2018). Fidaxomicin works against a narrow spectrum of species, which leads to a smaller impact on the microbiome. A study in a murine model showed that it impacted the microbiome less than vancomycin, with a smaller loss in diversity and a quicker diversity recovery time (Ajami *et al.*, 2018).

In the past it has been argued that evolved resistance towards Fidaxomicin is unlikely, as known resistance mutations either do not confer a high tolerance or cause a fitness decrease (Eyre *et al.*, 2014, Kuehne *et al.*, 2017). The currently highest known tolerance against Fidaxomicin is caused by the *rpoB*<sub>V1143D</sub> mutation, which confers a MIC of > 64  $\mu$ g/ml. Strains resistant to Fidaxomicin through mutations at the *rpoB*<sub>V1143D</sub> site display a reduction in growth rate, sporulation, and toxin formation (Kuehne *et al.*, 2017). Strains carrying such mutations would therefore be outcompeted

outside of Fidaxomicin selective pressure. In addition, strains resistant towards Fidaxomicin would presumably cause a milder form of CDI, due to the reduction in growth rate and toxin formation.

We previously generated a *C. difficile* 630 $\Delta$ *erm rpoB*<sub>V1143D</sub> mutant strain, in which we confirmed the described fitness defect of the mutation. In this report, we used this mutant in an in vitro evolution experiment and passaged the culture multiple times in the presence of sublethal Fidaxomicin concentrations, which should maintain the V1143D mutation. Isolates with higher growth rates were identified and compensatory mutations which could partly restore the growth defect were determined.

## 4.3 Materials and Methods

### 4.3.1 Media and strain cultivation

*C. difficile* 630 $\Delta$ *erm* strains were grown at 37 °C in BHIS (37 g/l brain heart infusion broth supplemented with 5 g/l yeast extract and 0.3 g/l cysteine), shaking at 180 rpm for liquid cultures. For plates, BHIS medium was supplemented with 15 g/l agar, or strains were grown on Columbia agar with 5 % sheep blood (COS, bioMérieux, Germany). Growth was always performed under anaerobic conditions using a COY anaerobic gas chamber (COY Laboratory Products, USA) flushed with gas consisting of 85 % N<sub>2</sub>, 10 % H<sub>2</sub>, and 5 % CO<sub>2</sub>. Medium was supplemented with 16 µg/ml Fidaxomicin where necessary.

### 4.3.2 Used strains

*C. difficile* 630 $\Delta$ *erm* (DSM 28645, RT012, CP016318.1) (Dannheim *et al.*, 2017), *C. difficile* 630 $\Delta$ *erm rpoB*<sub>V1143D</sub> (derived from DSM 28645 (Schwanbeck *et al.*, 2019)), *C. difficile* Goe-91 (DSM 105001, (Schwanbeck *et al.*, 2019)).

### 4.3.3 Strain evolution

*C. difficile* 630 $\Delta$ *erm* strains with a V1143D mutation in *rpoB* was grown in BHIS with 16 µg/ml Fidaxomicin. Four independent repeats were inoculated in either 10 or 4 ml BHIS. Strains were grown for 16 hours, after which the optical density was measured. Strains were then inoculated in fresh media to an OD<sub>600</sub> of 0.05.

#### 4.3.4 Growth curves

From a 4 ml BHIS overnight culture, 4 ml anoxic BHIS were inoculated to an OD<sub>600</sub> of 0.05 in Hungate tubes (Macy *et al.*, 1972). Cultures were incubated at 37 °C, 180 rpm. OD<sub>600</sub> was measured in a NanoColor<sup>®</sup> VisII spectrophotometer (Macherey-Nagel, Düren, Germany).

#### 4.3.5 Sequencing

Strain sequencing was performed as described in Schwanbeck *et al.* (2019).

#### 4.3.6 Mutation site analysis

Subunits of the RNA polymerase were compared using swissmodel<sup>6</sup> using standard settings. Templates were selected for highest global model quality estimation while disregarding recombinant proteins.

### 4.4 Results and Discussion

The growth impaired *C. difficile* 630 $\Delta$ *erm rpoB*<sub>V1143D</sub> mutant (Schwanbeck *et al.*, 2019) was subjected to an in vitro evolution experiment in order to select for isolates which harbour putative compensatory mutations that would lead to a restoration of the growth defect. Four cultures of the *rpoB*<sub>V1143D</sub> mutant were evolved in parallel. Cultures were diluted once a day to OD<sub>600</sub> 0.05 in BHIS supplemented with 16 µg/ml Fidaxomicin for a total of 16-20 days. Afterwards, the cultures were plated on BHIS agar supplemented with 16 µg/ml Fidaxomicin. One isolated colony per culture was randomly picked and subsequently subjected to growth rate analysis. Three of the four independently evolved isolates had a significantly increased replication rate in comparison to the initial *C. difficile* 630 $\Delta$ *erm rpoB*<sub>V1143D</sub> mutant (fig. 4.1). Sequencing of *rpoB* PCR products revealed that the V1143D mutation was maintained in all four isolates. The evolution experiment thus indicates that the *rpoB*<sub>V1143D</sub> associated growth defect can be partly compensated by either adaptive processes and/or compensatory mutations within current Fidaxomicin treatment time frames.

#### 4.4.1 Mutations in *rpoB* and *rpoC*

Isolates Evo\_1, Evo\_2 and Evo\_3 were subjected to whole genome sequencing. We found in addition to *rpoB*<sub>V1143D</sub> further mutations in the RNA polymerase subunits

---

<sup>6</sup>[swissmodel.expasy.org/](http://swissmodel.expasy.org/)



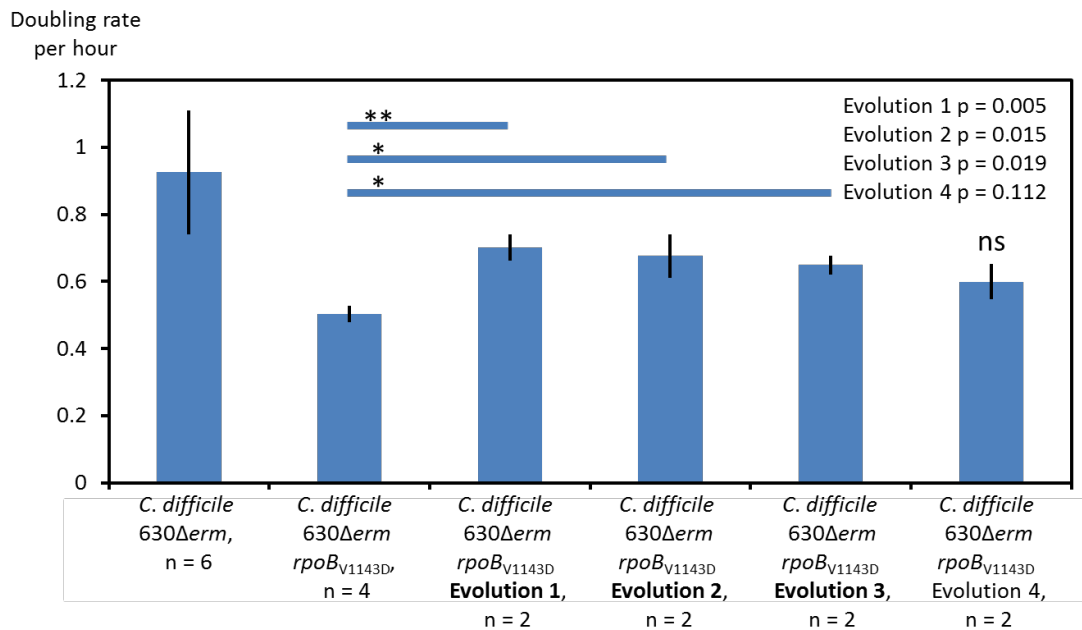


Figure 4.1: **Doubling rate per hour of various strains.** Strain *C. difficile* 630 $\Delta$ erm is the wild type. Strain *C. difficile* 630 $\Delta$ erm *rpoB*<sub>V1143D</sub> is the progenitor strain of the evolved strains. Strains Evo\_1 through Evo\_4 are compared to the doubling rate of the progenitor strain. Strains Evo\_1, Evo\_2, and Evo\_3 were significantly faster ( $p = 0.005$ ,  $0.015$ , and  $0.019$ , respectively), while strain Evo\_4 was not significant ( $P = 0.112$ )

in two strains. Isolate Evo\_3 possesses a Proline 244 to Threonine mutation in *rpoB*. This mutation is localised within a loop sequence between two beta barrels, containing two consecutive prolines, which can also be found in other species (fig. 4.2). The two beta barrels are positioned close to the non-translated DNA strand within the RNA polymerase holoenzyme during transcription. The mutation likely changes the angle between the two beta barrels, which may have an effect on the way the non-translated strand is guided.

The isolate Evo\_2 possesses a Glutamate 768 to valine mutation in *rpoC*. The glutamate 768 is an amino acid whose negative charge is conserved through several species. The Aspartate at that position in *Mycobacterium tuberculosis* is located at a position shortly before the translated and non-translated strands anneal again (fig. 4.3). The loss of the negative charge at that position could also have an impact on how the DNA is guided through the holoenzyme. Given the position of both mutations, we believe it is likely that compensations to the *rpoB*<sub>V1143D</sub> mutation can be achieved by changes to the way the DNA is guided through the RNA polymerase.

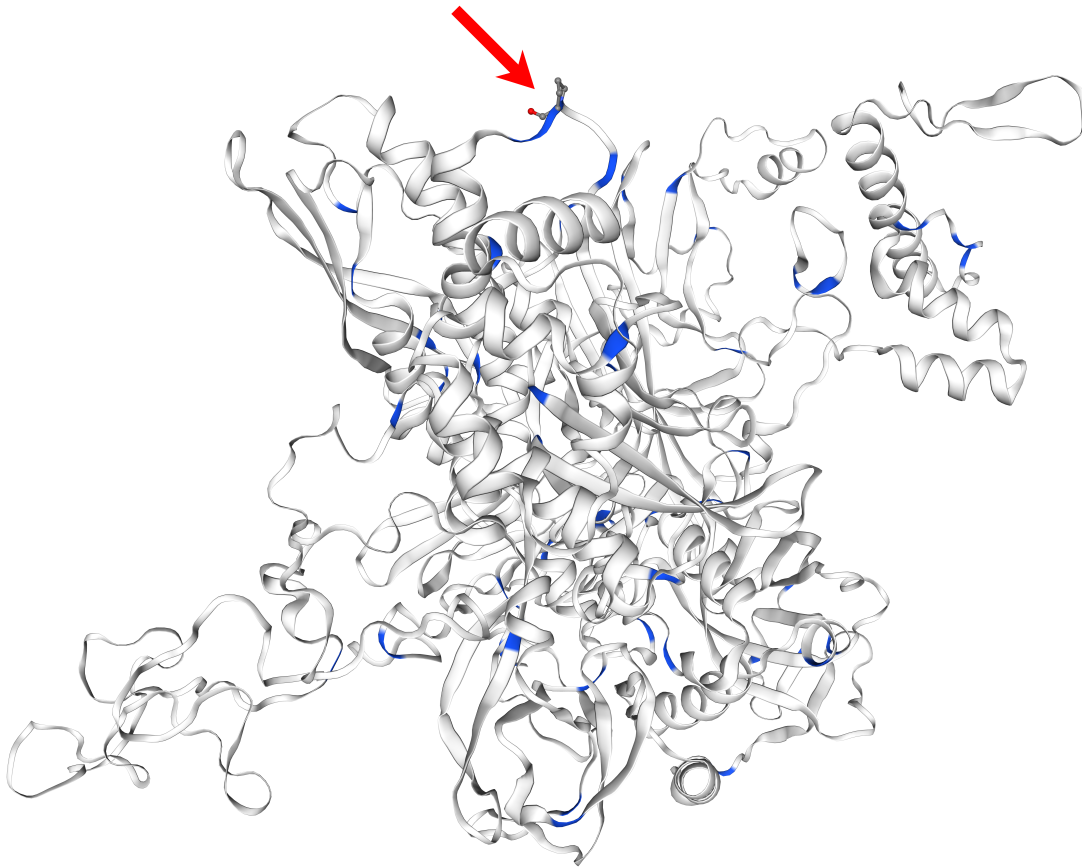


Figure 4.2: **Position of *rpoB* Proline 244**, marked with a red arrow and depicted as ball and stick model. Proline 255 sits between two beta barrels. Positions of prolines are highlighted in blue. Figure was created using swissmodel<sup>6</sup> using 5vi5.1.E of *Mycobacterium smegmatis* as comparison model.

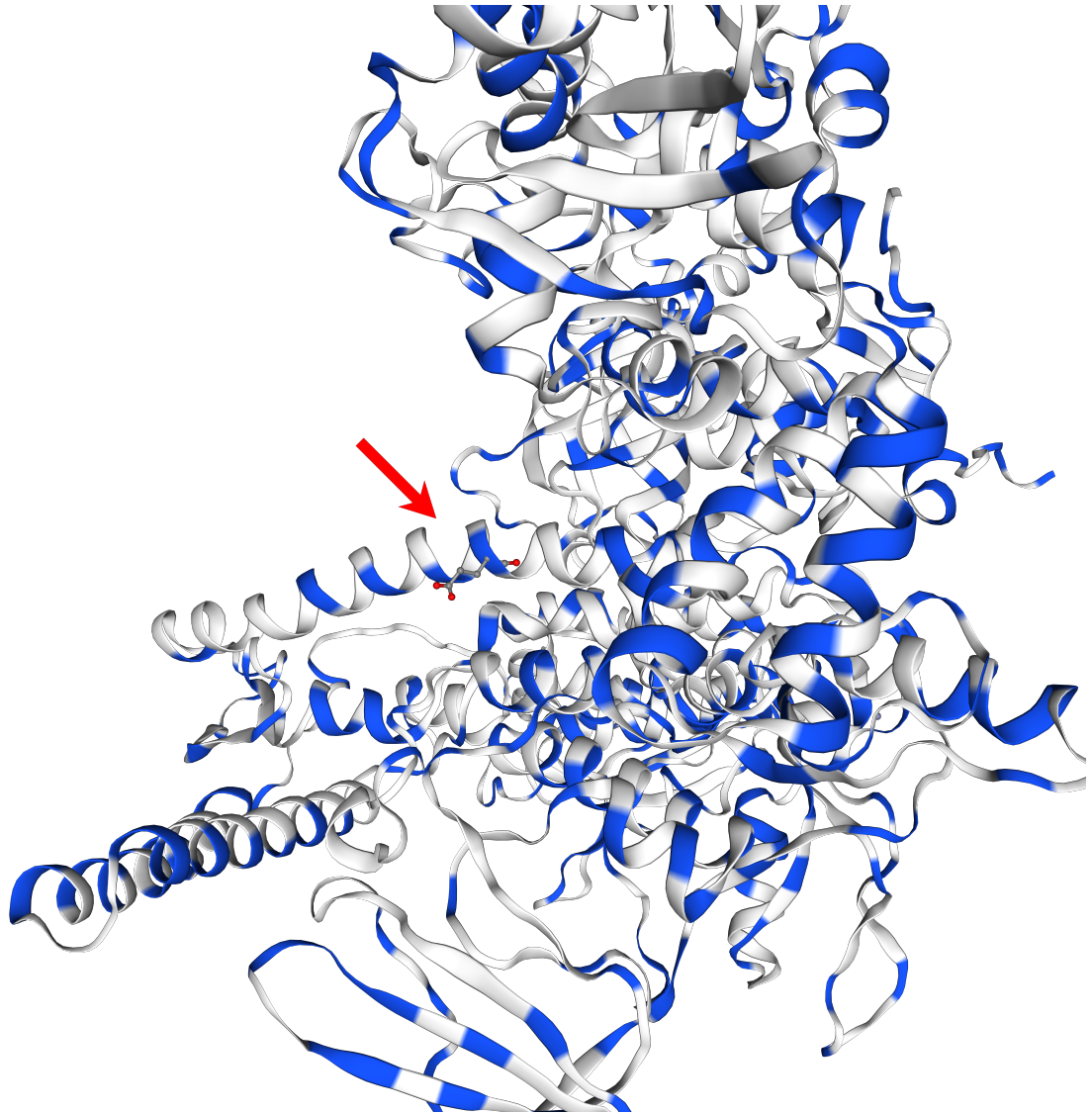


Figure 4.3: **Position of *rpoC* Glutamate 244** marked with a red arrow and depicted as ball and stick model. Charged side chains are highlighted in blue. Figure was created using swissmodel<sup>6</sup> using 6c04.1.D of *Mycobacterium tuberculosis* as comparison model.

### 4.4.2 Other Mutations

Two further mutations could be found in all three evolved strains versus the progenitor strain: *bclA3* and hypothetical protein CD630\_06320. CD630\_06320 largely consists of dipeptide repeats of Alanine–Arginine in the wild type from which in all evolved strains a region of 30-78 bp have been deleted, resulting in a frame shift in two evolved strains. The role of CD630\_06320 is currently unclear. BclA3 is an exosporangial glycoprotein under the expression control of  $\sigma^k$ , and the affected region consists of a "TPGTAG" repeat region from which 383 – 430 bp are deleted in the evolved strains (Strong *et al.*, 2014). We presume that both mutations are unlikely to be the cause of a compensatory effect.

## 4.5 Conclusion

We described earlier the first clinical isolate with a high Fidaxomicin tolerance, Goe-91. Goe-91 was isolated from a patient with symptoms indicative of CDI. Interestingly, the growth rate of Goe-91 was comparable to that of other wild type strains. Goe-91 carries the *rpoB*<sub>V1143D</sub> mutation, but no other mutations in the RNA polymerase. We could show in this study that the *rpoB*<sub>V1143D</sub> mutation associated growth defect can be reduced when bacteria are passaged continuously in the presence of Fidaxomicin for a period of 16-20 days. The passaging favours faster doubling rates, creating a selection bias against/ slower strains. The significant increase in doubling rate in three of the four strains shows that it is possible to create a faster growing *C. difficile* 630 $\Delta$ *erm* strain with a maintained Fidaxomicin resistance in vitro. The mutations of Evo\_2 and Evo\_3 within the RNA-Polymerase are likely candidates for a compensatory effect which we aim to confirm in the future. The mutations are on different parts of the holoenzyme, though both mutations indicate a change in the way the DNA is guided through the RNA-polymerase holoenzyme. These alterations may alleviate the impairing effects caused by the change in charge due to the *rpoB* Valine 1143 to Aspartate mutation.

Interestingly, both one of the evolved strains as well as the original Goe-91 strains have no amino acid substitutions within the RNA polymerase except for V1143D. We therefore hypothesise that other compensatory mutations outside of the RNA polymerase are possible. Multiple possible compensatory mutation sites for the restoration of the *rpoB*<sub>V1143D</sub> mediated growth defect are a troubling prospect for the future of therapeutic options for *C. difficile* 630 $\Delta$ *erm*.

## 4.6 Appendix

### 4.6.1 Acknowledgements

We would like to thank Igor Khassanov for contributions to the evolved strains.

### 4.6.2 Funding

This work was funded by the Federal State of Lower Saxony, Niedersächsisches Vorab (VWZN2889/3215/3266).

### 4.6.3 Declarations

Nothing to declare.

### 4.6.4 Author contributions

Conceptualization, Julian Schwanbeck (JS), Wolfgang Bohne (WB); methodology, JS, Thomas Riedel (TR), WB; software, TR; validation, JS, Katrina Funkner (KF), TR; formal analysis, JS, KF, TR; investigation, JS, TR, KF, Ines Oehmig (IO); resources, Jörg Overmann (JO), Uwe Groß (UG), Andreas E. Zautner (AEZ), WB; data curation, JS, KF, TR; writing—original draft preparation, JS, WB, AEZ; writing—review and editing, JS, TR, JO, UG, AEZ, WB; visualization, JS; supervision, JO, UG, AEZ, WB; project administration, JO, UG, AEZ, WB; funding acquisition, JO, UG.



## Part II

# *Clostridioides difficile* Single Cell

## Motility





## Chapter 5

# YSMR: a video tracking and analysis program for bacterial motility

Authors: Julian Schwanbeck<sup>1,2</sup>, Ines Oehmig<sup>1</sup>, Jérôme Dretzke<sup>3</sup>, Andreas E. Zautner<sup>1</sup>, Uwe Groß<sup>1</sup>, and Wolfgang Bohne<sup>1</sup>.

First sent to BMC Bioinformatics on 28th August 2019; returned on the 2nd January 2020, revised on the 19th February 2020, accepted on the 15th April 2020, published on the 29th April 2020. DOI: 10.1186/s12859-020-3495-9 (Schwanbeck *et al.*, 2020a).

Contributions: see subsection 5.8.1 on page 59.

## 5.1 Abstract

### 5.1.1 Background

Motility in bacteria forms the basis for taxis and is in some pathogenic bacteria important for virulence. Video tracking of motile bacteria allows the monitoring of bacterial swimming behaviour and taxis on the level of individual cells, which is a prerequisite to study the underlying molecular mechanisms.

### 5.1.2 Results

The open-source python program YSMR (Your Software for Motility Recognition) was designed to simultaneously track a large number of bacterial cells on standard computers from video files in various formats. In order to cope with the high number of tracked objects, we use a simple detection and tracking approach based on grey-value and position, followed by stringent selection against suspicious data points. The generated data can be used for statistical analyses either directly with YSMR or with external programs.

---

<sup>1</sup>Institute for Medical Microbiology, University Medical Center, Göttingen, Germany

<sup>2</sup>Corresponding Author. Tel.: 0049-551-3914018, E-Mail: j.schwanbeck@yahoo.de

<sup>3</sup>Institute of Applied Mathematics, Leibniz University Hannover, Hannover, Germany

### 5.1.3 Conclusion

In contrast to existing video tracking software, which either requires expensive computer hardware or only tracks a limited number of bacteria for a few seconds, YSMR is an open-source program which allows the 2-D tracking of several hundred objects over at least 5 minutes on standard computer hardware. The code is freely available at [github.com/schwanbeck/YSMR/](https://github.com/schwanbeck/YSMR/).

## 5.2 Background

Bacteria developed different types of motility, most of them driven by flagella or pili. The molecular processes that regulate motility in bacteria are an active area in research, as they form the basis for dispersion, tactile processes, and virulence in some pathogenic bacteria (Watts *et al.*, 2019).

The particular type of bacterial swimming varies significantly among bacterial species and depends on the number of flagella and their distribution on the bacterial cell body (Bastos-Arrieta *et al.*, 2018). The best studied example is the “run and tumble” motility type of *Escherichia coli*, in which counter clockwise rotation of flagella leads to a run phase, while clockwise rotation leads to a tumbling phase with a random cell rotation (Sarkar *et al.*, 2010). However, in recent years additional motility types were discovered, as the “forward–reverse–flick” motility type in *Vibrio alginolyticus* (Xie *et al.*, 2011) or the “stop–and–coil” type in *Rhodobacter sphaeroides* (Haya *et al.*, 2011).

To study bacterial motility patterns, microscopic monitoring and analysis of single cell motility is required. Manual analysis of motility videos increases the risk of inadvertent cherry picking, as well as being tedious. The application of video tracking software is thus advisable for the quantification of various motility parameters such as the average speed, the length of travel paths, the time of swimming and tumbling, arc-chord ratio, percentage of immotile cells, and preferred direction of travel.

To our knowledge, video tracking software, which can be used for this purpose, have been designed with a high priority on tracking accuracy, as for example TrackMate2 (Tinevez *et al.*, 2017), or require additional licences to be used (Taute *et al.*, 2015).

However, a high accuracy tracking program monitors several parameters per tracked object per frame and can therefore quickly run into hardware limitations when several hundred objects are simultaneously analysed. Using such programs forces the user to choose between fewer cells per frame or shorter videos in order to be still functional.

We therefore felt the need for an open-source tracking program which uses only simple parameters for tracking, in order to be able to cope with the large amount of tracked objects for at least five minutes. Here, we use the grey value of the bacterium for detection, and the distance between frames for tracking. As the sample size is very large, typically in the range of several hundred bacteria per frame, the loss of tracked objects is less important. After initial tracking, we subsequently filter out questionable data points and tracks in multiple steps. We also include the possibility for statistical analysis of the generated data.

## 5.3 Software

### 5.3.1 File requirements

During the initial setup, YSMR requires various parameters to be set in an automatically generated settings file, “tracking.ini”. The file was created with the idea in mind that it should be simple to set the basic values, but still allow for more in-depth configurations. Basic required settings are pixel per micrometre factor, frames per second, frame dimensions, whether the bacteria are brighter or darker than the background, as well as whether rod shaped or coccoid bacteria are tracked. In order to take advantage of multi-core CPUs, YSMR is designed to handle a video file per available processor core in parallel. Files can be loaded by specifying them in the file dialogue, as arguments for the YSMR function, or by specifying the path in the tracking.ini file. The user has to provide a video file in any format accepted by ffmpeg. We so far successfully tested .wmv, .avi, .mov, .mp4, and .mkv.

### 5.3.2 Bacteria detection by grey value

Recorded bacteria can be either brighter or darker than the background. The program reads one frame at a time. During the process of bacterial detection, the frame is first converted into grey-scale (see fig. 5.1). Recorded bacteria can be either brighter or darker than the background. The program reads one frame at a time. During the process of bacterial detection, the frame is first converted into grey-scale (fig. 5.1 A & B). The noise in the frame is reduced by a 2D Gaussian blur in order to reduce the rate of false positive areas (fig. 5.1 C). Outline areas are set using an adaptive threshold with an 11 by 11 Gaussian kernel (Fig. 1 d). In order to exclude erroneous detections, a second adaptive Gaussian threshold with an increased threshold is used to generate marker positions (fig. 5.1 E). Whenever no white area from fig. 5.1 E is

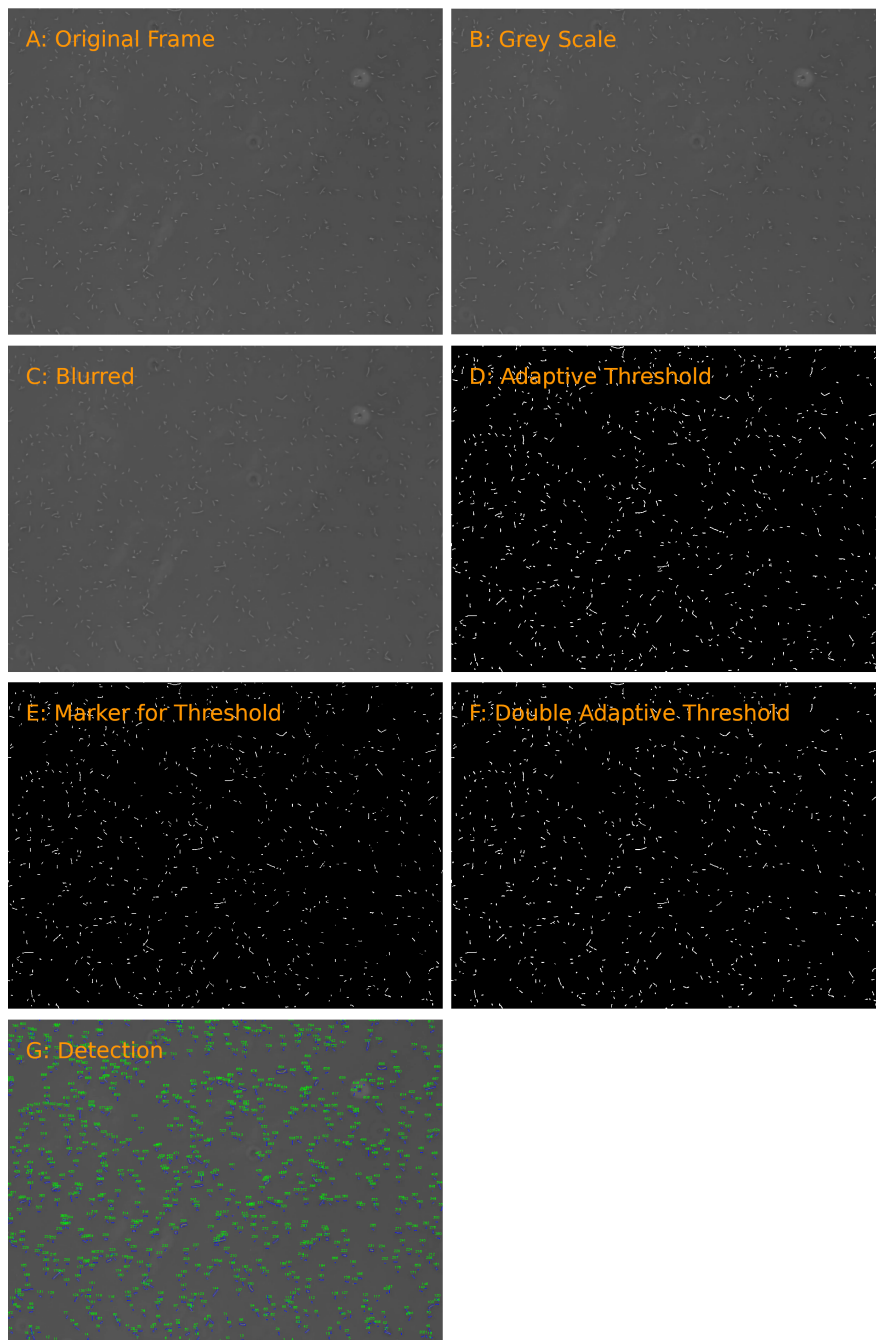


Figure 5.1: **From original frame to final detection.** A: the original frame from the video file. B: the frame is converted to grey scale. C: a Gaussian blur with a 3 by 3 kernel is applied. D: the adaptive threshold is applied, leaving white areas as potential bacteria. E: a second, higher, adaptive threshold is applied to generate markers. F: white areas from D which contain markers from E are used as outlines. G: each area is encased in a rectangle and assigned a unique ID, displayed on the original frame.

contained within a white area from fig. 5.1 D, that area is disregarded. From this, the frame depicted in fig. 5.1 F is generated. The outermost points of the edges in fig. 5.1 F are then used to create a rectangle and each newly generated rectangle receives a unique ID (fig. 5.1 G). The centre-point of the rectangle (named “tracking target”) is set as the x-, y-coordinate of the bacterium, which is used for tracking.

Optionally, either simple adaptive thresholding, without the marker based approach, or simple thresholding based on the grey value of the frame can be used.

### 5.3.3 The tracking process

Tracking is performed by calculating the distances of all tracking targets between each frame and joining the neighbours with the least distance between frames. In addition, a Gaussian sum finite impulse response filter using a constant velocity model is used to filter the measured signal as well as to produce predictions of positions for tracking (Pak, 2019). When a new frame has more tracking targets than a previous frame, new IDs are assigned to the additional tracking targets. Tracking targets which cannot be assigned will be given the width and height dimensions of 0.0 for missing frames, while their last predicted x-, y-coordinate will be used for tracking. Centre-points that cannot be assigned within one second of the last detection will be removed. The generated information per frame, consisting of ID, filtered position, width, height, time, and rotation angle, is periodically saved to disc in a .csv file. When all frames have been read, the resulting .csv file is sorted by ID and time.

### 5.3.4 Track selection

The data is then loaded as a pandas data frame and all tracks are checked for plausibility or errors before further calculations are performed. Track selection is performed in two parts, as some erroneous data points as well as entirely too short tracks can be excluded directly, which saves processing time and increases precision in the secondary finer selection step.

(i) In the initial step, entire tracks are discarded. This includes all tracks whose bounding rectangles are on average below or above user specified bacterial size limits. The lower limit discards most events which have a small bounding rectangle for a few frames, followed by frames with an area of zero for one second, averaging close to zero in total. The upper limit excludes areas of bright spots caused by dirt, chromatic aberrations in the microscope, or other unwanted objects. We find that using a lower limit of 20 % of the average bacterial size in  $\text{px}^2$  and an upper limit of five times that

area can be used as a rule of thumb for the initial broad exclusion limits. When a user defined minimum tracking time is given, all tracks below this limit at this stage are also excluded.

(ii) In the second step, erroneous single measurements are deleted. This includes all single measurement points where the area is zero. This is caused by the tracker, which zeros width and height when the track cannot be linked in between frames. The position given at such points is the last predicted position.

(iii) Optionally, single data points can be excluded if they surpass a specified multiple of the average bounding rectangle area of a track. This can occur when bacteria overlap, which increases the size of the bounding rectangle by the area of the second bacterium. In this case, one bacterium is erroneously assigned a larger size, while the other cannot be tracked.

After removing erroneous data points and tracks, each track is sequentially filtered through user defined criteria. A count of how often a track has been excluded through each criterion is reported afterwards. We will hereafter refer to removed measurement points as “gaps” in the measurement. The following criteria are included: (iv) first, the duration in time of the track must be above a user defined minimum time limit, if one is specified. (v) The track may not have more than a set amount of consecutive frame gaps, which ensures continuous tracking. (vi) Optionally, distance outliers within tracks can be calculated. Outliers are defined as those above the outer fence of all distances. As this is prone to error when too many tracked objects are immotile, the feature can optionally disable itself if the detected outliers are above a specified percentage of all data points. If too large consecutive gaps in measurement or distance outliers are present, the track is split and both halves are analysed again, starting at the first check. (vii) The data points of the track may not have more than a user defined percentage of gaps. (viii) The average bacterial size within a track can be used as an exclusion parameter. If the average size is outside a percentile of all size measurements, the track is excluded. The percentile is also defined by the user. Area outliers missed by the hard limit of the initial sorting step ‘i’ are excluded at the possible expense of excluding a fraction of correct tracks. (ix) The average position of the track must not be within a given percentage of the screen edges. These tracks can be excluded as a precaution, since IDs near the screen edges could be wrongly reassigned when other bacteria enter the frame.

If all checks are passed, the track is added to the results. If a track was split and several parts pass the checks, the longest part is selected and all others are discarded.

Optionally, tracks can be limited to a user defined maximal duration. When an upper time limit is set the track is shortened to the exact duration or, if a gap is at that position, the closest data point below the set time limit. This behaviour can be changed so that shortened tracks which fall below the limit are discarded instead.

## 5.4 Data processing, analysis and illustration

The tracking process can either be displayed during analysis or saved as an .avi file encoded in MJPEG. The generated raw data from the tracking, the results from the subsequent fine selection, as well as the results from the statistical analysis can each be saved as an individual .csv file. The statistical analysis .csv files can also as a convenience function be collated into a .xlsx file.

Tracks can be graphically visualized in a coordinate graph with a marker at the starting position, or as a rose graph with starting x-/y-coordinates set to 0,0. In each case, the tracks are coloured depending on travelled distance.

Tracks can be analysed for the following parameter: (i) total travelled distance ( $\mu\text{m}$ ), (ii) speed ( $\mu\text{m/s}$ ), (iii) duration (s), (iv) maximum distance between tracked positions ( $\mu\text{m}$ ), (v) percentage of time where bacterium was motile, (vi) turn points per second, and (vii) arc-chord ratio. Generated statistics can be displayed as violin plots.

## 5.5 Comparison to TrackMate

TrackMate is a widely used tracking program designed for sub-pixel localisation and tracking of eukaryotic cells (Tinevez *et al.*, 2017). Smaller objects, such as bacteria, can also be tracked. It is in contrast to YSMR a semi-automatic application requiring user supervision and input during tracking. A further limitation is the maximum video length when tracking a large number of objects due to increasing RAM requirements. We compared the performance and results between YSMR and TrackMate on the example video which was shortened to 30 s (Supplementary Figure 1, Supplementary Video 1, and Supplementary Table 1). The analysis was done in comparable time (YSMR 140.5 s, TrackMate 141.8 s) with default options for YSMR. However, YSMR used fewer computational resources, since it is designed for parallel analysis of multiple videos. YSMR used only one thread, whereas TrackMate used four. The peak RAM usage was 6.3 GB for TrackMate and 1.1 GB for YSMR. Comparing the results, when overlaid, YSMR detects 91.1 % of all positions that overlap with those detected by

TrackMate. Mean values for speed, distance, displacement, arc-chord ratio, and percentage of motility are in a similar range with variations between 6.23 % and 19.81 % of the means (Supplementary Table 1).

## 5.6 Discussion and Conclusion

YSMR is a python program for generating tracking data and statistics from video files depicting motile bacteria. It offers the possibility to determine and quantify the most relevant bacterial motility parameters, for example total travelled distance, speed, percentage of time where bacteria are motile and turn points per second, among others. A thorough analysis of these data can provide the basis for novel insights into the motility behaviour of bacteria and its regulation.

Existing tracking programs have a focus on the high accuracy of generated tracking trails from video files and were often performed on very small sample sizes, due to the need to track single cells frame-by-frame throughout the video. In contrast, YSMR is optimized for the simultaneous tracking of a very large number of bacteria, typically in the range of 100-1000 per frame from video files generated with a 10 $\times$  objective. YSMR is based on a moderate fidelity, high selectivity approach, which keeps the processing time short. Instead of using computational intensive approaches for bacterial detection, for example machine learning, we found that the detection could be reduced to a very simple approach, namely finding bacteria by grey value threshold. We concluded that we could simplify the whole process down to the described detection and tracking mechanism, as long as in a secondary step we rigorously select against suspect data points. The entire process is inexpensive enough to be run on standard desktop computers and was adapted to take advantage of multicore processors for parallelisation.

In our setup, efficient tracking of flagellated *Bacillus subtilis* was possible with YSMR by using video files generated with a 30 fps camera (Aptina CMOS Sensor 18MP 1/2.3" Color) on a microscope with a 10 $\times$  objective (Nikon Eclipse TE2000-S, Nikon PlanFluor 10 $\times$ ). The comparatively large depth of the focal plane of a 10 $\times$  objective minimizes the number of bacteria that move out of focus during tracking. A frequent experimental design is to analyse bacterial motility statistics for a population under varying conditions (for example different pH, nutrient availability, growth phase, or cell densities). YSMR can analyse generated video files for this purposes quickly and in parallel. On the other hand, if the exact motility pattern of single bacteria, the movement in 3D, or bacteria-bacteria interaction is of interest, or the cell density is below 50 objects per frame, other programs with higher tracking accuracy might be a



better choice. To assess the performance of YSMR for a given task, the debug option lets the user review the detection process. For a straightforward assessment of the generated data, the save video option displays the generated measurements directly on the original video. YSMR was optimized to analyse bacterial motility statistics from a large number of bacteria in short time. Even if more precision is required, YSMR can still be used as a simple and quick pre-screening in order to select files for more complex and time consuming processes.

## 5.7 Availability and requirements

Project name: YSMR v 0.1.0. Project home page: [github.com/schwanbeck/YSMR/](https://github.com/schwanbeck/YSMR/).  
Operating systems: Platform independent. Programming Language: Python  $\geq$  3.6.  
Other requirements: opencv (opencv-contrib-python/opencv-python v3/v4, v2 untested), numpy, pandas, tkinter, matplotlib, scipy, seaborn. Optional: xlsxwriter.

## 5.8 Declarations

Ethics approval and consent to participate: not applicable. Consent for publication: not applicable. Availability of data and materials: an example video of *Bacillus subtilis* is provided in the supplementary. Competing interests: the Authors declare no conflict of interest. Funding this work was funded by the Federal State of Lower Saxony, Niedersächsisches Vorab (VWZN2889/3215/3266).

### 5.8.1 Authors' contributions

JS was the main developer of YSMR. IO performed the laboratory work. JD implemented the Gaussian-sum FIR filter in Python and tested it. AZ, UG and WB tested the application on various systems, contributed ideas, supervised the project and were involved in the preparation of the manuscript. All authors read and approved the final manuscript.

### 5.8.2 Acknowledgements

We would like to thank Prof. Burkhard Morgenstern for reading the manuscript and supporting the project. We would like to thank Avril von Hoyningen-Huene for proof-reading and providing corrections for the manuscript.



## Chapter 6

# ***Clostridioides difficile* single cell swimming strategy: a novel motility pattern regulated by cysteine and viscoelastic properties of the environment**

Authors: Julian Schwanbeck<sup>1</sup>, Ines Oehmig<sup>1</sup>, Uwe Groß<sup>1</sup>, Andreas E. Zautner<sup>1</sup>, and Wolfgang Bohne<sup>1,2</sup>.

In preparation for submission. Contributions: see subsection 6.7.4 on page 77.

### **6.1 Abstract**

Flagellar motility is important for the pathogenesis of many intestinal pathogens, allowing bacteria to move to their preferred ecological niche. *Clostridioides difficile* is currently the major cause for health care-associated intestinal infections in the western world. Most clinical strains have flagella and thus the capability of motility. However, little knowledge exists on the *C. difficile* swimming behaviour and its regulation. We report here on the swimming strategy of *C. difficile* at the single cell level and its dependency on environmental parameters. *C. difficile* motility was found to be strongly dependent on the viscoelastic properties of the medium. Long run phases were only observed in the presence of high molecular weight polymers, which suggests an adaptation of the motility apparatus to the mucin-rich intestinal environment. The *C. difficile* swimming strategy appears to be different from previously described patterns of other species and is characterised by alternating forth and back run phases, interrupted by a short stop without an apparent reorientation. A quantification of motility parameters in the presence of different metabolites identified cysteine as a compound which reduces the swimming speed. Velocity regulation by cysteine is dependent on an intact chemotaxis system, since a strain lacking CheY, the central transmitter of the chemotaxis system, shows no responsiveness to cysteine. Our data suggest that *C. difficile* swimming velocity is regulated by cysteine levels, which would allow bacteria to accumulate

---

<sup>1</sup>Institute for Medical Microbiology, University Medical Center, Göttingen, Germany

<sup>2</sup>Corresponding Author. Tel.: 0049-551-395869, E-Mail: wbohne@gwdg.de

in the cysteine rich environment close to the intestinal epithelium.

## 6.2 Importance

Flagellar motility regulated by gradients of chemoattractants or chemo-repellents is essential for many bacteria to reach their preferred ecological niche. A few different swimming strategies have been described in the bacterial world so far. We report here on a novel swimming pattern identified for the human intestinal pathogen *Clostridioides difficile*. This strategy is characterised by long and curved run phases that occur alternating and equal in forward and backward orientation. Interestingly, there is no apparent reorientation, no “tumbling”, or “flick”, during the short stop in between, as is typical for many other bacteria. The reorientation phase usually plays a critical step in chemotaxis. Swimming velocity is high by default, but can be reduced by cysteine, which would allow *C. difficile* to accumulate in the cysteine rich environment close to the intestinal epithelium. This swimming pattern was induced only in the presence of high molecular weight polymers, such as mucin, which reflects the composition of the natural habitat of *C. difficile* in the larger intestine.

## 6.3 Introduction

*Clostridioides* (formerly *Clostridium*) *difficile* is a spore forming, obligate anaerobic pathogen, which has emerged in recent years as a major cause of hospital-associated diarrhoea and pseudomembranous colitis (Leffler and Lamont, 2015, Lessa *et al.*, 2015). Clinical symptoms are associated with toxin expression, in particular of toxin A and toxin B, which undergo a complex pattern of regulation (Chandrasekaran and Lacy, 2017, Just *et al.*, 1995, Kuehne *et al.*, 2010). An intact gut microbiome is believed to protect from *C. difficile* infection. Dysbiosis however, for example after antibiotic treatment, favours *C. difficile* spore germination and subsequent colonisation (Theriot and Young, 2015). Chemotaxis allows bacteria to swim up or down a chemical gradient and thus to optimise the colonisation process (Matilla and Krell, 2018). Flagellar motility and chemotaxis is important for successful colonisation and virulence of many gastrointestinal pathogens, for example *Campylobacter jejuni*, *Salmonella enterica* Serovar *Thyphimurium*, *Helicobacter pylori* and *Vibrio cholerae* (Boin *et al.*, 2004, Korolik, 2019, Lertsethtakarn *et al.*, 2011, Stecher *et al.*, 2004). Most *C. difficile* strains produce peritrichious flagella, which can mediate swimming motility in soft-agar based assays (Stevenson *et al.*, 2015, Twine *et al.*, 2009). The contribution of flagellar

motility for the pathogenesis in mice was studied with the aid of *C. difficile* flagellar mutants, which were found to be reduced in their colonisation efficiency (Baban *et al.*, 2013, Batah *et al.*, 2017, Stevenson *et al.*, 2015). It is also known that the *C. difficile* genome contains a genomic region which encodes for a complete set of chemotaxis genes (Dannheim *et al.*, 2017). However, in contrast to other gut pathogens, little knowledge exists how *C. difficile*'s motility and chemotaxis is regulated on the single cell as well as the molecular level. It was recently reported that N-acetylneuraminic acid reduced the velocity of bacteria during run phases (Courson *et al.*, 2019). Furthermore, motility in *C. difficile* was shown to be pH-dependent with reduced motility at low pH and increased motility at alkaline environments (Wetzel and McBride, 2019). We report in this study on the swimming behaviour of *C. difficile* and its dependency on the (i) viscoelastic properties of the medium, (ii) presence of different metabolites and (iii) an intact chemotaxis system. A comprehensive quantitative analysis of *C. difficile* motility parameter on single cell level was obtained with the aid of the recently developed bacterial tracking program YSMR (Schwanbeck *et al.*, 2020a).

## 6.4 Materials & Methods

### 6.4.1 Used *C. difficile* strains

*C. difficile* 630 $\Delta$ *erm* (DSM 28645, CP016318.1), *C. difficile* 630 *cheY::erm* (derived from DSM 28645, this study), *C. difficile* R20291 (DSM 27147), DSM 102860, DSM 28670, and DSM 29695.

### 6.4.2 Media and strain cultivation

*C. difficile* strains were grown at 37 °C in BHIS (37 g/L brain heart infusion broth supplemented with 5 g/L yeast extract and 0.3 g/L cysteine) shaking at 180 rpm for liquid cultures, alternatively with 15 g/L agar for plates, or on Columbia agar with 5% sheep blood (COS, bioMérieux, Germany). Growth was always performed under anaerobic conditions using a COY anaerobic gas chamber (COY Laboratory Products, USA). The chamber was gas-flushed with 85% N<sub>2</sub>, 10% H<sub>2</sub> and 5% CO<sub>2</sub>. For overnight cultures, where necessary, 5 mg/L erythromycin was added.

### 6.4.3 Video Microscopy

From overnight cultures 4 ml BHIS were inoculated to an OD<sub>600</sub> of 0.05 and incubated until an OD<sub>600</sub> of 0.5 ± 0.1 was reached. For videos of cultures in 100% BHIS, 4 µl of the

culture were placed on an objective slide, covered with a cover slip and immediately sealed with nail polish. Except when stated otherwise, slides were recorded 15 min after sealing on a microscope with a 10x objective (Nikon Eclipse TE2000-S, Nikon PlanFluor 10x). Videos were taken for 3 min at 30 fps using an Aptina CMOS Sensor 18 MP 1/2.3" Color.

#### 6.4.4 Video Microscopy with polyvinylpyrrolidone (PVP) or Mucin

For videos containing PVP (K 90, MW 360,000 g/mol, Carl Roth, Karlsruhe, order nr. CP15.1) or mucin (Bovine Submaxillary glands, Merck, Darmstadt, order nr. M3895-100MG), 1 ml of the mid exponential culture ( $OD_{600}$  0.4 – 0.6) was centrifuged at  $1,500 \times g$  for 15 min using a slow speed up and break protocol. The supernatant was removed, and the pellet resuspended to an  $OD_{600}$  of 6 in BHIS. From this, 10  $\mu$ l were added to a solution containing 36  $\mu$ l 10% PVP in PBS for a final concentration of 3.6% for 630 $\Delta$ *erm* (or 20  $\mu$ l 10% PVP in PBS for all other strains for a final concentration of 2%) and filled up to 100  $\mu$ l with PBS containing additives as specified. For mucin, a final concentration of 35 mg/ml mucin in PBS was used. From this, 4  $\mu$ l were used for video microscopy as described above. For 64x objective movies, a Leica DMR microscope with a PL APO 506082 63x objective was used. Movies were taken with a Nikon D7100 camera at 30 fps.

#### 6.4.5 YSMR settings

See the supplementary. In general, settings “supplementary S3\_tracking.rtf” were used, except for evaluating the video used for Figure 1a. There “supplementary S4\_tracking-100BHL.rtf” was used, as the very high frequency of turnarounds necessitated that the difference in frames used to calculate turnarounds is reduced. Except for figure 1a, all evaluations were done with the motile fraction. Motile bacteria were defined as those with a total travelled distance between turning points greater than 5 times their own cell length. Depiction of *C. difficile* population statistics analysis. Unless stated otherwise, only the motile fraction was used. In order to compare different experiments, we used kernel density estimate plots with a Gaussian kernel for displacement and speed. For displacement, a bin range between 0 and 220 was used, for speed a range between 0 and 20. In each case, we used 60 bins. All other settings remained as default as set in Seaborn v 0.10.0 ([doi.org/10.5281/zenodo.3629446](https://doi.org/10.5281/zenodo.3629446)). Turnarounds were grouped in steps of 0.2 per second and are depicted as a percentage of the total.

### 6.4.6 Insertion of *erm* into *cheY*

We used the ClosTron system to insertionally inactivate CheY in 630 $\Delta$ *erm* DSM 28645 as described in (Heap *et al.*, 2010). A detailed description is shown in Supplementary CheY Deletion. Live/Dead staining. Staining was performed as denoted in the LIVE/DEAD BacLight Bacterial Viability Kit (Invitrogen) manual, with the following changes: cells were prepared for video microscopy as described under “Video Microscopy with PVP”, except that the staining solutions were added to the 100  $\mu$ l bacterial solution. To check if the kit correctly identifies dead cells, one round was performed with cells, which were prior killed by incubation with ethanol. The kit correctly stained dead and live *C. difficile*.

## 6.5 Results

### 6.5.1 Quantification of *C. difficile* motility parameters

. We applied single cell video microscopy to analyse and quantify the motility characteristics of *C. difficile* under various conditions. A simple experimental setup was used, in which a cover slide was placed on a 4  $\mu$ l aliquot of bacteria in the medium to test, followed by immediate sealing with nail polish, in order to prevent further exposure to oxygen. For quantitative data of the *C. difficile* swimming parameters, we recorded video files and analysed a 10 s interval per detected bacteria with the aid of the recently developed bacterial tracking program YSMR (Schwanbeck *et al.*, 2020a). We used a low magnification objective (10x) for video recording in order to monitor the swimming behaviour of a large number of bacteria (100 - 1000) per video. YSMR is particularly suitable to generate tracking data from such a large number of bacteria. The following motility parameters were determined for each detected bacterium and its track: (i) average speed of the bacterium; (ii) net displacement of the bacterium from the start position; (iii) number of turnarounds within the track.

### 6.5.2 *C. difficile* swimming motility in BHIS medium

. When 630 $\Delta$ *erm* swimming behaviour was analysed in 100% BHI medium or in 10% BHI/PBS, the bacteria could be classified into two groups. A fraction of  $\sim 75$  % was completely non-motile, whereas the remaining  $\sim 25$  % displayed an unusual motility phenotype, which is characterised by alternating, short, forth and back run phases of 0.5-1 bacterial lengths, corresponding to 3–6  $\mu$ m (Movie S1). Forth and back run phases

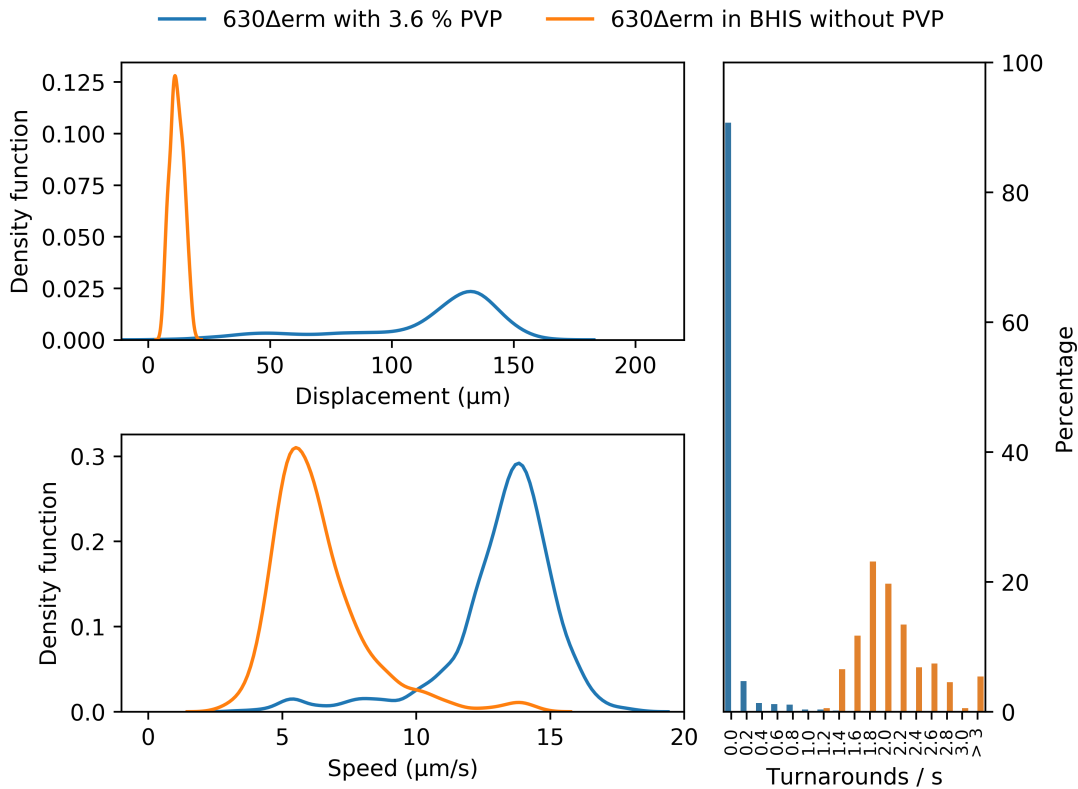


Figure 6.1: *C. difficile* 630 $\Delta$ erm motility parameter in the absence and presence of the high-molecular weight polymer PVP. Displacement, speed, and turnarounds in 10% BHIS/PBS without PVP ( $n = 343$ , orange line) and in 10% BHIS/PBS with 3.6% PVP ( $n = 1101$ , blue line).  $n$ : number of bacterial tracks included in motility parameter quantification by YSMR.



are indistinguishable in length and speed. The frequency of directional changes is very high with  $\sim 18$  turnarounds/10 s (section 6.5.3) and we thus refer to this behaviour as “jitter motility”. None of the bacteria displayed prolonged run phases and there is no substantial net displacement of the bacteria during movement (section 6.5.3). The motility of further five *C. difficile* strains from different clades was analysed under the same conditions. The clade 5 strain RT078, which is non-flagellated and non-motile in soft-agar assays was as expected completely lacking motile bacteria. All other tested strains, namely R20291 (clade 2), DSM 102860 (clade 3), DSM 28670 (clade 4), and DSM 29695 (clade 4) displayed the jitter-motility phenotype in BHI medium (data not shown). When  $630\Delta erm$  motility was analysed in 100% PBS instead of BHI medium, the jitter-motility fraction was absent and bacteria were completely non-motile.

### 6.5.3 The motility phenotype changes in the presence of the high molecular weight polymer PVP

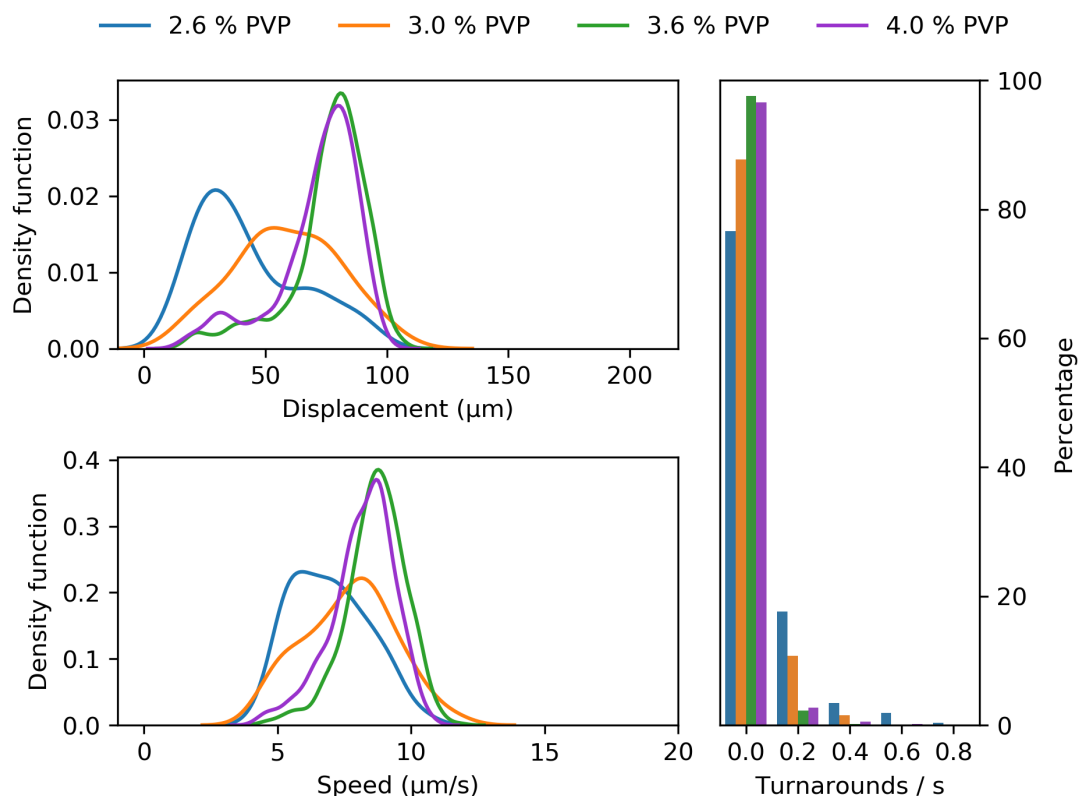


Figure 6.2: **Change of *C. difficile*  $630\Delta erm$  motility parameter at different PVP concentrations.** 2.6% PVP (blue,  $n = 264$ ); 3% PVP (orange,  $n = 65$ ); 3.6% PVP (green,  $n = 574$ ); 4% PVP (purple,  $n = 559$ ).  $n$ : number of bacterial tracks included in motility parameter quantification by YSMR.

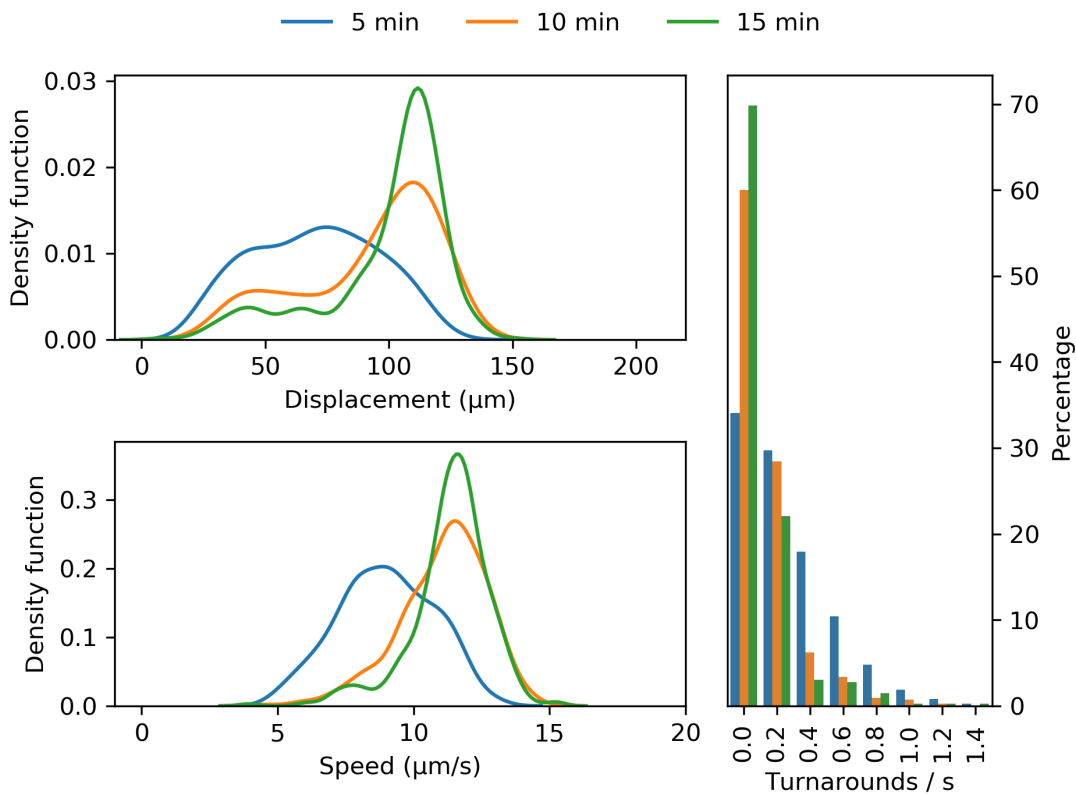


Figure 6.3: **Kinetics of PVP-induced motility parameter change in *C. difficile* 630 $\Delta$ erm.** Videos were taken from the same slide at the specified time after initial sealing of the cover slip. 5 min (blue,  $n = 307$ ); 10 min (orange,  $n = 230$ ), 15 min (green,  $n = 452$ ).  $n$ : number of bacterial tracks included in motility parameter quantification by YSMR.

High molecular weight polymers such as PVP were described to enhance motility in various bacteria in a concentration dependent manner (Greenberg and Canale-Parola, 1977, Schneider and Doetsch, 1974). When *C. difficile* was resuspended in a solution containing 3.6% PVP, bacteria displayed a dramatic change in motility behaviour (Movies S2 and S3). Length and duration of run phases were strongly increased, which leads to a sharp drop in the number of turnarounds. More than 90% of the bacteria displayed no turnarounds within 10 s in a 3.6% PVP solution. The PVP-induced change of the motility parameter is dose dependent and reaches a maximum at 3.6% PVP for 630 $\Delta$ *erm* (fig. 6.2). A kinetic of motility parameter after addition of 3.6% PVP reveals that maximum speed and displacement is reached after 10 min (fig. 6.3). The PVP-induced change of the motility phenotype occurred in all motile strains that we tested, including R20291 (clade 2), DSM 102860 (clade 3), DSM 28670 (clade 4), and DSM 29695 (clade 4) (data not shown). We wondered whether this change of the swimming pattern would also occur in the presence of high molecular weight polymers from the natural habitat of *C. difficile*. Natural high molecular weight polymers in the larger intestine are mucins, which cover the epithelial cell layer with a gel like structure. We tested *C. difficile* motility in a medium containing 35 mg/ml bovine mucin. Bacteria displayed under these conditions the same motility phenotype with long, alternating forward and backward run phases as in PVP (Movie S4).

#### 6.5.4 *C. difficile* displays a distinct motility phenotype

Exemplary tracks from a video (Movie S5) of 630 $\Delta$ *erm* as identified by the YSMR software are shown in fig. 6.4 A. A 1.8% PVP solution was chosen for this experiment, since in this concentration clear run phases are discernible, but turnarounds still occur often. The swimming motility phenotype in PVP is characterised by alternating forth and back run phases, which are indistinguishable in length and duration. There is a short stop between two run phases, but there is neither an obvious tumbling nor a sudden reorientation during the stop (fig. 6.4 B). Nevertheless, the direction of the back run can be different from the forth run. The curvature of tracks is independent of direction of travel and varies. This leads to a significant net displacement of the bacterium during movement. To exclude the possibility that the observed motility patterns are influenced by the relatively small distance between the microscope slide and the cover slide or the wall effect (Magariyama *et al.*, 2005), we monitored the swimming behaviour also on cavity slides. The same motility pattern as with the original setup was observed for experiments with and without PVP (data not shown).

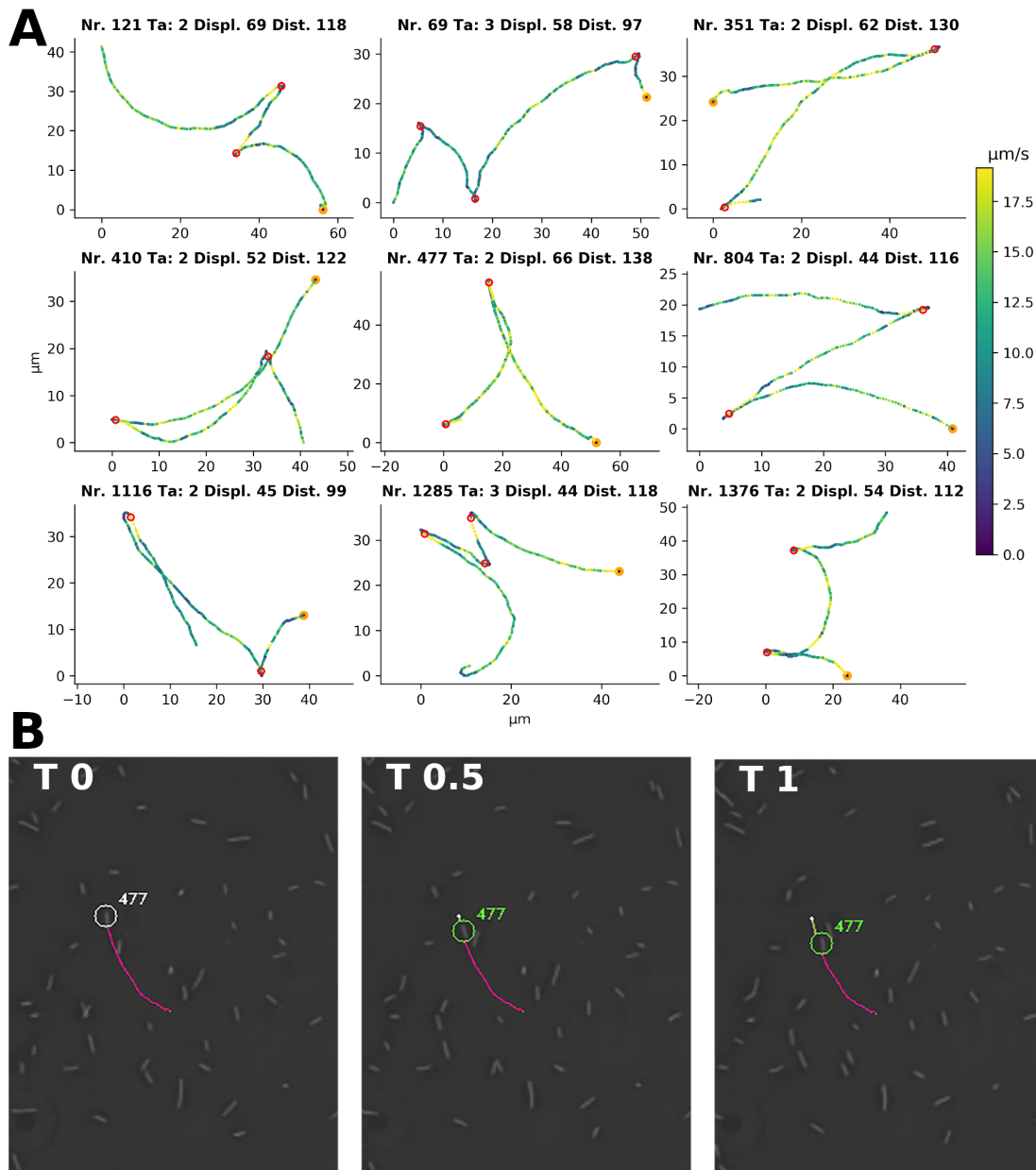


Figure 6.4: **Single cell motility of *C. difficile* 630 $\Delta$ erm in 1.8% PVP.** **A:** Representative single cell tracks from Movie S3 as detected by YSMR. Titles display track number, number of turnarounds (Ta), displacement (Displ.,  $\mu\text{m}$ ), and total travelled distance (Dist.,  $\mu\text{m}$ ) covered. Colour of the positions indicates speed at that time. The start of the track is marked in orange. Red circles show the positions for turnarounds. The bacteria associated with the displayed tracks are labelled in Movie S3. The formation of tracks is shown in Movie S3 by the extension of a coloured line behind the respective bacterium. **B:** A picture sequence taken from Movie S3 shows the first turnaround of track number 477, starting with the turnaround itself (0 s) and snapshots at 0.5 s and 1 s afterwards. The picture sequence shows the start of the backward movement without previous reorientation at the turnaround.

PVP leads to an increased viscosity of the medium and we thus wondered whether an increase in viscosity caused by a low molecular molecule such as glycerol had the same effect as PVP. 630 $\Delta$ *erm* were exposed to various glycerine concentrations from 0.05% to 25%. None of these conditions induced increased swimming motility as seen by PVP and the bacteria remained in their jitter-motility stage.

### 6.5.5 Dependency of *C. difficile* motility on the availability of various metabolites

We compared the motility parameter in 3.6% PVP solution in the presence of various metabolites that are known to play a role in *C. difficile* metabolism. Our standard PVP solution was supplemented with either (i) 2.2 mM glucose, (ii) a mixture of eight amino acids (alanine, proline, glutamine, valine, isoleucine, leucine, histidine, phenylalanine), each 5 mM, or (iii) 5 mM cysteine. Glucose and the mixture of eight amino acids had no effect on 630 $\Delta$ *erm* motility. Bacterial speed, net displacement, and frequency of turnarounds were unchanged (fig. 6.5 A, B). However, the addition of 5 mM cysteine reduced the average speed of the population with a peak at 8  $\mu$ m/s instead of 12  $\mu$ m/s. The net displacement was also reduced, while the frequency of turnarounds remained unchanged (fig. 6.6 A). In order to exclude the possibility that the reduction potential of cysteine could influence flagellar motility, we tested the effect of the strong reduction agent dithiothreitol (DTT) on *C. difficile* motility. All motility parameters remained unchanged in the presence of 10 mM DTT, suggesting that flagellar motility in *C. difficile* is unaffected by reducing agents at the tested concentrations (fig. S1). A live/dead staining was performed using LIVE/DEAD BacLight Bacterial Viability Kit (Invitrogen) to determine the viability of bacteria with and without cysteine. In each case, more than 98% of the bacteria showed green, but no red fluorescence, indicating that non-motile bacteria are largely viable. Since cysteine seems to influence *C. difficile* motility we wondered whether components of the chemotaxis system are involved in this regulation. 630 $\Delta$ *erm* contains a genomic region encoding for a complete chemosensory system (CD630\_05330 - CD630\_05410). CheY is usually a key player in chemotaxis systems and transduces the signal from the chemoreceptor to the flagellar motor complex (Porter *et al.*, 2011). The 630 $\Delta$ *erm* *cheY* is the first gene of the chemotaxis region (CD630\_05330) and we generated a *cheY* mutant by ClosTron mutagenesis (fig. S2). The motility of the *cheY* mutant was unaffected by cysteine (fig. 6.6 B), suggesting that an intact chemotaxis system is required for the cysteine dependent modulation of *C. difficile* motility. We attempted to restore the phenotype with a plasmid vector

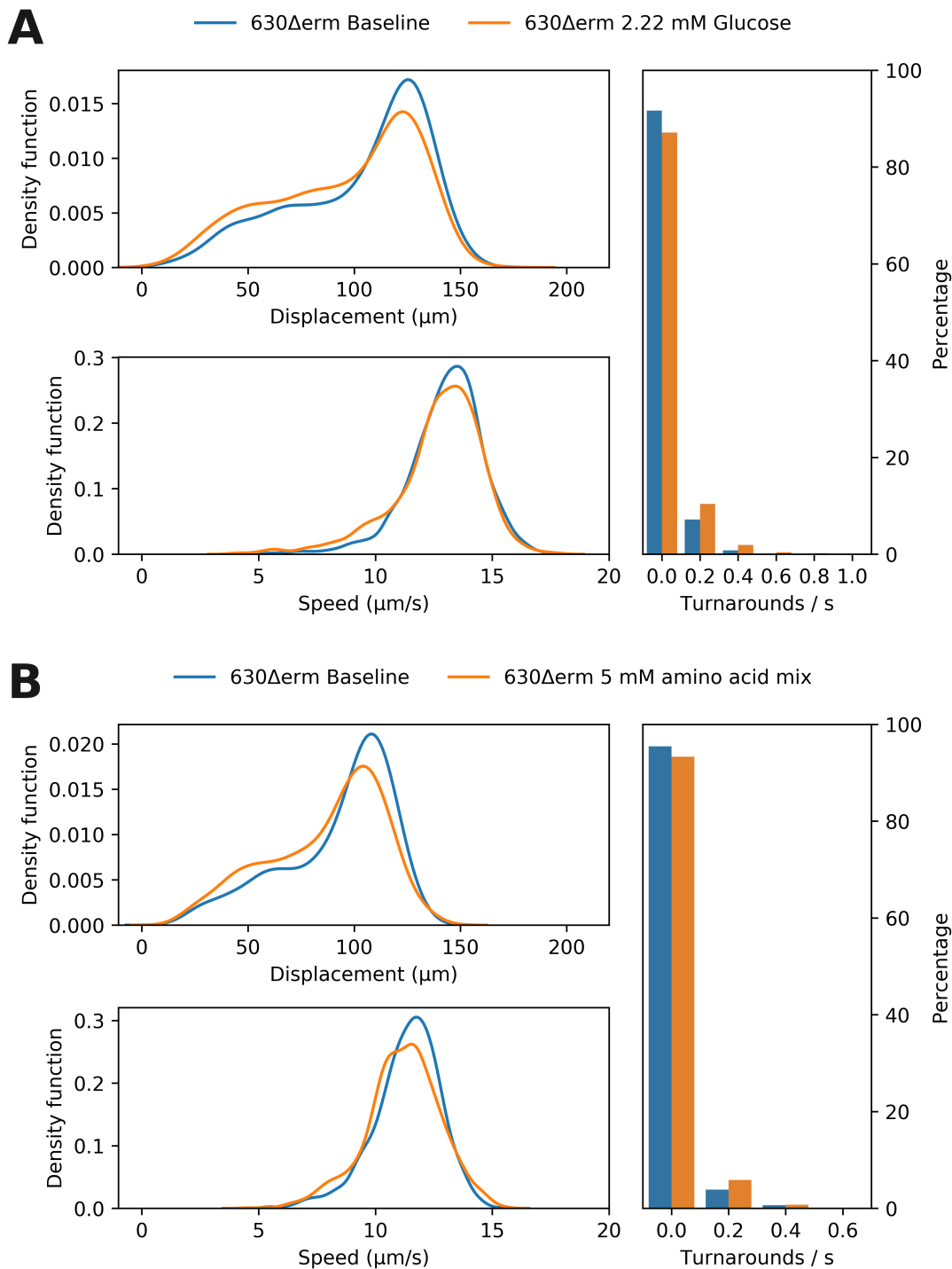


Figure 6.5: *C. difficile* 630 $\Delta$ erm motility parameters are neither affected by glucose nor by a mixture of 8 different amino acids. **A**: Motility parameters after addition of 2.22 mM Glucose (orange line,  $n = 1551$ ) in comparison to the regular setup without additional glucose (blue line,  $n = 1641$ ). **B**: Motility parameters after addition of 5 mM of each alanine, proline, glutamine, valine, isoleucine, leucine, histidine, phenylalanine (orange line,  $n = 1631$ ) in comparison to the regular setup without additional amino acids (blue line,  $n = 1733$ ).  $n$ : number of bacterial tracks included in motility parameter quantification by YSMR.

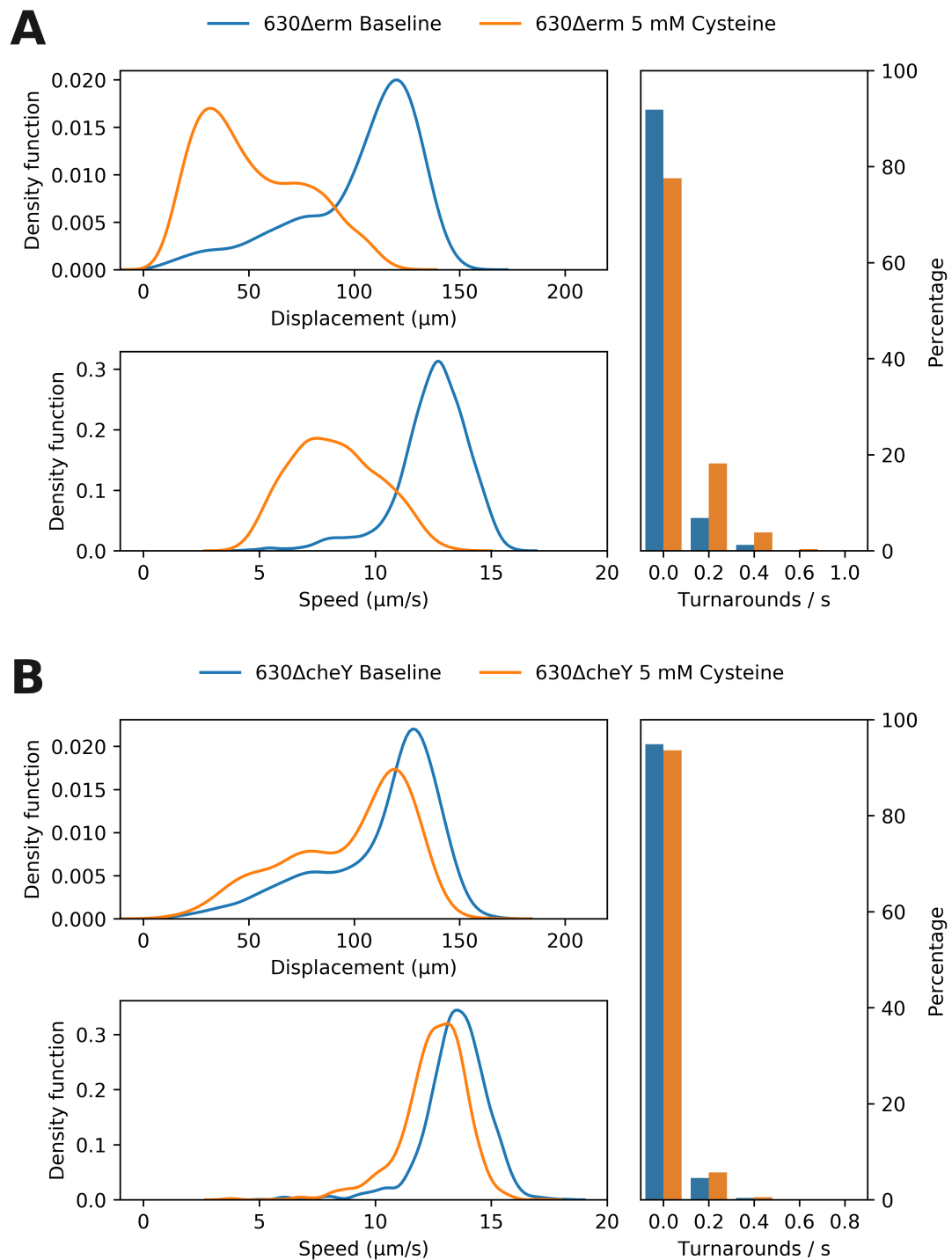


Figure 6.6: *C. difficile* swimming velocity is decreased by cysteine and this regulation depends on an intact chemotaxis system. **A**: Motility parameters after addition of 5 mM cysteine (orange line,  $n = 1363$ ) in comparison to the regular setup without additional cysteine (blue line,  $n=967$ ). **B**: *C. difficile* 630 *cheY::erm* with (orange line,  $n = 1578$ ) and without (blue line,  $n = 1759$ ) 5 mM cysteine. The velocity of the *cheY* knockout mutant is not reduced by cysteine.  $n$ : number of bacterial tracks included in motility parameter quantification by YSMR.

(pJS10, vector sequence in S2 CheY Deletion) that contains the *cheY* orf and 747 bp of the upstream region. However, complementation was not successful, since mutants harbouring this plasmid displayed the same unresponsiveness to cysteine as the  $\Delta cheY$  mutant. We did not further investigate the reason for this unresponsiveness. It is however conceivable that deletion of *cheY* had polar effects on downstream located genes of the chemotaxis operon.

## 6.6 Discussion

We used single cell video microscopy in conjunction with a software-based quantification of motility parameters to characterise the motility profile of *C. difficile* under various conditions. The applied YSMR software allowed the unbiased and automated analysis of a large number of tracks per frame.

*C. difficile* swimming motility with long run phases and a noticeable net displacement of bacteria was dependent on the presence of high molecular weight molecules such as PVP or mucin. Motility of bacteria in water-based medium without these compounds is characterised by short, forth and back movements at high frequency, which results in a trembling-like motility. This motility pattern appears to be futile, since no net displacement of the bacteria occurs. It is unclear whether this motility phenotype has any relevance for *C. difficile* physiology and it is possible that it does not occur under natural environmental conditions.

It is well investigated that flagellar motility of bacteria depends on the physical properties of the medium, for example on viscosity and on matrix elasticity (Gao *et al.*, 2014, Martinez *et al.*, 2014). Glycerol increases medium viscosity without affecting the matrix elasticity. A pure increase of viscosity by glycerol did not alter the swimming behaviour of *C. difficile*. However, increase of matrix elasticity by PVP or by mucins, which can form gel like structures, has a dramatic effect on *C. difficile* swimming motility. The most striking effect is the strong increase in the duration of run phases with > 90% of bacteria performing no turnarounds within 10 s, while in medium lacking high molecular weight additives > 90% of bacteria display  $\sim 15$  turnarounds within 10 s. In contrast, swimming speed is affected only moderately by PVP. These results suggest that viscoelasticity affects the *C. difficile* flagellar motor rotation state with a strong reduction of switching frequency in an environment of high matrix elasticity. Our findings lead to the conclusion that the motility apparatus in *C. difficile* is adapted to an environment of large, high molarity molecules. Such molecules can be found in the natural environment of *C. difficile*, for example in the mucin-rich lower intestines.



For further studies on single cell *C. difficile* motility in liquid media it appears thus advisable to work in the presence of high molecular weight molecules in order to avoid artificial results. In contrast, the viscoelastic properties of soft-agar seems to support *C. difficile* motility and soft-agar plate or tube assays were successfully applied in various motility studies on the population level (Stevenson *et al.*, 2015).

*C. difficile* displays a novel swimming strategy: Depending on the species and the number and location of flagella across the cell body, bacteria use different swimming strategies. At least four different swimming types are described in the literature, but none of them matches the observed *C. difficile* swimming strategy. The swimming pattern of the peritrichous flagellated model organism *E. coli* and its regulation is particularly well investigated. *E. coli* switches between a “run” mode and a “tumble” mode (Sarkar *et al.*, 2010). During the run mode, the counter-clockwise rotating flagella form a bundle that pushes the cell forward, leading to a straight swimming phase. In the “tumble” mode, the clockwise rotation of flagella leads to a breakup of the flagellar bundle followed by a random change of the cell orientation. Bacteria with a single flagellum, such as *Vibrio alginolyticus* and *Rhodobacter sphaeroides*, possess different swimming patterns. *V. alginolyticus* displays a three-step pattern, in which a forward swimming phase is followed by a reverse swimming phase and a reorientation (“flick”) phase (Stocker, 2011, Xie *et al.*, 2011). The flagellum of *R. sphaeroides* rotates in only one direction and the motility pattern follows a “stop and coil” pattern (Armitage and Macnab, 1987). Random reorientation occurs when the flagellar rotation stops. *Pseudomonas putida* produces a tuft of flagella on one cell pole. It can switch between a pushing mode, a pulling mode and a wrapping mode, with reorientation taking place during switches in modes (Hintsche *et al.*, 2017). The PVP-induced *C. difficile* motility pattern appears to be markedly different from those previously described. In particular, an obvious reorientation phase caused by a “tumble” or a “flick” appears to be absent. Instead, *C. difficile* stops in place at the end of a run phase and performs a  $\sim 180^\circ$  turnaround by changing the movement direction from forward to backward. Alternating forth and back run phases are comparable in length and speed, suggesting that *C. difficile* has no preferred direction of travel. Individual run phases can last for more than 10 s and can be highly curved. The curvature leads to a net displacement of the bacterium and prevents a return to the starting position after a forth and back run.

Nutrient dependency: We found that the velocity during run phases was reduced by cysteine. It was not affected by eight other tested amino acids, namely alanine, pro-

line, glutamine, valine, isoleucine, leucine, histidine and phenylalanine, and also not by glucose. *C. difficile* growth and virulence gene expression is strongly dependent on the nutritional availability in the environment and cysteine was shown to play a critical role for these processes. Amino acid utilisation studies revealed that cysteine, proline and leucine are the preferred carbon and energy sources in the growing state (Neumann-Schaal *et al.*, 2015). Cysteine availability was also shown to be critical during shift to the stationary phase (Hofmann *et al.*, 2018). A central role of cysteine availability for *C. difficile* physiology was demonstrated in transcriptomic studies. Regulation of various genes involved in energy metabolism, fermentation, transport, amino acid biosynthesis, stress response and iron acquisition was dependent on cysteine (Dubois *et al.*, 2016, Gu *et al.*, 2018). Furthermore, cysteine was shown to be involved in the modulation of virulence gene expression, for example toxin production was found to be reduced in the presence of cysteine (Karlsson *et al.*, 2000, Martin-Verstraete *et al.*, 2016).

Cysteine was also shown to reduce flagellar gene expression (Gu *et al.*, 2018). This suggests that cysteine influences *C. difficile* motility at least at two different levels: by reducing the swimming velocity and by reducing the transcript level of flagellar genes. A reduction in swimming velocity was also reported when *C. difficile* was exposed to high concentrations (32 mM) of N-acetylneuraminic acid (Courson *et al.*, 2019). These findings are in agreement with a *C. difficile* motility model in which the swimming velocity by default is at a maximum level and only decreased in the presence of molecules recognised by the chemotaxis system. This type of regulation would allow the bacterium to leave hostile environments as fast as possible and to enrich in favourable areas. Aside from its nutritional role, cysteine was also shown to play an important role for maintaining the redox status in the intestinal lumen. Cysteine is exported by enterocytes into the lumen, where it can be oxidised to cystine. The cysteine/cystine redox system is together with the glutathione and the thioredoxin system responsible for preserving tissue redox homeostasis (Circu and Aw, 2011). High cysteine levels might thus serve as an indicator for *C. difficile* to be localised at a preferred niche close to the intestinal epithelium.

Regulation of motility by the chemotaxis system is well investigated for a variety of bacterial species. Chemical gradients are sensed by chemoreceptors, which transfer the signal via the adapter protein CheW and the histidine kinase CheA to the transducer CheY, which becomes phosphorylated (Porter *et al.*, 2011). The phosphorylated CheY finally interacts with the flagellar motor and leads to a modulation of motility character-

istics. We could demonstrate with the aid of a *cheY* mutant that the cysteine-induced velocity reduction requires an intact chemotaxis system. Although the modulation of motility by the chemotaxis system is the expected result, the specific characteristics of this modulation and the mode of action of the involved components can vary from species to species. For example, phosphorylated CheY causes counterclockwise rotation of the flagella in *B. subtilis*, but clockwise rotation in *E. coli* (Rao *et al.*, 2008). The velocity of the *cheY* knockout mutant appears to be at maximum level without any responsiveness to the cysteine level as seen in the wild type. This would be consistent with a model in which the CheY-P interaction with the flagellar motor complex leads to a reduction in the rotation frequency of the flagellum, but not necessarily in a switch between clockwise and counter-clockwise rotation.

## 6.7 Appendix

### 6.7.1 Acknowledgements

We would like to thank Anna Klassen and Carina Fischer for their work with the *cheY* mutant strain.

### 6.7.2 Funding

This work was funded by the Federal State of Lower Saxony, Niedersächsisches Vorab (VWZN2889/3215/3266). This publication was funded by the Open Access support program of the Deutsche Forschungsgemeinschaft and the publication fund of the Georg August Universitaät Göttingen.

### 6.7.3 Transparency declaration

Nothing to declare.

### 6.7.4 Author contributions

Conceptualization, Julian Schwanbeck (JS), Wolfgang Bohne (WB), Ines Oehmig (IO); methodology, JS, IO, WB; software, JS; validation, JS, IO, WB; formal analysis, JS; investigation, JS, IO; resources, Uwe Groß (UG), Andreas E. Zautner (AEZ), WB; data curation, JS; writing—original draft preparation, JS, WB; writing-review and editing, JS, UG, AEZ, WB; visualization, JS; supervision, UG, AEZ, WB; project administration, UG, AEZ, WB; funding acquisition, UG.

**6.7.5 Supplementary data**

Movies S1 – S5, Fig. S1 – S2.

## Chapter 7

### Discussion

#### 7.1 Antibiotic Resistance in *Clostridioides difficile*

Rifaximin and Fidaxomicin are both effective drugs against *C. difficile*, and both components target the  $\beta$ -subunit of the RNA polymerase (*rpoB*). Rifaximin resistant mutant strains frequently occur, particularly in patients previously treated for Tuberculosis. The underlying mutations that confer Rifaximin-resistance differ to those conferring Fidaxomicin resistance, and binding studies indicate that binding sites of both drugs differ. In this study we have identified a so far undescribed *rpoB* allele which confers Rifaximin-resistance in patients from Indonesia. In contrast to Rifaximin, Fidaxomicin resistant isolates from patients are very rare so far. However, tolerance development against Fidaxomicin has previously been studied *in vitro*. These studies identified various sites of interest within the genome, which confer increased tolerance. The most notable site is a valine to aspartate mutation at position 1143 (V1143D) in *rpoB*, the  $\beta$ -subunit of the RNA polymerase. This conferred the highest tolerance towards Fidaxomicin, which was previously found to be  $> 32$  mg/L (Kuehne *et al.*, 2017). The mutation has been shown to be associated with several disadvantages for the cell, namely decreases in growth, maximal optical density, sporulation rates, as well as toxin A and B formation. This has led to the assumption that any *C. difficile* carrying such a tolerance would easily be out-competed, both by other organisms and by other *C. difficile* strains, and therefore not commonly occur (Kuehne *et al.*, 2017).

We screened a total of 50 isolates from patients with cases of severe CDI for Fidaxomicin tolerance. Two isolates from one patient were tolerant to all initially used concentrations of Fidaxomicin. We characterised the strains further and noted that their growth rate was comparable to the lab strain *C. difficile* 630 $\Delta$ *erm* as well as a more closely related strain DSM29678. Sequencing of the *rpoB* and *rpoC* locus, the  $\beta$ - and  $\beta'$ -subunits of the RNA polymerase, revealed that both isolates carry the *rpoB*<sub>V1143D</sub> mutation. The isolating of strains with an *rpoB*<sub>V1143D</sub> mutation from a patient with *C. difficile* symptoms and no growth defects is not only unexpected, but a worrying development, due to the previous predictions that this would be unlikely.

As the effect of an *rpoB*<sub>V1143D</sub> mutation was previously only assessed in a R20291 background, which is a widely used lab strain of *C. difficile*, we hypothesised that its

defects may be strain or clade specific (Kuehne *et al.*, 2017). We therefore repeated the insertion of the V1143D mutation in the  $\beta$ -subunit of the RNA polymerase of *C. difficile* 630 $\Delta$ *erm*, which belongs to clade 1, while R20291 belongs to clade 2. We obtained comparable results in growth rate, toxin formation and sporulation to the decreases observed in *C. difficile* R20291 *rpoB*<sub>V1143D</sub>, leading to the conclusion that the mutation deficits are likely strain and clade unspecific (Schwanbeck *et al.*, 2019).

This opens up the question how Goe-91 can maintain both its growth rate and Fidaxomicin tolerance. Sequencing of the Goe-91 genome showed no obvious characteristics that would explain its improved growth behaviour. In order to test if the compensation is caused by a single nucleotide polymorphism (SNP) an evolution experiment was performed on the *C. difficile* 630 $\Delta$ *erm* *rpoB*<sub>V1143D</sub> strain. For this purpose, *C. difficile* 630 $\Delta$ *erm* *rpoB*<sub>V1143D</sub> cultures were continuously re-inoculated with Fidaxomicin in the medium to exert selective pressure for Fidaxomicin tolerance. If a compensatory SNP causes improved growth rates, it can be developed again by individual bacteria over time. Given the resulting increase in growth rate, the strain will then out-compete others and subsequently dominate the medium. If the compensatory mutation is based on a SNP, we could then detect it by comparing the genome of the evolved strain to that of its progenitor strain. If no growth increase can be obtained this would indicate that the Goe-91 strain has received its compensatory mechanism by other means, for example horizontal gene transfer. Another possibility could be the need for multiple mutations, which would require a far longer time scale.

We started out with four independent replicates. After 16 days of continuous growth with Fidaxomicin, one strain showed an increase in OD<sub>600</sub> at the end of its growth period. The other strains were grown until day 20. We then measured the growth rate and compared it to the progenitor strain. Three of the four strains had a significant increase while the fourth strain was also faster than its progenitor, though not significantly so. The evolution experiment indicates that genetic changes are likely responsible for compensating the deficits caused by the *rpoB*<sub>V1143D</sub> mutation. The 16 to 20 days of continuous growth at a generation time of less than two hours comes down to more than two hundred bacterial generations. Adaptive mechanisms would likely result in an earlier increase in growth, as they would be present but dormant in the cells. Horizontal gene transfer can be excluded as three independent replicates showed a significantly increased growth rate without contact to other organisms. The variable time frame for growth increase to occur further indicates mutations.

Upon analysing the genomes of the evolved strains, we found various mutations,

though no congruent sites across all strains which would likely explain the observed phenotype. An increase in growth rate could potentially be achieved through various means. Since we sequenced only three strains, it is possible that each strain could have evolved a different compensatory mechanism. We have found four mutations of interest in total. Two mutation sites in the genes *bclA3* and CD630\_06320 were congruent across the strains, though are questionable, as both regions have repetitive sequences which are known to cause difficulty during sequencing. The protein BclA3 is an exosporangial glycoprotein. All evolved strains have deletions within in the range of 383 to 430 bp. Considering its characterised function, it is unlikely that BclA3 plays a large role during exponential growth. The hypothetical protein CD630\_06320 consists largely of alanine arginine repeats and has not been further characterised. The evolved strains and Goe-91 have deletions in this gene ranging from 30 to 78 bp. This leads to a frame shift in strains Evo\_1 and Evo\_2. Arginine repeats have been implicated as DNA and RNA binding regions, though more often in combination with glycine (Ntountoumi *et al.*, 2019). Determining the function of CD630\_06320 is unlikely to be helpful in our case, especially as the outcome of the mutation differs between the strains. We therefore disregarded the two congruent sites for the time being.

The strains Evo\_1 and Evo\_3, which each have a mutation in their RNA polymerase, could point in the direction of a possible compensatory mechanism. Evo\_1 has a proline 244 to threonine mutation in the  $\beta$ -subunit of the RNA polymerase. The area of the mutation consists of two prolines between two predicted alpha helices, which would change the angle between the helices. The helices are positioned close to the single stranded untranslated DNA strand which is guided through the RNA polymerase holoenzyme during transcription. The mutation in Evo\_2, glutamate 768 to valine in the  $\beta'$ -subunit of the RNA polymerase, changes the negative charge of the side chain. The predicted position is located close to the point in the RNA polymerase where the single stranded DNA anneals back into double stranded DNA. The change in charge could influence how the DNA is guided through the holoenzyme. Based on the assumption, that the *rpoB*<sub>V1143D</sub> mutation negatively impacts how the DNA is guided through the RNA polymerase, these mutations present themselves as obvious candidates warranting further investigation.

Both the Goe-91 and Evo\_2 strain have no additional mutations in the RNA polymerase. No further promising candidates for a compensatory mutation were found in either strain. It is possible that we overlooked mutations at promoter sites. While taken on its own the compensatory mechanism in Goe-91 could have been acquired through

horizontal gene transfer, the evolved mechanism in *Evo\_2* shows that this is unlikely. Instead, we believe that both strains have evolved a mechanism which is independent of further mutations in the RNA polymerase, but was not detected in this study.

The time frame in which the strains increased their growth rate during the evolution experiment should be viewed with concern. During the experiment we relied solely on natural mutation rates and did not add any mutagens. Current recommended Fidaxomicin course regimes are in the range of 10 to 14 days (Ooijevaar *et al.*, 2018). Extended-pulsed Fidaxomicin regimes have been tested, during which patients receive Fidaxomicin for a period of up to 25 days (Guery *et al.*, 2020, 2017). Considering the timeline, if a patient is infected with *C. difficile* and receives a prolonged Fidaxomicin regime, our evolutionary experiment could be replicated *in vivo*. Increases in tolerance against Fidaxomicin have already been achieved through a single high dose pulse of Fidaxomicin (Leeds, 2016). If the patient is either infected with a strain carrying the *rpoB*<sub>V1143D</sub> mutation or the mutation evolves *de novo*, the strain would then be positioned to grow without direct competition. Within the following 10 to 25 days, depending on the regimen, and given our demonstrated timetable, compensatory mutations can develop. The development of further Fidaxomicin tolerant strains is therefore simply a question of time.

In the ClosER study, which collected samples across Europe over a five year period, a single strain with increased tolerance towards Fidaxomicin was found (Freeman *et al.*, 2020). The strain harboured a Fidaxomicin tolerance above 4 mg/ml; with no specified upper limit. The tolerance mechanism was not discussed, but merits further investigation.

It has been shown that the concentration of Fidaxomicin in stool during treatment is at around 0.27 – 1 mg/g (Sears *et al.*, 2012, Zhanel *et al.*, 2015). Excepting for *rpoB*<sub>V1143D</sub>, *in vivo* concentration of Fidaxomicin have been used to question whether hitherto found tolerances warrant concern, as the concentrations far exceed the MICs (Leeds, 2016, Zhanel *et al.*, 2015). Generally, they do insofar as accumulation of minor tolerance effects against an antibiotic can result in a strong resistance (Wistrand-Yuen *et al.*, 2018). While this is a long-term scenario, it should nevertheless be regarded. In the specific case of the *rpoB*<sub>V1143D</sub> mutation the actual MIC for Fidaxomicin has not been determined (Kuehne *et al.*, 2017, Schwanbeck *et al.*, 2019). Our tested ceiling of 64 mg/ml was limited by precipitation of Fidaxomicin at higher concentrations (data not shown). Whether Goe-91 can grow *in vivo* during a course of Fidaxomicin has therefore not been determined, though it is questionable how much of the antibiotic is



active at concentrations above the solubility limit.

### 7.1.1 Outlook

Several open questions remain to be solved. First, the effect of the mutations in the RNA polymerase within strains Evo\_1 and Evo\_3 should be verified. The mutation can be introduced together with a *rpoB*<sub>V1143D</sub> point mutation into a *C. difficile* 630 $\Delta$ *erm* strain. If the resulting strain has a smaller growth defect than *C. difficile* 630 $\Delta$ *erm* *rpoB*<sub>V1143D</sub>, changes in the mechanical characteristics of the RNA polymerase caused by the second mutation should be further investigated. Secondly, the rate of translation efficiency of the base RNA polymerase variant, the *rpoB*<sub>V1143D</sub> mutation, as well as the double mutation observed in strains Evo\_1 and Evo\_3 could be compared. If feasible, X-ray crystallography of the doubly mutated polymerase in action could explain the mechanism in detail.

Elucidating the compensatory mechanisms of Goe-91 and Evo\_2 may be achieved by repeating the evolution experiment with more independent replicates. If further strains can be generated which lack additional mutations in the RNA polymerase, these can be compared for overlapping changes within their genome sequences.

At the time of writing, there are no EUCAST cut-off guidelines determining resistance levels for Fidaxomicin, though given the distribution of MICs in the currently described strains the cut-off values can be estimated. Nevertheless, setting guideline points is of importance, as this allows official allocation of strains into the categories susceptible, tolerant, and resistant. This would help in creating awareness of how problematic specific strains can be.

It should be noted that Fidaxomicin is metabolised to OP-1118, which also acts as a narrow-spectrum antibiotic. It is bactericidal against *C. difficile*, albeit at increased MIC levels (Babakhani *et al.*, 2011, Goldstein *et al.*, 2012). We did not test whether the *rpoB*<sub>V1143D</sub> mutation also confers resistance against OP-1118. It may be possible that some mutations have led to different MIC changes for the two compounds. Testing the Fidaxomicin tolerance mutations against OP-1118, as well as studying the interaction between the RNA-Polymerase and OP-1118 should be considered in future Fidaxomicin resistance research.

The antibiotic Rifaximin also targets the RNA polymerase and can be used against *C. difficile*, though currently only off-label within Germany (Shayto *et al.*, 2016). The resistance mechanism also consists of mutations in the RNA polymerase, though has a different site of action and does not come with strong negative side effects (Curry *et al.*,

2009, Dang *et al.*, 2016). We created a Fidaxomicin Rifaximin double resistant strain, which suffered from major growth defects and was barely viable (data not shown). As some resistance effects are mutually exclusive, it would be valuable to see if a doubly resistant strain can become viable over time. If it cannot, the combination should be considered in future therapeutic research.

## 7.2 Motility of single cell *Clostridioides difficile*

Previous studies describing motility most often employed an assay in which bacteria were inoculated either on or in media with low concentrations of agarose (Anjuwon-Foster and Tamayo, 2017, Baban *et al.*, 2013, Dingle *et al.*, 2011, Riedel *et al.*, 2017, Walter *et al.*, 2015). The assay works demonstrably well for the distinction between motile and non-motile strains. During our own initial experiments, we noted that results suffer from a considerable variance for motile *C. difficile* strains, not just between experiments but also within technical replicates (data not shown). Another option to measure motility and chemotactile behaviour is the chemical-in-plug assay. Effectors are placed via plugs on a medium in which bacteria are dispersed, which then aggregate around attractants or withdraw from repellents. However, this assay has been shown to be prone to false positive responses (Li *et al.*, 2010). During the outset, motility of *C. difficile* had not been described on a single cell level. We, therefore, saw this as an opportunity to address all three issues at once. Microscopy based observations would clearly demonstrate the ability for motility, allow for direct quantification on the single cell level, as well as provide the opportunity to analyse chemotactile behaviour. In addition, we could directly observe the result instead of relying on indirect cell counting measures as employed by other assays (Cerna-Vargas *et al.*, 2019, Law and Aitken, 2005, Li *et al.*, 2010). Due to the size and speed of *C. difficile*, we could evaluate a high number of observations per experiment, which would increase the statistical certainty within each replicate.

To take full advantage of video-based microscopy analysis, we required an automated evaluation system. Observations of several thousand bacteria per video were common but could not feasibly be tracked by hand. An automated system would also decrease the likelihood for inadvertent cherry picking. Currently available tracking software is mostly aimed at eukaryote or animal tracing, which usually involves monitoring various identifiers per tracked object. If used for our purposes, the large number of bacteria per frame in combination with the number of data points tracked for each bacterium adds up to unfeasible computational demands. A core requirement for animal and eukaryotic cells generally is the ability to recognise a previously lost object. This is useful when objects travel in and out of the field of vision, as it allows for continuous tracking and correct assignment without the need for subsequent manual correction. Due to their morphological similarity, however, distinction between individual cells with any degree of certainty is not possible in our case. We were therefore

able to forgo this requirement, and track cells based on their current and predicted position as well as their size. As now only few data points per cell need to be kept in the memory, tracking large numbers of cells per frame is a comparatively cheap operation, with regard to computational requirements. Due to the lower requirements, analysis can be performed on desktop PCs.

Detection of eukaryotes can likewise be a difficult or costly process, depending on the environmental background and target of interest. Here the experimental setup offers an easy solution in that bacteria are darker than the background. Object detection can therefore be done based on edge detection. Since the characteristics of the *C. difficile* shape can be measured beforehand, other objects can be excluded based on their general outline. A general advantage of the large number of tracked bacteria is that any exclusion criteria can be overzealous, as enough tracked objects will remain. Based on these criteria a tracking program, YSMR, was developed and released under GPL-3.0 (Schwanbeck *et al.*, 2020a).

It is now possible to analyse videos of motile single cells on a large scale with the aid of YSMR. Population based metrics can only indicate whether cells are motile, as well as providing rough metrics such as inhabited area after 24 hours. With microscopic analysis general observations about mode of motility, such as swarming or swimming motility, can be made. Single cell tracking further allows for detailed observations, such as changes in median speed, tumble frequency, percentage of motile cells, and general direction of travel.

The natural environment of viable *C. difficile* cells is the lower intestine, specifically the end of the ileum and the ascending colon. The colon is host to the largest fraction of the gastrointestinal microbiome, estimated at an order of  $10^{11}$  cells per ml. The high cell density is supported by the long retention time of stool, neutral pH, low bile acid concentration, and lack of Paneth cells excreting antimicrobial molecules (McGuckin *et al.*, 2011, Sender *et al.*, 2016). The mucus layer protecting the epithelial cells in the large intestine is divided into an outer and an inner layer. The inner layer, spanning 0.1 mm, is generally sterile. It consists of densely packed and cross-linked mucin which physically bars access to the epithelial layer. Upon perception of pathogens, new mucin layers can rapidly be released to try and displace them. The inner layer is converted to the outer layer by degradation of some of the cross-links via proteolytic cleavage. Despite degradation, the basic net-like structure of the mucins is maintained, which subsequently expands in volume. The outer layer is roughly 0.7 mm thick. Passable for bacteria, the outer layer is actively degraded by commensals for use as nutrient

source (Johansson *et al.*, 2011). *C. difficile* motility likely is adapted especially to its environment, as it is generally dormant outside of it. Its motility therefore needs to be effective in a medium consisting in large parts of long chained, net like structures.

All tested *C. difficile* strains showed either no motility, or an inexplicable phenotype in water-based media. If motile, cells move rapidly back and forth within a maximum range of two cell lengths which does not lead to a substantial displacement of the cell. This observation does not change noticeably with increased glycerol concentrations, except for a decrease in frequency of turnarounds. As mentioned earlier, *C. difficile* is motile in media containing low concentrations of agarose. Single cells within agarose blocks showed seemingly elongated travel paths under the microscope, though the maximal travel path was still shorter than one cell length (data not shown).

This led to the hypothesis, that *C. difficile* cannot swim in water based medium which has not the correct viscoelastic properties created by long chained molecules or net like structures. Polyvinylpyrrolidone (PVP) was tested as an alternative additive to agarose. PVP is a polymer with a molecular weight of 360 kDa that has previously been used in motility research and consists of very long hydrophilic chains (Greenberg and Canale-Parola, 1977, Martinez *et al.*, 2014). In its presence, *C. difficile* cells displayed a marked change in motility behaviour: cells did not twitch rapidly in place; instead, the distance covered per run phase far exceeded five cell lengths. Motile cells showed a steady speed throughout the run phase. After stopping, cells reversed and carried on in the opposite direction with no discernible preference for direction of travel.

The first takeaway from this result is that *C. difficile* is optimised to move through either a net like structure or media containing a framework of long chained molecules. Motility is specialised to such a degree, that outside of such an environment its motility malfunctions. Adding mucin to the medium had a comparable effect on the motility to that of PVP. As PVP seemingly replicates some of the same physical properties to those of mucin, it is reasonable to assume that *C. difficile* is optimised to swim in the mucin layer or other substrates containing high molecular weight polymers within the gastrointestinal tract.

Compared to the hitherto described motility patterns, the pattern of *C. difficile* appears to be novel. The model organisms *Escherichia coli* and *Bacillus subtilis* employ the well-known run and tumble pattern. During the run phase their flagella form a bundle, which propels the bacteria. During tumble events, the flagellar bundle disintegrates due to a change in rotational direction, resulting in free rotation of the flagella. This leads to a random course change, after which the next run phase starts. In *E. coli*

and *B. subtilis* the rotational direction of the flagellum is tied to the mode of motility: counter-clockwise rotation is associated with run phases, clockwise with the tumble (Rao *et al.*, 2008, Sarkar *et al.*, 2010). Besides the run and tumble pattern of *B. subtilis* and *E. coli*, other motility patterns have been described. The forward-reverse-flick of *Vibrio alginolyticus* is split into three phases. During forwards oriented travel long distances are covered. Reverse phases are short and without change in direction. When reverting to forward travel, the bacteria perform a flick to reorient the cell (Stocker, 2011, Xie *et al.*, 2011). *Rhodobacter sphaeroides* has a single flagellum which always rotates in the same direction. During a stop, the flagellum coils around the cell and reorients the bacterium (Armitage and Macnab, 1987). *Pseudomonas putida* employs three different run modes: push, pull, and wrap, with reorientations occurring during mode switches (Hintsche *et al.*, 2017).

Each of these patterns has a reorientation event which occurs either during a stop-phase, or during a phase switch. Such a dedicated event seems to be lacking in *C. difficile*. Forward and backward travel phases have a similar curvature on average, while turnaround events do not lead to strong reorientation. The observed motility pattern of *C. difficile* does not fit well with any of the hitherto described models.

We therefore postulate that *C. difficile* has a novel motility pattern consisting of run and turnaround phases. The run phases, which have a variable curvature and are not associated with a particular heading, prevent a back-and-forth in one place. Turnaround-phases are likewise without a strong tumbling effect and lead to a reversal in travel direction (Schwanbeck *et al.*, 2020b).

The motility of pathogens can generally serve three distinct goals: to reach the preferred site of infection, to avoid an unfavourable environment, or to disperse in order to find a new host. The motility phenotype of *C. difficile* does not properly fit into the first two categories. Both require some form of chemotactile behaviour. However, chemotaxis in bacteria generally involves tumbling events, which change the heading of the cell. The frequency of the tumble events allows bacteria to head in the right direction. The turnarounds, which invert the travel direction of *C. difficile*, appear to occur without preference of direction or difference in curvature between travel directions. Based on the turnaround events, it could therefore be assumed, that *C. difficile* uses its motility for dispersal.

When testing the effect of additives on the motility behaviour, we noted that *C. difficile* had a strongly reduced velocity in the presence of 5 mM cysteine with a resulting net reduction in displacement. Adding 5 mM of the amino acids alanine, proline, glu-

tamine, valine, isoleucine, leucine, histidine and phenylalanine had no influence, nor did tripling the glucose concentration in the medium. These additives were selected as they are metabolised by *C. difficile* or were previously described to influence motility on a regulatory level. Addition of dithiothreitol, a further reducing agent, or Glutathione showed no effect (Schwanbeck *et al.* (2020b), data not shown). The redox potential of cysteine can therefore likely be excluded as the reason for the difference in motility. A *C. difficile* strain lacking *cheY*, the diffusible secondary messenger in the chemotaxis pathway, showed no response to increases in cysteine in the medium.

The phenotype of the *C. difficile*  $\Delta cheY$  mutant shows that the role of phosphorylated CheY (CheY-p) is likely different in *C. difficile*, as the role described in *E. coli* and *B. subtilis*. The role of CheY-p, the intracellular secondary messenger, differs in both organisms. In *E. coli*, CheY-p leads to clockwise rotation and therefore a tumbling event, whereas in *B. subtilis* CheY-p leads to counter-clockwise rotation (Rao *et al.*, 2008, Sarkar *et al.*, 2010, Ward *et al.*, 2019). In *C. difficile* without a functional chemotaxis system, the velocity is always at maximum level, whereas the intact chemotaxis system in the wild type responds to attractants by a decrease in speed. Instead of affecting the rotational direction of the flagellum, which likely would influence either the turnarounds or lead to another observable change in motility behaviour, the velocity of the bacterium is affected. We therefore postulate, that changes in CheY-p concentration lead to a change in rotation rate of the flagella rather than a stop phase, switch in rotational direction, or other mode switch.

The change in motility behaviour affected by cysteine poses the question if it is conducive to a form of chemotaxis, or if it serves a different purpose. As previously discussed, the run-turnaround motility pattern is conceivably ill suited for a chemotactile process. A decrease in speed keeps the cell in the vicinity of the attractant, but does not help in navigating the cell towards it.

Cysteine plays a key role in the redox system of the lumen within the gastrointestinal tract. Glutathione is the main conductor for establishment of a redox potential on the lumen-side. It is a tripeptide consisting of glutamate, cysteine, and glycine with a gamma link between glutamate and cysteine. Glutathione can be degraded into its amino acids through  $\gamma$ -glutamyl transferase and dipeptidase-catalyzed hydrolysis. It is oxidised to Glutathione-disulphide as part of the redox system of the lower intestine. Glutathione-disulphide is reduced to glutathione by cysteine, which is further oxidised to cystine. The cysteine concentration is maintained by export from the epithelial cells (Circu and Aw, 2011). Cysteine is therefore present near the epithelial cell surface

through export and glutathione degradation, and may serve as a positional indicator for *C. difficile*. If this is the case, the deceleration of *C. difficile* could be used to give it time to attach to the cell surface.

Taken together, it can be hypothesised that the motility pattern of *C. difficile* is employed for a stochastic search aimed at cell surface attachment in a mucin rich environment. The curvature during run phases and intermittent turnarounds lead to continuous reorientation while the turnarounds help prevent cells from getting stuck. If a *C. difficile* cell detects an increase in cysteine it slows down and subsequently attaches to the cell surface. The motility pattern of *C. difficile* therefore plays a significant role in its pathogenicity.

### 7.2.1 Outlook

All clade 5 strains of *C. difficile* seem to have lost the motility operon, yet retained a functional chemotaxis operon (data not shown). As no sequenced clade 5 strain appears to have nonsense mutations in the chemotaxis operon, it seems likely that it still serves a purpose. Regulation of motility in *C. difficile* is closely linked to pathogenicity through c-di-GMP,  $\sigma^D$ , and the regulatory RNA Cdi4 (Anjuwon-Foster and Tamayo, 2017, El Meouche *et al.*, 2013, McKee *et al.*, 2018b, 2013, Purcell *et al.*, 2012). It would therefore be of interest to investigate the possibility whether the chemotaxis pathway is used as a sensory system for other intracellular processes besides motility, and if pathogenicity factors are involved.

While the *cheY* deletion phenotype is currently not confirmed through ectopic expression, it is possible that the deletion has unintended up-/downstream effects. Fusing larger parts or the entire chemotaxis operon into a plasmid might alleviate this issue. Optionally, the deletion and ectopic expression could be performed in another strain for confirmation.

The role of the chemotaxis receptor of *C. difficile* remains unknown. Its interaction with cysteine should be checked by expressing and purifying the MCP binding domain and performing isothermal titration calorimetry including putative interaction partners. Its position may be investigated by expressing a PhiLov tagged variant and performing fluorescence microscopy (Buckley *et al.*, 2016).

To our knowledge, the only current other study on *C. difficile* motility was published by Courson *et al.* (Courson *et al.*, 2019). Their findings are fundamentally different to ours, as they were able to observe motile *C. difficile* cells without PVP or equivalent substances in the medium. As, to our knowledge, the study is based on only one strain,



the differences could perceivably arise from strain specific differences. Their other main result, the change in speed due to *N*-acetylneuraminic acid, could not be replicated in our experiments (data not shown). Comparing their strain in our setup and vice versa may provide further insight into the underlying causes.



# List of Figures

1.1	Original microscopy pictures of <i>C. difficile</i> from Hall and O'Toole . . . . .	2
2.1	Growth curves of strain Goe-91 and <i>C. difficile</i> 630 $\Delta$ erm rpoB <sub>V1143D</sub> . . . . .	22
2.2	Toxin & Spore production . . . . .	23
3.1	Frequency distribution of MIC [RFX] in <i>C. difficile</i> isolates . . . . .	30
3.2	Scheme of the Antimicrobial Susceptibility Testing workflow . . . . .	35
4.1	Doubling rate per hour of FDX resistant strains . . . . .	43
4.2	rpoB mutation site of strain Evo_3 . . . . .	44
4.3	rpoC mutation site of strain Evo_2 . . . . .	45
5.1	From original frame to final detection in YSMR . . . . .	54
6.1	<i>C. difficile</i> motility in the absence and presence of PVP . . . . .	66
6.2	<i>C. difficile</i> motility parameter at different PVP concentrations . . . . .	67
6.3	Kinetics of PVP-induced motility parameter change in <i>C. difficile</i> . . . . .	68
6.4	Single cell motility of <i>C. difficile</i> in 1.8% PVP . . . . .	70
6.5	<i>C. difficile</i> motility parameters are neither affected by glucose nor by a mixture of 8 different amino acids. . . . .	72
6.6	<i>C. difficile</i> swimming velocity is decreased by cysteine . . . . .	73



## References

- Abt, M. C., McKenney, P. T., and Pamer, E. G. 2016. *Clostridium difficile* colitis: pathogenesis and host defence. *Nat. Rev. Microbiol.*, **14**(10):609–620.
- Ajami, N. J., Cope, J. L., Wong, M. C., Petrosino, J. F., and Chesnel, L. 2018. Impact of oral fidaxomicin administration on the intestinal microbiota and susceptibility to *Clostridium difficile* colonization in mice. *Antimicrob. Agents Chemother.*, **62**(February):AAC.02112–17.
- Aktories, K., Papatheodorou, P., and Schwan, C. 2018. Binary *Clostridium difficile* toxin (CDT) - A virulence factor disturbing the cytoskeleton. *Anaerobe*, **53**:21–29.
- Al-Nassir, W. N., Sethi, A. K., Li, Y., Pultz, M. J., Riggs, M. M., and Donskey, C. J. 2008. Both Oral Metronidazole and Oral Vancomycin Promote Persistent Overgrowth of Vancomycin-Resistant Enterococci during Treatment of *Clostridium difficile*-Associated Disease. *Antimicrob. Agents Chemother.*, **52**(7):2403–2406.
- Al Saif, N. and Brazier, J. S. 1996. The distribution of *Clostridium difficile* in the environment of South Wales. *J. Med. Microbiol.*, **45**(2):133–137.
- Albenberg, L., Esipova, T. V., Judge, C. P., Bittinger, K., Chen, J., Laughlin, A., Grunberg, S., Baldassano, R. N., Lewis, J. D., Li, H., Thom, S. R., Bushman, F. D., Vinogradov, S. A., and Wu, G. D. 2014. Correlation Between Intraluminal Oxygen Gradient and Radial Partitioning of Intestinal Microbiota. *Gastroenterology*, **147**(5):1055–1063.e8.
- Anjuwon-Foster, B. R. and Tamayo, R. 2017. A genetic switch controls the production of flagella and toxins in *Clostridium difficile*. *PLOS Genet.*, **13**(3):e1006701.
- Antunes, L. C. M., Han, J., Ferreira, R. B. R., Lolić, P., Borchers, C. H., and Finlay, B. B. 2011. Effect of Antibiotic Treatment on the Intestinal Metabolome. *Antimicrob. Agents Chemother.*, **55**(4):1494–1503.
- Armitage, J. P. and Macnab, R. M. 1987. Unidirectional, intermittent rotation of the flagellum of *Rhodobacter sphaeroides*. *J. Bacteriol.*, **169**(2):514–518.
- Artsimovitch, I., Seddon, J., and Sears, P. 2012. Fidaxomicin is an inhibitor of the initiation of bacterial RNA synthesis. *Clin. Infect. Dis.*, **55**(SUPPL.2):127–131.

- Babakhani, F., Gomez, A., Robert, N., and Sears, P. 2011. Killing kinetics of fidaxomicin and its major metabolite, OP-1118, against *Clostridium difficile*. *J. Med. Microbiol.*, **60**(8):1213–1217.
- Babakhani, F., Seddon, J., and Sears, P. 2014. Comparative microbiological studies of transcription inhibitors fidaxomicin and the rifamycins in *Clostridium difficile*. *Antimicrob. Agents Chemother.*, **58**(5):2934–2937.
- Baban, S. T., Kuehne, S. A., Barketi-Klai, A., Cartman, S. T., Kelly, M. L., Hardie, K. R., Kansau, I., Collignon, A., and Minton, N. P. 2013. The Role of Flagella in *Clostridium difficile* Pathogenesis: Comparison between a Non-Epidemic and an Epidemic Strain. *PLoS One*, **8**(9).
- Bandelj, P., Harmanus, C., Blagus, R., Cotman, M., Kuijper, E. J., Ocepek, M., and Vengust, M. 2018. Quantification of *Clostridioides (Clostridium) difficile* in feces of calves of different age and determination of predominant *Clostridioides difficile* ribotype 033 relatedness and transmission between family dairy farms using multilocus variable-number ta. *BMC Vet. Res.*, **14**(1):1–10.
- Bastos-Arrieta, J., Revilla-Guarinos, A., Uspal, W. E., and Simmchen, J. 2018. Bacterial Biohybrid Microswimmers. *Front. Robot. AI*, **5**(August):1–16.
- Batah, J., Kobeissy, H., Bui Pham, P. T., Denève-Larrazet, C., Kuehne, S., Collignon, A., Janoir-Jouveshomme, C., Marvaud, J.-C., and Kansau, I. 2017. *Clostridium difficile* flagella induce a pro-inflammatory response in intestinal epithelium of mice in cooperation with toxins. *Sci. Rep.*, **7**(1):3256.
- Boin, M. A., Austin, M. J., and Håase, C. C. 2004. Chemotaxis in *Vibrio cholerae*. *FEMS Microbiol. Lett.*, **239**(1):1–8.
- Bradshaw, W. J., Roberts, A. K., Shone, C. C., and Acharya, K. R. 2018. The structure of the S-layer of *Clostridium difficile*. *J. Cell Commun. Signal.*, **12**(1):319–331.
- Brown, K. A., Khanafer, N., Daneman, N., and Fisman, D. N. 2013. Meta-Analysis of Antibiotics and the Risk of Community-Associated *Clostridium difficile* Infection. *Antimicrob. Agents Chemother.*, **57**(5):2326–2332.
- Buckley, A. M., Jukes, C., Candlish, D., Irvine, J. J., Spencer, J., Fagan, R. P., Roe, A. J., Christie, J. M., Fairweather, N. F., and Douce, G. R. 2016. Lighting Up *Clostridium difficile*: Reporting Gene Expression Using Fluorescent Lov Domains. *Sci. Rep.*, **6**:23463.

- Buffie, C. G., Bucci, V., Stein, R. R., McKenney, P. T., Ling, L., Gobourne, A., No, D., Liu, H., Kinnebrew, M., Viale, A., Littmann, E., van den Brink, M. R. M., Jenq, R. R., Taur, Y., Sander, C., Cross, J. R., Toussaint, N. C., Xavier, J. B., and Pamer, E. G. 2015. Precision microbiome reconstitution restores bile acid mediated resistance to *Clostridium difficile*. *Nature*, **517**(7533):205–8.
- Burdet, C., Nguyen, T. T., Duval, X., Ferreira, S., Andremont, A., Guedj, J., and Mentré, F. 2019. Impact of antibiotic gut exposure on the temporal changes in microbiome diversity. *Antimicrob. Agents Chemother.*, **63**(10):1–11.
- Calabi, E., Calabi, F., Phillips, A. D., and Fairweather, N. F. 2002. Binding of *Clostridium difficile* Surface Layer Proteins to Gastrointestinal Tissues. *Infect. Immun.*, **70**(10):5770–5778.
- Campbell, E. A., Korzheva, N., Mustaev, A., Murakami, K., Nair, S., Goldfarb, A., and Darst, S. A. 2001. Structural Mechanism for Rifampicin Inhibition of Bacterial RNA Polymerase. *Cell*, **104**(6):901–912.
- Cassini, A., Plachouras, D., Eckmanns, T., Abu Sin, M., Blank, H.-P., Ducomble, T., Haller, S., Harder, T., Klingeberg, A., Sixtensson, M., Velasco, E., Weiß, B., Kramarz, P., Monnet, D. L., Kretzschmar, M. E., and Suetens, C. 2016. Burden of Six Healthcare-Associated Infections on European Population Health: Estimating Incidence-Based Disability-Adjusted Life Years through a Population Prevalence-Based Modelling Study. *PLOS Med.*, **13**(10):e1002150.
- Cerna-Vargas, J. P., Santamaría-Hernando, S., Matilla, M. A., Rodríguez-Herva, J. J., Daddaoua, A., Rodríguez-Palenzuela, P., Krell, T., and López-Solanilla, E. 2019. Chemoperception of Specific Amino Acids Controls Phytopathogenicity in *Pseudomonas syringae* pv. tomato. *MBio*, **10**(5):1–14.
- Chandrasekaran, R. and Lacy, D. B. 2017. The role of toxins in *Clostridium difficile* infection. *FEMS Microbiol. Rev.*, **41**(6):723–750.
- Chilton, C. H., Crowther, G. S., Ashwin, H., Longshaw, C. M., and Wilcox, M. H. 2016. Association of Fidaxomicin with *C. difficile* Spores: Effects of Persistence on Subsequent Spore Recovery, Outgrowth and Toxin Production. *PLoS One*, **11**(8):e0161200.
- Chlebek, J. L., Hughes, H. Q., Ratkiewicz, A. S., Rayyan, R., Wang, J. C.-Y., Herrin, B. E., Dalia, T. N., Biais, N., and Dalia, A. B. 2019. PilT and PilU are homohexameric ATPases that coordinate to retract type IVa pili. *PLOS Genet.*, **15**(10):e1008448.

- Circu, M. L. and Aw, T. Y. 2011. Redox biology of the intestine. *Free Radic. Res.*, **45**(11-12):1245–1266.
- Cluzel, P., Surette, M., and Leibler, S. 2000. An ultrasensitive bacterial motor revealed by monitoring signaling proteins in single cells. *Science*, **287**(5458):1652–5.
- Collins, D. A., Hawkey, P. M., and Riley, T. V. 2013. Epidemiology of *Clostridium difficile* infection in Asia. *Antimicrob. Resist. Infect. Control*, **2**(1):21.
- Courson, D. S., Pokhrel, A., Scott, C., Madrill, M., Rinehold, A. J., Tamayo, R., Cheney, R. E., and Purcell, E. B. 2019. Single cell analysis of nutrient regulation of *Clostridioides (Clostridium) difficile* motility. *Anaerobe*, **59**:205–211.
- Crobach, M. J. T., Vernon, J. J., Loo, V. G., Kong, L. Y., Péchiné, S., Wilcox, M. H., and Kuijper, E. J. 2018. Understanding *Clostridium difficile* Colonization. *Clin. Microbiol. Rev.*, **31**(2):e00021–17.
- Curry, S. R. R., Marsh, J. W. W., Shutt, K. A. A., Muto, C. A. A., O’Leary, M. M. M., Saul, M. I. I., Pasculle, A. W. W., and Harrison, L. H. H. 2009. High Frequency of Rifampin Resistance Identified in an Epidemic *Clostridium difficile* Clone from a Large Teaching Hospital. *Clin. Infect. Dis.*, **48**(4):425–429.
- Dang, U. T., Zamora, I., Hevener, K. E., Adhikari, S., Wu, X., and Hurdle, J. G. 2016. Rifamycin resistance in *Clostridium difficile* is generally associated with a low fitness burden. *Antimicrob. Agents Chemother.*, **60**(9):5604–5607.
- Dannheim, H., Riedel, T., Neumann-Schaal, M., Bunk, B., Schober, I., Spröer, C., Chibani, C. M., Gronow, S., Liesegang, H., Overmann, J., and Schomburg, D. 2017. Manual curation and reannotation of the genomes of *Clostridium difficile* 630 $\Delta$ erm and *Clostridium difficile* 630. *J. Med. Microbiol.*, **66**(3):286–293.
- De Gunzburg, J., Ghozlane, A., Ducher, A., Le Chatelier, E., Duval, X., Ruppé, E., Armand-Lefevre, L., Sablier-Gallis, F., Burdet, C., Alavoine, L., Chachaty, E., Augustin, V., Varastet, M., Levenez, F., Kennedy, S., Pons, N., Mentré, F., and Andremont, A. 2018. Protection of the human gut microbiome from antibiotics. *J. Infect. Dis.*, **217**(4):628–636.
- Debast, S., Bauer, M., and Kuijper, E. 2014. European Society of Clinical Microbiology and Infectious Diseases: Update of the Treatment Guidance Document for *Clostridium difficile* Infection. *Clin. Microbiol. Infect.*, **20**(S2):1–26.



- Dharmasena, M. and Jiang, X. 2018. Isolation of Toxigenic *Clostridium difficile* from Animal Manure and Composts Being Used as Biological Soil Amendments. *Appl. Environ. Microbiol.*, **84**(16):1–12.
- Di Bella, S., Ascenzi, P., Siarakas, S., Petrosillo, N., and di Masi, A. 2016. *Clostridium difficile* Toxins A and B: Insights into Pathogenic Properties and Extraintestinal Effects. *Toxins (Basel)*, **8**(5):134.
- Dingle, T. C., Mulvey, G. L., and Armstrong, G. D. 2011. Mutagenic Analysis of the *Clostridium difficile* Flagellar Proteins, FliC and FliD, and Their Contribution to Virulence in Hamsters. *Infect. Immun.*, **79**(10):4061–4067.
- Drózdź, M., Biesiada, G., Piątek, A., Świstek, M., Michalak, M., Stażyk, K., Garlicki, A., and Czepiel, J. 2018. Analysis of risk factors and outcomes of *Clostridium difficile* infection. *Folia Med. Cracov.*, **58**(4):105–116.
- Dubois, T., Dancer-Thibonnier, M., Monot, M., Hamiot, A., Bouillaut, L., Soutourina, O., Martin-Verstraete, I., and Dupuy, B. 2016. Control of *Clostridium difficile* Physiopathology in Response to Cysteine Availability. *Infect. Immun.*, **84**(8):2389–2405.
- Edwards, A. N., Karim, S. T., Pascual, R. A., Jowhar, L. M., Anderson, S. E., and McBride, S. M. 2016. Chemical and Stress Resistances of *Clostridium difficile* Spores and Vegetative Cells. *Front. Microbiol.*, **7**(OCT):1–13.
- El Meouche, I., Peltier, J., Monot, M., Soutourina, O., Pestel-Caron, M., Dupuy, B., and Pons, J. L. 2013. Characterization of the SigD regulon of *C. difficile* and its positive control of toxin production through the regulation of *tcdR*. *PLoS One*, **8**(12):1–17.
- Engelmann, T. W. 1882. Ueber Sauerstoffausscheidung von Pflanzenzellen im Mikrospektrum. *Pflüger, Arch. für die Gesamte Physiol. des Menschen und der Thiere*, **27**(1):485–489.
- Eyre, D. W., Babakhani, F., Griffiths, D., Seddon, J., Del Ojo Elias, C., Gorbach, S. L., Peto, T. E. A., Crook, D. W., and Walker, A. S. 2014. Whole-genome sequencing demonstrates that fidaxomicin is superior to vancomycin for preventing reinfection and relapse of infection with *Clostridium difficile*. *J. Infect. Dis.*, **209**(9):1446–51.
- Faust, L., Ruhwald, M., Schumacher, S., and Pai, M. 2020. How are high burden countries implementing policies and tools for latent tuberculosis infection? A survey of current practices and barriers. *Heal. Sci. Reports*, **3**(2).

- Freeman, J., Vernon, J., Pilling, S., Morris, K., Nicolson, S., Shearman, S., Clark, E., Palacios-Fabrega, J. A., and Wilcox, M. 2020. Five-year Pan-European, longitudinal surveillance of *Clostridium difficile* ribotype prevalence and antimicrobial resistance: the extended ClosER study. *Eur. J. Clin. Microbiol. Infect. Dis.*, **39**(1):169–177.
- Gao, Y., Neubauer, M., Yang, A., Johnson, N., Morse, M., Li, G., and Tang, J. X. 2014. Altered motility of *Caulobacter crescentus* in viscous and viscoelastic media. *BMC Microbiol.*, **14**(1):322.
- Gettelfinger, B. and Cussler, E. L. 2004. Will humans swim faster or slower in syrup? *AIChE J.*, **50**(11):2646–2647.
- Goldstein, E. J. C., Babakhani, F., and Citron, D. M. 2012. Antimicrobial activities of fidaxomicin. *Clin. Infect. Dis.*, **55**(SUPPL.2):143–148.
- Goldstein, E. J. C., Citron, D. M., Sears, P., Babakhani, F., Sambol, S. P., and Gerding, D. N. 2011. Comparative Susceptibilities to Fidaxomicin (OPT-80) of Isolates Collected at Baseline, Recurrence, and Failure from Patients in Two Phase III Trials of Fidaxomicin against *Clostridium difficile* Infection. *Antimicrob. Agents Chemother.*, **55**(11):5194–5199.
- Gómez, S., Chaves, F., and Orellana, M. A. 2017. Clinical, epidemiological and microbiological characteristics of relapse and re-infection in *Clostridium difficile* infection. *Anaerobe*, **48**:147–151.
- Greenberg, E. P. and Canale-Parola, E. 1977. Relationship between cell coiling and motility of spirochetes in viscous environments. *J. Bacteriol.*, **131**(3):960–969.
- Griffiths, D., Fawley, W., Kachrimanidou, M., Bowden, R., Crook, D. W., Fung, R., Golubchik, T., Harding, R. M., Jeffery, K. J. M., Jolley, K. A., Kirton, R., Peto, T. E., Rees, G., Stoesser, N., Vaughan, A., Walker, A. S., Young, B. C., Wilcox, M., and Dingle, K. E. 2010. Multilocus Sequence Typing of *Clostridium difficile*. *J. Clin. Microbiol.*, **48**(3):770–778.
- Gu, H., Shi, K., Liao, Z., Qi, H., Chen, S., Wang, H., Li, S., Ma, Y., and Wang, J. 2018. Time-resolved transcriptome analysis of *Clostridium difficile* R20291 response to cysteine. *Microbiol. Res.*, **215**(May):114–125.
- Gude, S., Pinçe, E., Taute, K. M., Seinen, A.-B., Shimizu, T. S., and Tans, S. J. 2020. Bacterial coexistence driven by motility and spatial competition. *Nature*, **578**(7796):588–592.

- Guery, B., Georgopali, A., Karas, A., Kazeem, G., Michon, I., Wilcox, M. H., and Cornely, O. A. 2020. Pharmacokinetic analysis of an extended-pulsed fidaxomicin regimen for the treatment of *Clostridioides (Clostridium) difficile* infection in patients aged 60 years and older in the EXTEND randomized controlled trial. *J. Antimicrob. Chemother.*, **75**(4):1014–1018.
- Guery, B., Menichetti, F., Anttila, V.-j., Adomakoh, N., Aguado, J. M., Bisnauthsing, K., Georgopali, A., Goldenberg, S. D., Karas, A., Kazeem, G., Longshaw, C., Palacios-Fabrega, J. A., Cornely, O. A., Vehreschild, M. J. G. T., and EXTEND Clinical Study Group 2017. Extended-pulsed fidaxomicin versus vancomycin for *Clostridium difficile* infection in patients 60 years and older (EXTEND): a randomised, controlled, open-label, phase 3b/4 trial. *Lancet Infect. Dis.*, **in press**(17):1–12.
- Hall, B. A., Armitage, J. P., and Sansom, M. S. P. 2012. Mechanism of Bacterial Signal Transduction Revealed by Molecular Dynamics of Tsr Dimers and Trimers of Dimers in Lipid Vesicles. *PLoS Comput. Biol.*, **8**(9):e1002685.
- Hall, I. C. and O’Toole, E. 1935. INTESTINAL FLORA IN NEW-BORN INFANTS. *Am. J. Dis. Child.*, **49**(2):390.
- Haya, S., Tokumaru, Y., Abe, N., Kaneko, J., and Aizawa, S. I. 2011. Characterization of lateral flagella of *Selenomonas ruminantium*. *Appl. Environ. Microbiol.*, **77**(8):2799–2802.
- Heap, J. T., Kuehne, S. A., Ehsaan, M., Cartman, S. T., Cooksley, C. M., Scott, J. C., and Minton, N. P. 2010. The ClosTron: Mutagenesis in *Clostridium* refined and streamlined. *J. Microbiol. Methods*, **80**(1):49–55.
- Hemmasi, S., Czulkies, B. A., Schorch, B., Veit, A., Aktories, K., and Papatheodorou, P. 2015. Interaction of the *Clostridium difficile* Binary Toxin CDT and Its Host Cell Receptor, Lipolysis-stimulated Lipoprotein Receptor (LSR). *J. Biol. Chem.*, **290**(22):14031–44.
- Himsworth, C. G., Patrick, D. M., Mak, S., Jardine, C. M., Tang, P., and Scott Weese, J. 2014. Carriage of *Clostridium difficile* by wild urban Norway rats (*Rattus norvegicus*) and black rats (*Rattus rattus*). *Appl. Environ. Microbiol.*, **80**(4):1299–1305.
- Hintsche, M., Waljor, V., Großmann, R., Kühn, M. J., Thormann, K. M., Peruani, F., and Beta, C. 2017. A polar bundle of flagella can drive bacterial swimming by pushing, pulling, or coiling around the cell body. *Sci. Rep.*, **7**(1):16771.

- Hofmann, J. D., Otto, A., Berges, M., Biedendieck, R., Michel, A.-M., Becher, D., Jahn, D., and Neumann-Schaal, M. 2018. Metabolic Reprogramming of *Clostridioides difficile* During the Stationary Phase With the Induction of Toxin Production. *Front. Microbiol.*, **9**(AUG):1–17.
- Howerton, A., Ramirez, N., and Abel-Santos, E. 2011. Mapping interactions between germinants and *Clostridium difficile* spores. *J. Bacteriol.*, **193**(1):274–82.
- Huhulescu, S., Sagel, U., Fiedler, A., Pecavar, V., Blaschitz, M., Wewalka, G., Allerberger, F., and Indra, A. 2011. Rifaximin disc diffusion test for *in vitro* susceptibility testing of *Clostridium difficile*. *J. Med. Microbiol.*, **60**(8):1206–1212.
- Igarashi, H., Maeda, S., Ohno, K., Horigome, A., Odamaki, T., and Tsujimoto, H. 2014. Effect of Oral Administration of Metronidazole or Prednisolone on Fecal Microbiota in Dogs. *PLoS One*, **9**(9):e107909.
- Jabr, F. 2013. The Science of the Great Molasses Flood.
- Janssen, I., Cooper, P., Gunka, K., Rupnik, M., Wetzel, D., Zimmermann, O., and Groß, U. 2016. High prevalence of nontoxigenic *Clostridium difficile* isolated from hospitalized and non-hospitalized individuals in rural Ghana. *Int. J. Med. Microbiol.*, **306**(8):652–656.
- Johansson, M. E. V., Larsson, J. M. H., and Hansson, G. C. 2011. The two mucus layers of colon are organized by the MUC2 mucin, whereas the outer layer is a legislator of host-microbial interactions. *Proc. Natl. Acad. Sci.*, **108**(Supplement\_1):4659–4665.
- Johnson, S., Schriever, C., Galang, M., Kelly, C. P., and Gerding, D. N. 2007. Interruption of Recurrent *Clostridium difficile*-Associated Diarrhea Episodes by Serial Therapy with Vancomycin and Rifaximin. *Clin. Infect. Dis.*, **44**(6):846–848.
- Johnson, S., Schriever, C., Patel, U., Patel, T., Hecht, D. W., and Gerding, D. N. 2009. Rifaximin Redux: Treatment of recurrent *Clostridium difficile* infections with Rifaximin immediately post-vancomycin treatment. *Anaerobe*, **15**(6):290–291.
- Just, I., Selzer, J., Wilm, M., Eichel-Streiber, C. V., Mann, M., and Aktories, K. 1995. Glucosylation of Rho proteins by *Clostridium difficile* toxin B. *Nature*, **375**(6531):500–503.
- Kanehisa, M. KEGG *Clostridioides difficile* Flagellar Assembly.

- Kapoor, G., Saigal, S., and Elongavan, A. 2017. Action and resistance mechanisms of antibiotics: A guide for clinicians. *J. Anaesthesiol. Clin. Pharmacol.*, **33**(3):300.
- Karlsson, S., Lindberg, A., Norin, E., Burman, L. G., and Akerlund, T. 2000. Toxins, Butyric Acid, and Other Short-Chain Fatty Acids Are Coordinately Expressed and Down-Regulated by Cysteine in *Clostridium difficile*. *Infect. Immun.*, **68**(10):5881–5888.
- Kearns, D. B. 2010. A field guide to bacterial swarming motility. *Nat. Rev. Microbiol.*, **8**(9):634–644.
- Keller, J. J., Vehreschild, M. J., Hvas, C. L., Jørgensen, S. M., Kupciskas, J., Link, A., Mulder, C. J., Goldenberg, S. D., Arasaradnam, R., Sokol, H., Gasbarrini, A., Hoegenauer, C., Terveer, E. M., Kuijper, E. J., and Arkkila, P. 2019. Stool for fecal microbiota transplantation should be classified as a transplant product and not as a drug. *United Eur. Gastroenterol. J.*, **7**(10):1408–1410.
- Kim, S., de los Reyes V, A. A., and Jung, E. 2020. Country-specific intervention strategies for top three TB burden countries using mathematical model. *PLoS One*, **15**(4):e0230964.
- Koenigsnecht, M. J., Theriot, C. M., Bergin, I. L., Schumacher, C. A., Schloss, P. D., and Young, V. B. 2015. Dynamics and Establishment of *Clostridium difficile* Infection in the Murine Gastrointestinal Tract. *Infect. Immun.*, **83**(3):934–941.
- Korolik, V. 2019. The role of chemotaxis during *Campylobacter jejuni* colonisation and pathogenesis. *Curr. Opin. Microbiol.*, **47**:32–37.
- Krijger, I. M., Meerburg, B. G., Harmanus, C., and Burt, S. A. 2019. *Clostridium difficile* in wild rodents and insectivores in the Netherlands. *Lett. Appl. Microbiol.*, **69**(1):35–40.
- Kuehne, S. A., Cartman, S. T., Heap, J. T., Kelly, M. L., Cockayne, A., and Minton, N. P. 2010. The role of toxin A and toxin B in *Clostridium difficile* infection. *Nature*, **467**(7316):711–713.
- Kuehne, S. A., Dempster, A. W., Collery, M. M., Joshi, N., Jowett, J., Kelly, M. L., Cave, R., Longshaw, C. M., and Minton, N. P. 2017. Characterization of the impact of *rpoB* mutations on the *in vitro* and *in vivo* competitive fitness of *Clostridium difficile* and susceptibility to fidaxomicin. *J. Antimicrob. Chemother.*, (December):1–8.

- Lai, S. K., O'Hanlon, D. E., Harrold, S., Man, S. T., Wang, Y.-Y., Cone, R., and Hanes, J. 2007. Rapid transport of large polymeric nanoparticles in fresh undiluted human mucus. *Proc. Natl. Acad. Sci.*, **104**(5):1482–1487.
- Lai, S. K., Wang, Y.-Y., Wirtz, D., and Hanes, J. 2009. Micro- and macrorheology of mucus. *Adv. Drug Deliv. Rev.*, **61**(2):86–100.
- Law, A. M. J. and Aitken, M. D. 2005. Continuous-Flow Capillary Assay for Measuring Bacterial Chemotaxis. *Appl. Environ. Microbiol.*, **71**(6):3137–3143.
- Lawson, P. A., Citron, D. M., Tyrrell, K. L., and Finegold, S. M. 2016. Reclassification of *Clostridium difficile* as *Clostridioides difficile* (Hall and O'Toole 1935) Prévot 1938. *Anaerobe*, **40**:95–99.
- Lee, H. Y., Hsiao, H. L., Chia, C. Y., Cheng, C. W., Tsai, T. C., Deng, S. T., Chen, C. L., and Chiu, C. H. 2019. Risk factors and outcomes of *Clostridium difficile* infection in hospitalized patients. *Biomed. J.*, **42**(2):99–106.
- Leeds, J. A. 2016. Antibacterials Developed to Target a Single Organism: Mechanisms and Frequencies of Reduced Susceptibility to the Novel Anti-*Clostridium difficile* Compounds Fidaxomicin and LFF571. *Cold Spring Harb. Perspect. Med.*, **6**(2):a025445.
- Leeds, J. A., Sachdeva, M., Mullin, S., Whitney Barnes, S., and Ruzin, A. 2014. *In vitro* selection, via serial passage, of *Clostridium difficile* mutants with reduced susceptibility to fidaxomicin or vancomycin. *J. Antimicrob. Chemother.*, **69**(1):41–44.
- Leffler, D. A. and Lamont, J. T. 2015. *Clostridium difficile* Infection. *N. Engl. J. Med.*, **372**(16):1539–1548.
- Lertsethtakarn, P., Ottemann, K. M., and Hendrixson, D. R. 2011. Motility and Chemotaxis in *Campylobacter* and *Helicobacter*. *Annu. Rev. Microbiol.*, **65**(1):389–410.
- Lessa, F. C., Mu, Y., Bamberg, W. M., Beldavs, Z. G., Dumyati, G. K., Dunn, J. R., Farley, M. M., Holzbauer, S. M., Meek, J. I., Phipps, E. C., Wilson, L. E., Winston, L. G., Cohen, J. A., Limbago, B. M., Fridkin, S. K., Gerding, D. N., and McDonald, L. C. 2015. Burden of *Clostridium difficile* Infection in the United States. *N. Engl. J. Med.*, **372**(9):825–834.
- Lew, T., Putsathit, P., Sohn, K. M., Wu, Y., Ouchi, K., Ishii, Y., Tateda, K., Riley, T. V., and Collins, D. A. 2020. Antimicrobial Susceptibilities of *Clostridium diffi-*

- cile Isolates from 12 Asia-Pacific Countries in 2014 and 2015. *Antimicrob. Agents Chemother.*, **64**(7).
- Li, H. and Durbin, R. 2009. Fast and accurate short read alignment with Burrows-Wheeler transform. *Bioinformatics*, **25**(14):1754–1760.
- Li, H. and Durbin, R. 2010. Fast and accurate long-read alignment with Burrows-Wheeler transform. *Bioinformatics*, **26**(5):589–595.
- Li, J., Go, A. C., Ward, M. J., and Ottemann, K. M. 2010. The chemical-in-plug bacterial chemotaxis assay is prone to false positive responses. *BMC Res. Notes*, **3**(1):77.
- Lin, W., Das, K., Degen, D., Mazumder, A., Duchi, D., Wang, D., Ebright, Y. W., Ebright, R. Y., Sineva, E., Gigliotti, M., Srivastava, A., Mandal, S., Jiang, Y., Liu, Y., Yin, R., Zhang, Z., Eng, E. T., Thomas, D., Donadio, S., Zhang, H., Zhang, C., Kapanidis, A. N., and Ebright, R. H. 2018. Structural Basis of Transcription Inhibition by Fidaxomicin (Lipiarmycin A3). *Mol. Cell*, **70**(1):60–71.e15.
- Liu, W., Cremer, J., Li, D., Hwa, T., and Liu, C. 2019. An evolutionarily stable strategy to colonize spatially extended habitats. *Nature*, **575**(7784):664–668.
- Luciano, J., Agrebi, R., Le Gall, A. V., Wartel, M., Fiegna, F., Ducret, A., Brochier-Armanet, C., and Mignot, T. 2011. Emergence and Modular Evolution of a Novel Motility Machinery in Bacteria. *PLoS Genet.*, **7**(9):e1002268.
- Macy, J. M., Snellen, J. E., and Hungate, R. E. 1972. Use of syringe methods for anaerobiosis. *Am. J. Clin. Nutr.*, **25**(12):1318–23.
- Magariyama, Y., Ichiba, M., Nakata, K., Baba, K., Ohtani, T., Kudo, S., and Goto, T. 2005. Difference in bacterial motion between forward and backward swimming caused by the wall effect. *Biophys. J.*, **88**(5):3648–3658.
- Major, G., Bradshaw, L., Boota, N., Sprange, K., Diggle, M., Montgomery, A., Jawhari, A., Spiller, R. C., and RAPID Collaboration Group 2019. Follow-on RifAximin for the Prevention of recurrence following standard treatment of Infection with *Clostridium Difficile* (RAPID): a randomised placebo controlled trial. *Gut*, **68**(7):1224–1231.
- Martin-Verstraete, I., Peltier, J., and Dupuy, B. 2016. The Regulatory Networks That Control *Clostridium difficile* Toxin Synthesis. *Toxins (Basel)*, **8**(5):153.

- Martinez, V. A., Schwarz-Linek, J., Reufer, M., Wilson, L. G., Morozov, A. N., and Poon, W. C. K. 2014. Flagellated bacterial motility in polymer solutions. *111*(50):17771–17776.
- Matilla, M. A. and Krell, T. 2017. Chemoreceptor-based signal sensing. *Curr. Opin. Biotechnol.*, **45**:8–14.
- Matilla, M. A. and Krell, T. 2018. The effect of bacterial chemotaxis on host infection and pathogenicity. *FEMS Microbiol. Rev.*, **42**(1):40–67.
- McDonald, L. C., Gerding, D. N., Johnson, S., Bakken, J. S., Carroll, K. C., Coffin, S. E., Dubberke, E. R., Garey, K. W., Gould, C. V., Kelly, C., Loo, V., Shaklee Sammons, J., Sandora, T. J., and Wilcox, M. H. 2018. Clinical Practice Guidelines for *Clostridium difficile* Infection in Adults and Children: 2017 Update by the Infectious Diseases Society of America (IDSA) and Society for Healthcare Epidemiology of America (SHEA). *Clin. Infect. Dis.*, **66**(7):987–994.
- McDonnell, G. and Russell, A. D. 1999. Antiseptics and disinfectants: Activity, action, and resistance. *Clin. Microbiol. Rev.*, **12**(1):147–179.
- McGuckin, M. A., Lindén, S. K., Sutton, P., and Florin, T. H. 2011. Mucin dynamics and enteric pathogens. *Nat. Rev. Microbiol.*, **9**(4):265–278.
- McKee, R. W., Aleksanyan, N., Garrett, E. M., and Tamayo, R. 2018a. Type IV Pili Promote *Clostridium difficile* Adherence and Persistence in a Mouse Model of Infection. *Infect. Immun.*, **86**(5):1–13.
- McKee, R. W., Harvest, C. K., and Tamayo, R. 2018b. Cyclic Diguanilate Regulates Virulence Factor Genes via Multiple Riboswitches in *Clostridium difficile*. *mSphere*, **3**(5):1–15.
- McKee, R. W., Mangalea, M. R., Purcell, E. B., Borchardt, E. K., and Tamayo, R. 2013. The second messenger cyclic Di-GMP regulates *Clostridium difficile* toxin production by controlling expression of sigD. *J. Bacteriol.*, **195**(22):5174–5185.
- McLaughlin, R. W., Cochran, P. A., Dowd, S. E., Andersen, K., Anderson, N., Brennan, R., Brook, N., Callaway, T., Diamante, K., Duberstine, A., Fitch, K., Freiheit, H., Godlewski, C., Gorman, K., Haubrich, M., Hernandez, M., Hirtreiter, A., Ivanoski, B., Jaminet, X., Kirkpatrick, T., Kratowicz, J., Latus, C., Leable, T., Lingafelt, N., Lowe, D., Lowrance, H., Malsack, L., Mazurkiewicz, J., Merlos, P., Messley,



- J., Montemurro, D., Nakitare, S., Nelson, C., Nye, A., Pazera, V., Pierangeli, G., Rellora, A., Reyes, A., Roberts, J., Robins, S., Robinson, J., Schultz, A., Seifert, S., Sigler, E., Spangler, J., Swift, E., TenCate, R., Thurber, J., Vallee, K., Wamboldt, J., Whitten, S., Woods, D., Wright, A., and Yankunas, D. 2014. Draft Genome Sequence of *Clostridium mangenotii* TR, Isolated from the Fecal Material of a Timber Rattlesnake. *Genome Announc.*, **2**(1):2164.
- Merrigan, M. M., Venugopal, A., Roxas, J. L., Anwar, F., Mallozzi, M. J., Roxas, B. A., Gerding, D. N., Viswanathan, V. K., and Vedantam, G. 2013. Surface-Layer Protein A (SlpA) is a major contributor to host-cell adherence of *Clostridium difficile*. *PLoS One*, **8**(11):1–12.
- Merz, A. J., So, M., and Sheetz, M. P. 2000. Pilus retraction powers bacterial twitching motility. *Nature*, **407**(6800):98–102.
- Morimoto, Y. V. and Minamino, T. 2014. Structure and function of the bi-directional bacterial flagellar motor. *Biomolecules*, **4**(1):217–234.
- Mukherjee, S. and Kearns, D. B. 2014. The Structure and Regulation of Flagella in *Bacillus subtilis*. *Annu. Rev. Genet.*, **48**(1):319–340.
- Munita, J. M. and Arias, C. A. 2016. Mechanisms of Antibiotic Resistance. *Microbiol. Spectr.*, **4**(2):1–37.
- Nasiri, M. J., Goudarzi, M., Hajikhani, B., Ghazi, M., Goudarzi, H., and Pouriran, R. 2018. *Clostridium difficile* infection in hospitalized patients with antibiotic-associated diarrhea: A systematic review and meta-analysis. *Anaerobe*, **50**:32–37.
- Neumann-Schaal, M., Hofmann, J. D., Will, S. E., and Schomburg, D. 2015. Time-resolved amino acid uptake of *Clostridium difficile* 630 $\Delta$ *erm* and concomitant fermentation product and toxin formation. *BMC Microbiol.*, **15**(1):1–12.
- Ng, J., Hirota, S. A., Gross, O., Li, Y., Ulke-Lemee, A., Potentier, M. S., Schenck, L. P., Vilaysane, A., Seamone, M. E., Feng, H., Armstrong, G. D., Tschopp, J., MacDonald, J. A., Muruve, D. A., and Beck, P. L. 2010. *Clostridium difficile* Toxin-Induced Inflammation and Intestinal Injury Are Mediated by the Inflammasome. *Gastroenterology*, **139**(2):542–552.e3.
- Ntountoumi, C., Vlastaridis, P., Mossialos, D., Stathopoulos, C., Iliopoulos, I., Promponas, V., Oliver, S. G., and Amoutzias, G. D. 2019. Low complexity regions

- in the proteins of prokaryotes perform important functional roles and are highly conserved. *Nucleic Acids Res.*, **47**(19):9998–10009.
- O'Connor, J. R., Galang, M. A., Sambol, S. P., Hecht, D. W., Vedantam, G., Gerding, D. N., and Johnson, S. 2008. Rifampin and rifaximin resistance in clinical isolates of *Clostridium difficile*. *Antimicrob. Agents Chemother.*, **52**(8):2813–2817.
- Olmsted, S. S., Padgett, J. L., Yudin, A. I., Whaley, K. J., Moench, T. R., and Cone, R. A. 2001. Diffusion of Macromolecules and Virus-Like Particles in Human Cervical Mucus. *Biophys. J.*, **81**(4):1930–1937.
- Ooijevaar, R. E., van Beurden, Y. H., Terveer, E. M., Goorhuis, A., Bauer, M. P., Keller, J. J., Mulder, C. J., and Kuijper, E. J. 2018. Update of treatment algorithms for *Clostridium difficile* infection. *Clin. Microbiol. Infect.*, **24**(5):452–462.
- Ottemann, K. M. 1999. A Piston Model for Transmembrane Signaling of the Aspartate Receptor. *Science (80-. )*, **285**(5434):1751–1754.
- Oughton, M. T., Loo, V. G., Dendukuri, N., Fenn, S., and Libman, M. D. 2009. Hand Hygiene with Soap and Water Is Superior to Alcohol Rub and Antiseptic Wipes for Removal of *Clostridium difficile*. *Infect. Control Hosp. Epidemiol.*, **30**(10):939–944.
- Pak, J. M. 2019. Gaussian Sum FIR Filtering for 2D Target Tracking. *Int. J. Control. Autom. Syst.*, **17**(2017):1–7.
- Palleja, A., Mikkelsen, K. H., Forslund, S. K., Kashani, A., Allin, K. H., Nielsen, T., Hansen, T. H., Liang, S., Feng, Q., Zhang, C., Pyl, P. T., Coelho, L. P., Yang, H., Wang, J., Typas, A., Nielsen, M. F., Nielsen, H. B., Bork, P., Wang, J., Vilsbøll, T., Hansen, T., Knop, F. K., Arumugam, M., and Pedersen, O. 2018. Recovery of gut microbiota of healthy adults following antibiotic exposure. *Nat. Microbiol.*, **3**(11):1255–1265.
- Parkinson, J. S., Parker, S. R., Talbert, P. B., and Houts, S. E. 1983. Interactions between chemotaxis genes and flagellar genes in *Escherichia coli*. *J. Bacteriol.*, **155**(1):265–274.
- Partridge, J. D. and Harshey, R. M. 2013. Swarming: Flexible roaming plans. *J. Bacteriol.*, **195**(5):909–918.
- Partridge, J. D., Nhu, N. T. Q., Dufour, Y. S., and Harshey, R. M. 2020. Tumble Suppression Is a Conserved Feature of Swarming Motility. *MBio*, **11**(3):1–5.

- Pecavar, V., Blaschitz, M., Hufnagl, P., Zeinzinger, J., Fiedler, A., Allerberger, F., Maass, M., and Indra, A. 2012. High-resolution melting analysis of the single nucleotide polymorphism hot-spot region in the *rpoB* gene as an indicator of reduced susceptibility to rifaximin in *Clostridium difficile*. *J. Med. Microbiol.*, **61**(6):780–785.
- Pfeffer, W. 1884. Locomotorische Richtungsbewegungen durch chemische Reize. *Untersuchungen aus dem Bot. Inst. zu Tübingen*, **1**:363–482.
- Piepenbrink, K. H., Maldarelli, G. A., de la Peña, C. F. M., Mulvey, G. L., Snyder, G. A., De Masi, L., von Rosenvinge, E. C., Günther, S., Armstrong, G. D., Donnenberg, M. S., and Sundberg, E. J. 2014. Structure of *Clostridium difficile* PilJ Exhibits Unprecedented Divergence from Known Type IV Pilins. *J. Biol. Chem.*, **289**(7):4334–4345.
- Porter, S. L., Wadhams, G. H., and Armitage, J. P. 2011. Signal processing in complex chemotaxis pathways. *Nat. Rev. Microbiol.*, **9**(3):153–165.
- Purcell, E. B., McKee, R. W., McBride, S. M., Waters, C. M., and Tamayo, R. 2012. Cyclic diguanylate inversely regulates motility and aggregation in *Clostridium difficile*. *J. Bacteriol.*, **194**(13):3307–3316.
- Purcell, E. M. 1977. Life at low Reynolds number. *Am. J. Phys.*, **45**(1):3–11.
- Rao, C. V., Glekas, G. D., and Ordal, G. W. 2008. The three adaptation systems of *Bacillus subtilis* chemotaxis. *Trends Microbiol.*, **16**(10):480–487.
- Rashid, T., Haghghi, F., Hasan, I., Bassères, E., Jahangir Alam, M., Sharma, S. V., Lai, D., DuPont, H. L., and Garey, K. W. 2020. Activity of Hospital Disinfectants against Vegetative Cells and Spores of *Clostridioides difficile* Embedded in Biofilms. *Antimicrob. Agents Chemother.*, **64**(1):1–10.
- Reigadas, E., Muñoz-Pacheco, P., Vázquez-Cuesta, S., Alcalá, L., Marín, M., Martín, A., and Bouza, E. 2017. Rifaximin-resistant *Clostridium difficile* strains isolated from symptomatic patients. *Anaerobe*, **48**:269–272.
- Renault, T. T., Abraham, A. O., Bergmiller, T., Paradis, G., Rainville, S., Charpentier, E., Guet, C. C., Tu, Y., Namba, K., Keener, J. P., Minamino, T., and Erhardt, M. 2017. Bacterial flagella grow through an injection-diffusion mechanism. *Elife*, **6**:1–22.
- Riedel, T., Bunk, B., Thürmer, A., Spröer, C., Brzuszkiewicz, E., Abt, B., Gronow, S., Liesegang, H., Daniel, R., and Overmann, J. 2015a. Genome Resequencing of the

- Virulent and Multidrug-Resistant Reference Strain *Clostridium difficile* 630. *Genome Announc.*, **3**(2):15–16.
- Riedel, T., Bunk, B., Wittmann, J., Thürmer, A., Spröer, C., Gronow, S., Liesegang, H., Daniel, R., and Overmann, J. 2015b. Complete Genome Sequence of the *Clostridium difficile* Type Strain DSM 1296 T. *Genome Announc.*, **3**(5):3–4.
- Riedel, T., Wetzel, D., Hofmann, J. D., Plorin, S. P. E. O., Dannheim, H., Berges, M., Zimmermann, O., Bunk, B., Schober, I., Spröer, C., Liesegang, H., Jahn, D., Overmann, J., Groß, U., and Neumann-Schaal, M. 2017. High metabolic versatility of different toxigenic and non-toxigenic *Clostridioides difficile* isolates. *Int. J. Med. Microbiol.*, **307**(6):311–320.
- Rodriguez-Palacios, A., Mo, K. Q., Shah, B. U., Msuya, J., Bijedic, N., Deshpande, A., and Ilic, S. 2020. Global and Historical Distribution of *Clostridioides difficile* in the Human Diet (1981–2019): Systematic Review and Meta-Analysis of 21886 Samples Reveal Sources of Heterogeneity, High-Risk Foods, and Unexpected Higher Prevalence Toward the Tropic. *Front. Med.*, **7**(February).
- Rohlfing, A. E., Eckenroth, B. E., Forster, E. R., Kevorkian, Y., Donnelly, M. L., Benito de la Puebla, H., Doublé, S., and Shen, A. 2019. The CspC pseudoprotease regulates germination of *Clostridioides difficile* spores in response to multiple environmental signals. *PLOS Genet.*, **15**(7):e1008224.
- Rohlke, F. and Stollman, N. 2012. Fecal microbiota transplantation in relapsing *Clostridium difficile* infection. *Therap. Adv. Gastroenterol.*, **5**(6):403–420.
- Rothenburger, J. L., Rousseau, J. D., Weese, J. S., and Jardine, C. M. 2018. Livestock-associated methicillin-resistant *Staphylococcus aureus* and *Clostridium difficile* in wild Norway rats (*Rattus norvegicus*) from ontario swine farms. *Can. J. Vet. Res.*, **82**(1):66–69.
- Sachsenheimer, F., Yang, I., Zimmermann, O., Wrede, C., Müller, L., Gunka, K., Groß, U., and Suerbaum, S. 2018. Genomic and phenotypic diversity of *Clostridium difficile* during long-term sequential recurrences of infection. *Int. J. Med. Microbiol.*, **308**(3):364–377.
- Samatey, F. A., Matsunami, H., Imada, K., Nagashima, S., Shaikh, T. R., Thomas, D. R., Chen, J. Z., DeRosier, D. J., Kitao, A., and Namba, K. 2004. Structure of the

- bacterial flagellar hook and implication for the molecular universal joint mechanism. *Nature*, **431**(7012):1062–1068.
- Sarkar, M. K., Paul, K., and Blair, D. 2010. Chemotaxis signaling protein CheY binds to the rotor protein FliN to control the direction of flagellar rotation in *Escherichia coli*. *Proc. Natl. Acad. Sci.*, **107**(20):9370–9375.
- Schneider, W. R. and Doetsch, R. N. 1974. Effect of Viscosity on Bacterial Motility. *J. Bacteriol.*, **117**(2):696–701.
- Schuech, R., Hoehfurtner, T., Smith, D. J., and Humphries, S. 2019. Motile curved bacteria are Pareto-optimal. *Proc. Natl. Acad. Sci.*, **116**(29):14440–14447.
- Schwalbe, R., Steele-Moore, L., and Goodwin, A. C. 2007. *Antimicrobial Susceptibility Testing Protocols*. CRC Press, Boca Raton.
- Schwan, C., Kruppke, A. S., Nölke, T., Schumacher, L., Koch-Nolte, F., Kudryashev, M., Stahlberg, H., and Aktories, K. 2014. *Clostridium difficile* toxin CDT hijacks microtubule organization and reroutes vesicle traffic to increase pathogen adherence. *Proc. Natl. Acad. Sci. U. S. A.*, **111**(6):2313–2318.
- Schwanbeck, J., Oehmig, I., Dretzke, J., Zautner, A. E., Groß, U., and Bohne, W. 2020a. YSMR: a video tracking and analysis program for bacterial motility. *BMC Bioinformatics*, **21**(1):166.
- Schwanbeck, J., Oehmig, I., Groß, U., Zautner, A. E., and Bohne, W. 2020b. *Clostridioides difficile* single cell swimming strategy: a novel motility pattern regulated by cysteine and viscoelastic properties of the environment.
- Schwanbeck, J., Riedel, T., Laukien, F., Schober, I., Oehmig, I., Zimmermann, O., Overmann, J., Groß, U., Zautner, A. E., and Bohne, W. 2019. Characterization of a clinical *Clostridioides difficile* isolate with markedly reduced fidaxomicin susceptibility and a V1143D mutation in *rpoB*. *J. Antimicrob. Chemother.*, **74**(1):6–10.
- Sears, P., Crook, D. W., Louie, T. J., Miller, M. A., and Weiss, K. 2012. Fidaxomicin Attains High Fecal Concentrations With Minimal Plasma Concentrations Following Oral Administration in Patients With *Clostridium difficile* Infection. *Clin. Infect. Dis.*, **55**(suppl 2):S116–S120.
- Seddon, J., Babakhani, F., Gomez, A., and Griffiths, D. 2011. RNA polymerase target modification in *Clostridium difficile* with reduced susceptibility to fidaxomicin.

- Seddon, S. V., Hemingway, I., and Borriello, S. P. 1990. Hydrolytic enzyme production by *Clostridium difficile* and its relationship to toxin production and virulence in the hamster model. *J. Med. Microbiol.*, **31**(3):169–174.
- Sender, R., Fuchs, S., and Milo, R. 2016. Revised Estimates for the Number of Human and Bacteria Cells in the Body. *PLoS Biol.*, **14**(8):1–14.
- Seoane, A. S. and Levy, S. B. 1995. Characterization of MarR, the repressor of the multiple antibiotic resistance (*mar*) operon in *Escherichia coli*. *J. Bacteriol.*, **177**(12):3414–3419.
- Seugendo, M., Janssen, I., Lang, V., Hasibuan, I., Bohne, W., Cooper, P., Daniel, R., Gunka, K., Kusumawati, R. L., Mshana, S. E., von Müller, L., Okamo, B., Ortlepp, J. R., Overmann, J., Riedel, T., Rupnik, M., Zimmermann, O., and Groß, U. 2018. Prevalence and Strain Characterization of *Clostridioides (Clostridium) difficile* in Representative Regions of Germany, Ghana, Tanzania and Indonesia – A Comparative Multi-Center Cross-Sectional Study. *Front. Microbiol.*, **9**(AUG):1–7.
- Sharma, P., Haycocks, J. R. J., Middlemiss, A. D., Kettles, R. A., Sellars, L. E., Ricci, V., Piddock, L. J. V., and Grainger, D. C. 2017. The multiple antibiotic resistance operon of enteric bacteria controls DNA repair and outer membrane integrity. *Nat. Commun.*, **8**(1):1444.
- Shayto, R. H., Abou Mrad, R., and Sharara, A. I. 2016. Use of rifaximin in gastrointestinal and liver diseases. *World J. Gastroenterol.*, **22**(29):6638–51.
- Shrestha, R. and Sorg, J. A. 2017. Hierarchical recognition of amino acid co-germinants during *Clostridioides difficile* spore germination. *Anaerobe*.
- Siani, H., Cooper, C., and Maillard, J.-Y. 2011. Efficacy of “sporicidal” wipes against *Clostridium difficile*. *Am. J. Infect. Control*, **39**(3):212–218.
- Sievers, S., Metzendorf, N. G., Dittmann, S., Troitzsch, D., Gast, V., Tröger, S. M., Wolff, C., Zühlke, D., Hirschfeld, C., Schlüter, R., and Riedel, K. 2019. Differential View on the Bile Acid Stress Response of *Clostridioides difficile*. *Front. Microbiol.*, **10**(February):1–13.
- Smits, W. K., Lyras, D., Lacy, D. B., Wilcox, M. H., and Kuijper, E. J. 2016. *Clostridium difficile* infection. *Nat. Rev. Dis. Prim.*, **2**:1–20.

- Songer, J. G., Trinh, H. T., Killgore, G. E., Thompson, A. D., McDonald, L. C., and Limbago, B. M. 2009. *Clostridium difficile* in Retail Meat Products, USA, 2007. *Emerg. Infect. Dis.*, **15**(5):819–821.
- Sorg, J., Theriot, C. M., Viswanathan, V. K., Smits, W. K., Baktash, A., Terveer, E. M., Zwiittink, R. D., Hornung, B. V. H., Corver, J., and Kuijper, E. J. 2018. Mechanistic Insights in the Success of Fecal Microbiota Transplants for the Treatment of *Clostridium difficile* Infections. **9**(June):1–15.
- Sorg, J. A. and Sonenshein, A. L. 2008. Bile salts and glycine as cogerminants for *Clostridium difficile* spores. *J. Bacteriol.*, **190**(7):2505–2512.
- Sourjik, V. and Armitage, J. P. 2010. Spatial organization in bacterial chemotaxis. *EMBO J.*, **29**(16):2724–2733.
- Stecher, B., Hapfelmeier, S., Muller, C., Kremer, M., Stallmach, T., and Hardt, W.-D. 2004. Flagella and Chemotaxis Are Required for Efficient Induction of *Salmonella enterica* Serovar Typhimurium Colitis in Streptomycin-Pretreated Mice. *Infect. Immun.*, **72**(7):4138–4150.
- Steindl, G., Fiedler, A., Huhulescu, S., Wewalka, G., and Allerberger, F. 2015. Effekt von gasförmigem Wasserstoffperoxid auf Sporen von *Clostridium difficile*. *Wien. Klin. Wochenschr.*, **127**(11-12):421–426.
- Stevenson, E., Minton, N. P., and Kuehne, S. A. 2015. The role of flagella in *Clostridium difficile* pathogenicity. *Trends Microbiol.*, **23**(5):275–282.
- Stocker, R. 2011. Reverse and flick: Hybrid locomotion in bacteria. *Proc. Natl. Acad. Sci.*, **108**(7):2635–2636.
- Strong, P. C. R., Fulton, K. M., Aubry, A., Foote, S., Twine, S. M., and Logan, S. M. 2014. Identification and Characterization of Glycoproteins on the Spore Surface of *Clostridium difficile*. *J. Bacteriol.*, **196**(14):2627–2637.
- Suzuki, S., Horinouchi, T., and Furusawa, C. 2017. Acceleration and suppression of resistance development by antibiotic combinations. *BMC Genomics*, **18**(1):328.
- Tarrant, J., Jenkins, R. O., and Laird, K. T. 2018. From ward to washer: The survival of *Clostridium difficile* spores on hospital bed sheets through a commercial UK NHS healthcare laundry process. *Infect. Control Hosp. Epidemiol.*, **39**(12):1406–1411.

- Tasteyre, A., Barc, M.-C., Collignon, A., Boureau, H., and Karjalainen, T. 2001. Role of FliC and FliD Flagellar Proteins of *Clostridium difficile* in Adherence and Gut Colonization. *Infect. Immun.*, **69**(12):7937–7940.
- Taute, K. M., Gude, S., Tans, S. J., and Shimizu, T. S. 2015. High-throughput 3D tracking of bacteria on a standard phase contrast microscope. *Nat. Commun.*, **6**(May):8776.
- Taylor, J. A., Sichel, S. R., and Salama, N. R. 2019. Bent Bacteria: A Comparison of Cell Shape Mechanisms in *Proteobacteria*. *Annu. Rev. Microbiol.*, **73**(1):457–480.
- Teng, C., Reveles, K. R., Obodozie-Ofoegbu, O. O., and Frei, C. R. 2019. *Clostridium difficile* infection risk with important antibiotic classes: An analysis of the FDA adverse event reporting system. *Int. J. Med. Sci.*, **16**(5):630–635.
- Theriot, C. M., Bowman, A. A., and Young, V. B. 2016. Antibiotic-Induced Alterations of the Gut Microbiota Alter Secondary Bile Acid Production and Allow for *Clostridium difficile* Spore Germination and Outgrowth in the Large Intestine. *mSphere*, **1**(1):e00045–15.
- Theriot, C. M., Koenigsknecht, M. J., Carlson, P. E., Hatton, G. E., Nelson, A. M., Li, B., Huffnagle, G. B., Z Li, J., and Young, V. B. 2014. Antibiotic-induced shifts in the mouse gut microbiome and metabolome increase susceptibility to *Clostridium difficile* infection. *Nat. Commun.*, **5**:3114.
- Theriot, C. M. and Young, V. B. 2015. Interactions Between the Gastrointestinal Microbiome and *Clostridium difficile*. *Annu. Rev. Microbiol.*, **69**(1):445–461.
- Thiem, S., Kentner, D., and Sourjik, V. 2007. Positioning of chemosensory clusters in *E. coli* and its relation to cell division. *EMBO J.*, **26**(6):1615–1623.
- Tinevez, J. Y., Perry, N., Schindelin, J., Hoopes, G. M., Reynolds, G. D., Laplantine, E., Bednarek, S. Y., Shorte, S. L., and Eliceiri, K. W. 2017. TrackMate: An open and extensible platform for single-particle tracking. *Methods*, **115**:80–90.
- Twine, S. M., Reid, C. W., Aubry, A., McMullin, D. R., Fulton, K. M., Austin, J., and Logan, S. M. 2009. Motility and Flagellar Glycosylation in *Clostridium difficile*. *J. Bacteriol.*, **191**(22):7050–7062.
- Varga, J. J., Nguyen, V., O'Brien, D. K., Rodgers, K., Walker, R. A., and Melville, S. B. 2006. Type IV pili-dependent gliding motility in the Gram-positive pathogen *Clostridium perfringens* and other Clostridia. *Mol. Microbiol.*, **62**(3):680–694.



- Wallace, R. L., Ouellette, M., and Jean, J. 2019. Effect of UV-C light or hydrogen peroxide wipes on the inactivation of methicillin-resistant *Staphylococcus aureus*, *Clostridium difficile* spores and norovirus surrogate. *J. Appl. Microbiol.*, **127**(2):586–597.
- Walter, B. M., Cartman, S. T., Minton, N. P., Butala, M., and Rupnik, M. 2015. The SOS response master regulator LexA is associated with sporulation, motility and biofilm formation in *Clostridium difficile*. *PLoS One*, **10**(12):1–17.
- Ward, E., Kim, E. A., Panushka, J., Botelho, T., Meyer, T., Kearns, D. B., Ordal, G., and Blair, D. F. 2019. Organization of the flagellar switch complex of *Bacillus subtilis*. *J. Bacteriol.*, **201**(8):1–22.
- Watts, K. J., Vaknin, A., Fuqua, C., and Kazmierczak, B. I. 2019. New Twists and Turns in Bacterial Locomotion and Signal Transduction. *J. Bacteriol.*, (July).
- Wei, Y., Sun, M., Zhang, Y., Gao, J., Kong, F., Liu, D., Yu, H., Du, J., and Tang, R. 2019. Prevalence, genotype and antimicrobial resistance of *Clostridium difficile* isolates from healthy pets in Eastern China. *BMC Infect. Dis.*, **19**(1):1–7.
- Weingarden, A. R., Dosa, P. I., DeWinter, E., Steer, C. J., Shaughnessy, M. K., Johnson, J. R., Khoruts, A., and Sadowsky, M. J. 2016. Changes in colonic bile acid composition following fecal microbiota transplantation are sufficient to control *Clostridium difficile* germination and growth. *PLoS One*, **11**(1):1–16.
- Wetzel, D. and McBride, S. M. 2019. The Impact of pH on *Clostridioides difficile* Sporulation and Physiology. *Appl. Environ. Microbiol.*, **86**(4):1–13.
- Wistrand-Yuen, E., Knopp, M., Hjort, K., Koskiniemi, S., Berg, O. G., and Andersson, D. I. 2018. Evolution of high-level resistance during low-level antibiotic exposure. *Nat. Commun.*, **9**(1):1599.
- Wiström, J., Norrby, S. R., Myhre, E. B., Eriksson, S., Granström, G., Lagergren, L., Englund, G., Nord, C. E., and Svenungsson, B. 2001. Frequency of antibiotic-associated diarrhoea in 2462 antibiotic-treated hospitalized patients: a prospective study. *J. Antimicrob. Chemother.*, **47**(1):43–50.
- Xie, L. L., Altindal, T., Chattopadhyay, S., and Wu, X.-L. 2011. Bacterial flagellum as a propeller and as a rudder for efficient chemotaxis. *Proc. Natl. Acad. Sci.*, **108**(6):2246–2251.

- Xu, L., Surathu, A., Raplee, I., Chockalingam, A., Stewart, S., Walker, L., Sacks, L., Patel, V., Li, Z., and Rouse, R. 2020. The effect of antibiotics on the gut microbiome: a metagenomics analysis of microbial shift and gut antibiotic resistance in antibiotic treated mice. *BMC Genomics*, **21**(1):263.
- Young, V. B. and Schmidt, T. M. 2004. Antibiotic-Associated Diarrhea Accompanied by Large-Scale Alterations in the Composition of the Fecal Microbiota. *J. Clin. Microbiol.*, **42**(3):1203–1206.
- Zhanel, G. G., Walkty, A. J., and Karlowsky, J. A. 2015. Fidaxomicin: A Novel Agent for the Treatment of *Clostridium difficile* Infection. *Can. J. Infect. Dis. Med. Microbiol.*, **26**(6):305–312.
- Zheng, L., Kelly, C. J., and Colgan, S. P. 2015. Physiologic hypoxia and oxygen homeostasis in the healthy intestine. A Review in the Theme: Cellular Responses to Hypoxia. *Am. J. Physiol. Physiol.*, **309**(6):C350–C360.
- Zidaric, V., Beigot, S., Lapajne, S., and Rupnik Maja, M. 2010. The occurrence and high diversity of *Clostridium difficile* genotypes in rivers. *Anaerobe*, **16**(4):371–375.
- Zimmer, M. A., Tiu, J., Collins, M. A., and Ordal, G. W. 2000. Selective Methylation Changes on the *Bacillus subtilis* Chemotaxis Receptor McpB Promote Adaptation. *J. Biol. Chem.*, **275**(32):24264–24272.

# Curriculum vitae

## Julian Schwanbeck

Date of birth            1. July 1990

Place of birth            Henstedt–Ulzburg

Nationality              German

## Education

06/2017    present    **Doctor rerum naturalium**  
Within the GGNB program “Microbiology & Biochemistry”  
Georg–August–Universität Göttingen

10/2014    09/2016    **Master of Science**  
Microbiology & Biochemistry  
Georg–August–Universität Göttingen

10/2010    05/2014    **Bachelor of Science**  
Biology  
Georg–August–Universität Göttingen

08/2001    07/2010    **Abitur**  
Heinrich–Heine–Gymnasium, Hamburg